

ACTA PHARMACEUTICA SCIENCIA

International Journal in Pharmaceutical Sciences, Published Quarterly

ISSN: 2636-8552

e-ISSN: 1307-2080,

Volume: 57, No: 2, 2019

Formerly: Eczacılık Bülteni

Acta Pharmaceutica Turcica

ACTA PHARMACEUTICA SCIENCIA

International Journal in Pharmaceutical Sciences
is Published Quarterly

ISSN: 2636-8552

e-ISSN: 1307-2080,

Volume: 57, No: 2, 2019

Formerly: Eczacılık Bülteni/Acta Pharmaceutica Turcica

Founded in 1953 by Kasım Cemal Güven

Editor

Şeref Demirayak

Associate Editors

Gülden Zehra Omurtag

Barkın Berk

Coordinators

M. Eşref Tatlıpınar

Gökberk Karabay

Language Editor

Recep Murat Nurlu

M. Eşref Tatlıpınar

Neda Taner

Biostatistics Editor

Pakize Yiğit

Graphic Design

Sertan Vural

Levent Karabağlı

Address

İstanbul Medipol Üniversitesi

Kavacık Güney Kampüsü

Göztepe Mah. Atatürk Cad.

No: 40 34810 Beykoz/İSTANBUL

Tel: 0216 681 51 00

E-mail

editor@actapharmsci.com

secretary@actapharmsci.com

Web site

<http://www.actapharmsci.com>

Editorial Board

Sabahattin Aydın

(İstanbul Medipol University, Turkey)

Ahmet Aydın (Yeditepe University, Turkey)

Ahmet Çağrı Karaburun (Anadolu University, Turkey)

Aristidis Tsatsakis (University of Crete, Greece)

Ayfer Beceren (Marmara University, Turkey)

Dilek Ak (Anadolu University, Turkey)

Ebrahim Razzazi-Fazeli

(University of Veterinary Medicine, Vienna)

Erem Memişoğlu Bilensoy

(Hacettepe University, Turkey)

Fatma Tosun

(İstanbul Medipol University, Turkey)

Fatih Demirci (Anadolu University, Turkey)

Hakan Göker (Ankara University, Turkey)

Hanefi Özbek

(İstanbul Medipol University, Turkey)

Hayati Çelik (Yeditepe University, Turkey)

İhsan Çalış (Near East University, Cyprus)

Julide Akbuğa (Altınbaş University, Turkey)

Kenneth A. Jacobson

(National Institutes of Health, USA)

Leyla Yurttaş (Anadolu University, Turkey)

Mahmud Miski (İstanbul University, Turkey)

Mesut Sancar (Marmara University, Turkey)

Murat Duran

(Eskişehir Osmangazi University, Turkey)

Nesrin Emekli

(İstanbul Medipol University, Turkey)

Nilay Aksoy (Altınbaş University, Turkey)

Nurşen Başaran (Hacettepe University, Turkey)

Özgen Özer (Ege University, Turkey)

Roberta Ciccocioppo

(University of Camerino, Italy)

Selma Saraç Tarhan

(Hacettepe University, Turkey)

Semra Şardaş (İstinye University, Turkey)

Sevda Süzgeç Selçuk

(İstanbul University, Turkey)

Stefano Constanzi (American University, USA)

Süreyya Ölgen (Biruni University, Turkey)

Şule Apikoğlu Rabuş

(Marmara University, Turkey)

Tuncer Değim (Biruni University, Turkey)

Yıldız Özsoy (İstanbul University, Turkey)

Yusuf Öztürk (Anadolu University, Turkey)

Printing Office

Forat Basımevi

Ziya Gökalp Mah.

Süleyman Demirel Bulvarı

Simpaş İş Modern Zemin Kat A 17-18

İkitelli - İstanbul

Tel: (0212) 501 82 20

Contents

Aims and Scope of Acta Pharmaceutica Scientia	
Şeref Demirayak	113
Instructions for Authors	114
Original articles	128
Synthesis, Characterization and Evaluation of the Anti-cancer Activity of Silver Nanoparticles by Natural Organic Compounds Extracted from <i>Cyperus sp.</i> rhizomes	
Rasim Farraj Muslim, Mustafa Nadhim Owaid	129
Anti-inflammatory and Analgesic Potential of Acetone Leaf Extract of <i>Combretum Sordidum</i> and its Fractions	
Babatunde Samuel, Olayinka Oridupa, Fisayo Gbadegesin	147
Combination of Cumulative Area Pre-Processing and Partial Least Squares for Handling Intensely Overlapping Binary and Ternary Drug Systems	
Yahya Al-Degs, Amjad El-Sheikh, Eman Abu Saaleek, Reema Omeir, Musab Al-Ghodran	161
Chemical Composition and Comparative Antibacterial Properties of Basil Essential Oil against Clinical and Standard Strains of <i>Campylobacter spp.</i>	
Aysegul Mutlu-Ingok, Burcu Firtin, Funda Karbancioglu-Guler	183
In vitro Antimicrobial and Antioxidant Evaluation of <i>Melampyrum Arvense</i> Var. <i>Elatius L.</i> and <i>Sedum Spurium M. Bieb.</i> Extracts	
Ayşe Esra Karadağ, Fatma Tosun	193
Preparation and In vitro Characterization of a Fluconazole Loaded Chitosan Particulate System	
Gülsel Yurtdaş-Kırımlıoğlu, Yenilmez Evrim, Başaran Ebru, Yazan Yasemin	
Review articles	216
Pharmaceutical Properties of Marine Polyphenols: An Overview	
Thanh Sang Vo, Dai Hung Ngo, Se-Kwon Kim.	217

Aims and Scope of Acta Pharmaceutica Scientia

Acta Pharmaceutica Scientia is a continuation of the former “Eczacılık Bülteni” which was first published in 1953 by Prof. Dr. Kasım Cemal Güven’s editorship. At that time, “Eczacılık Bülteni” hosted scientific papers from the School of Medicine-Pharmacy at Istanbul University, Turkey.

In 1984, the name of the journal was changed to “Acta Pharmaceutica Turcica” and it became a journal for national and international manuscripts, in all fields of pharmaceutical sciences in both English and Turkish. (1984-1995, edited by Prof. Dr. Kasım Cemal Güven, 1995-2001, edited by Prof. Dr. Erden Güler, 2002-2011, edited by Prof. Dr. Kasım Cemal Güven)

Since 2006, the journal has been published only in English with the name, “Acta Pharmaceutica Scientia” which represents internationally accepted high-level scientific standards. The journal has been published quarterly except for an interval from 2002 to 2009 in which its issues were released at intervals of four months. The publication was also temporarily discontinued at the end of 2011 but since 2016, Acta Pharmaceutica Scientia has continued publication with the reestablished Editorial Board and also with the support of you as precious scientists.

Yours Faithfully

Prof. Dr. Şeref DEMİRAYAK

Editor

INSTRUCTIONS FOR AUTHORS

1. Scope and Editorial Policy

1.1. Scope of the Journal

Acta Pharmaceutica Scientia (Acta Pharm. Sci.), formerly known as Bulletin of Pharmacy and Acta Pharmaceutica Turcica is a peer-reviewed scientific journal publishing current research and reviews covering all fields of pharmaceutical sciences since 1953.

The original studies accepted for publication must be unpublished work and should contain data that have not been published elsewhere as a whole or a part. The reviews must provide critical evaluation of the state of knowledge related with the subject.

All manuscripts has to be written in clear and concise English. Starting from 2016, the journal will be issued quarterly both in paper and online formates also publish special issues for national or international scientific meetings and activities in the coverage field.

1.2 Manuscript Categories

Manuscripts can be submitted as Research Articles and Reviews.

1.2.1 Research Articles are definitive accounts of significant, original studies. They are expected to present important new data or provide a fresh approach to an established subject.

1.2.2 Reviews integrate, correlate, and evaluate results from published literature on a particular subject. They expected to report new and up to date experimental findings. They have to have a well-defined theme, are usually critical, and may present novel theoretical interpretations. Up to date experimental procedures may be included. Reviews are usually submitted at the invitation of the Editors. However, experts are welcome to contact the Editors to ensure that a topic is suitable. Approval is recommended prior to submission.

1.3 Prior Publication

Authors should submit only original work that has not been previously published and is not under consideration for publication elsewhere. Academic theses, including those on the Web or at a college Web site, are not considered to be prior publication.

1.4 Patents and Intellectual Property

Authors need to resolve all patent and intellectual property issues. Acceptance

and publication will not be delayed for pending or unresolved issues of this type. Note that Accepted manuscripts and online manuscripts are considered as published documents.

1.5 Professional Ethics

Editors, reviewers, and authors are expected to adhere to internationally accepted criteria's for scientific publishing.

1.5.1 Author Consent. Submitting authors are reminded that consent of all coauthors must be obtained prior to submission of manuscripts. If an author is removed after submission, the submitting author must have the removed author consent to the change by e-mail or faxed letter to the assigned Editor.

1.5.2. Plagiarism. Manuscripts must be original with respect to concept, content, and writing. It is not appropriate for an author to reuse wording from other publications, including one's own previous publications, whether or not that publication is cited. Suspected plagiarism should be reported immediately to the editorial office. Report should specifically indicate the plagiarized material within the manuscripts. Acta Pharmaceutica Scientia uses iThenticate or Turnitin software to screen submitted manuscripts for similarity to published material. Note that your manuscript may be screened during the submission process.

1.5.3. Use of Human or Animal Subjects. For research involving biological samples obtained from animals or human subjects, editors reserve the right to request additional information from authors. Studies submitted for publication approval must present evidence that the described experimental activities have undergone local institutional review assessing safety and humane usage of study subject animals. In the case of human subjects authors must also provide a statement that study samples were obtained through the informed consent of the donors, or in lieu of that evidence, by the authority of the institutional board that licensed the use of such material. Authors are requested to declare the identification or case number of institution approval as well as the name of the licensing committee in a statement placed in the section describing the studies' Material and Methods.

1.6 Issue Frequency

The Journal publishes 4 issues per year.

2. Preparing the Manuscript

2.1 General Considerations

Manuscripts should be kept to a minimum length. Authors should write in cle-

ar, concise English, employing an editing service if necessary. For professional assistance with improving the English, figures, or formatting in the manuscript before submission please contact to editorial office by e-mail for suggestions.

The responsibility for all aspects of manuscript preparation rests with the authors. Extensive changes or rewriting of the manuscript will not be undertaken by the Editors. A standard list of Abbreviations, Acronyms and Symbols is in section 5.

It is best to use the fonts “Times” and “Symbol.” Other fonts, particularly those that do not come bundled with the system software, may not translate properly. Ensure that all special characters (e.g., Greek characters, math symbols) are present in the body of the text as characters and not as graphic representations. Be sure that all characters are correctly represented throughout the manuscript—e.g., 1 (one) and l (letter l), o (zero) and O (letter o).

All text (including the title page, abstract, all sections of the body of the paper, figure captions, scheme or chart titles, and footnotes and references) and tables should be in one file. Graphics may be included with the text or uploaded as separate files. Manuscripts that do not adhere to the guidelines may be returned to authors for correction.

2.1.1 Articles of all kind. Use page size A4. Vertically orient all pages. Articles of all kind must be double-spaced including text, references, tables, and legends. This applies to figures, schemes, and tables as well as text. They do not have page limitations but should be kept to a minimum length. The experimental procedures for all of experimental steps must be clearly and fully included in the experimental section of the manuscripts.

2.1.2 Nomenclature. It is the responsibility of the authors to provide correct nomenclature. It is acceptable to use semisynthetic or generic names for certain specialized classes of compounds, such as steroids, peptides, carbohydrates, etc. In such a case, the name should conform to the generally accepted nomenclature conventions for the compound class. Chemical names for drugs are preferred. If these are not practical, generic names, or names approved by the World Health Organization, may be used.

Authors may find the following sources useful for recommended nomenclature:

- The ACS Style Guide; Coghill, A. M., Garson, L. R., Eds.; American Chemical Society: Washington DC, 2006.
- Enzyme Nomenclature; Webb, E. C., Ed.; Academic Press: Orlando, 1992.

· IUPHAR database of receptors and ion channels (<http://www.guidetopharmacology.org/>).

2.1.3 Compound Code Numbers. Code numbers (including peptides) assigned to a compound may be used as follows:

- Once in the manuscript title, when placed in parentheses AFTER the chemical or descriptive name.
- Once in the abstract.
- Once in the text (includes legends) and once to label a structure. Code numbers in the text must correspond to structures or, if used only once, the chemical name must be provided before the parenthesized code number, e.g., “chemical name (JEM-398).” If appearing a second time in the text, a bold Arabic number must be assigned on first usage, followed by the parenthesized code number, e.g., “1 (JEM-398).” Subsequently, only the bold Arabic number may be used. All code numbers in the text must have a citation to a publication or a patent on first appearance.

Compounds widely employed as research tools and recognized primarily by code numbers may be designated in the manuscript by code numbers without the above restrictions. Their chemical name or structure should be provided as above. Editors have the discretion of determining which code numbers are considered widely employed.

2.1.4 Trademark Names. Trademark names for reagents or drugs must be used only in the experimental section. Do not use trademark or service mark symbols.

2.1.5 Interference Compounds. Active compounds from any source must be examined for known classes of assay interference compounds and this analysis must be provided in the General Experimental section. Many of these compounds have been classified as Pan Assay Interference Compounds (PA-INS; see Baell & Holloway, *J. Med. Chem.* 2010, 53, 2719-2740). These compounds shown to display misleading assay readouts by a variety of mechanisms by forming reactive compounds. Provide firm experimental evidence in at least two different assays that reported compounds with potential PAINS liability are specifically active and their apparent activity is not an artifact.

2.2 Manuscript Organization

2.2.1 Title Page. Title: The title of the manuscript should reflect the purposes and findings of the work in order to provide maximum information in a

computerized title search. Minimal use of nonfunctional words is encouraged. Only commonly employed abbreviations (e.g., DNA, RNA, ATP) are acceptable. Code numbers for compounds may be used in a manuscript title when placed in parentheses AFTER the chemical or descriptive name.

Authors' Names and Affiliations: The authors' full first names, middle initials, last names, and affiliations with addresses at time of work completion should be listed below the title. The name of the corresponding author should be marked with an asterisk (*).

2.2.2 Abstract and keywords. Articles of all types must have an abstract following the title page. The maximum length of the Abstract should be 150 words, organized in a findings-oriented format in which the most important results and conclusions are summarized. Code numbers may be used once in the abstract.

After the abstract, a section of Keywords not more than five has to be given. Be aware that the keywords, chosen according to the general concept, are very significant during searching and indexing of the manuscripts.

2.2.3 Introduction. The rationale and objectives of the research should be discussed in this section. The background material should be brief and relevant to the research described.

2.2.4. Methodology. Materials, synthetic, biological, demographic, statistical or experimental methods of the research should be given detailed in this section. The authors are free to subdivide this section in the logical flow of the study. For the experimental sections, authors should be as concise as possible in experimental descriptions. General reaction, isolation, preparation conditions should be given only once. The title of an experiment should include the chemical name and a bold Arabic identifier number; subsequently, only the bold Arabic number should be used. Experiments should be listed in numerical order. Molar equivalents of all reactants and percentage yields of products should be included. A general introductory section should include general procedures, standard techniques, and instruments employed (e.g., determination of purity, chromatography, NMR spectra, mass spectra, names of equipment) in the synthesis and characterization of compounds, isolates and preparations described subsequently in this section. Special attention should be called to hazardous reactions or toxic compounds. Provide analysis for known classes of assay interference compounds.

The preferred forms for some of the more commonly used abbreviations are mp, bp, °C, K, min, h, mL, µL, g, mg, µg, cm, mm, nm, mol, mmol, µmol, ppm,

TLC, GC, NMR, UV, and IR. Units are abbreviated in table column heads and when used with numbers, not otherwise. (See section 4 for more abbreviations)

2.2.5 Results and Discussion. This section could include preparation, isolation, synthetic schemes and tables of biological and statistical data. The discussions should be descriptive. Authors should discuss the analysis of the data together with the significance of results and conclusions. An optional conclusions section is not required.

2.2.6 Ancillary Information. Include pertinent information in the order listed immediately before the references.

PDB ID Codes: Include the PDB ID codes with assigned compound Arabic number. Include the statement “Authors will release the atomic coordinates and experimental data upon article publication.”

Homology Models: Include the PDB ID codes with assigned compound Arabic number. Include the statement “Authors will release the atomic coordinates upon article publication.”

Corresponding Author Information: Provide telephone numbers and email addresses for each of the designated corresponding authors.

Present/Current Author Addresses: Provide information for authors whose affiliations or addresses have changed.

Author Contributions: Include statement such as «These authors contributed equally.»

Acknowledgment: Authors may acknowledge people, organizations, and financial supporters in this section.

Abbreviations Used: Provide a list of nonstandard abbreviations and acronyms used in the paper, e.g., YFP, yellow fluorescent protein. Do not include compound code numbers in this list. It is not necessary to include abbreviations and acronyms from the Standard Abbreviations and Acronyms listed in section 4.

2.2.7 References and Notes. Number literature references and notes in one consecutive series by order of mention in the text. Numbers in the text are non-parenthesized superscripts. The accuracy of the references is the responsibility of the author. List all authors; do not use et al. Provide inclusive page numbers. Titles may have capitalization of first word only (excluding, for example, acronyms and trade names) or standard capitalization as shown below. The chosen style should be used consistently throughout the references. Double-space the references using the following format.

· For journals: Rich, D. H.; Green, J.; Toth, M. V.; Marshall, G. R.; Kent, S. B. H. Hydroxyethylamine Analogues of the p17/p24 Substrate Cleavage Site Are Tight Binding Inhibitors of HIV Protease. *J. Med. Chem.* **1990**, *33*, 1285-1288.

· For online early access: Rubner, G.; Bendsdorf, K.; Wellner, A.; Kircher, B.; Bergemann, S.; Ott, I.; Gust, R. Synthesis and Biological Activities of Transition Metal Complexes Based on Acetylsalicylic Acid as Neo-Anticancer Agents. *J. Med. Chem.* [Online early access]. DOI: 10.1021/jm101019j. Published Online: September 21, 2010.

· For periodicals published in electronic format only: Author 1; Author 2; Author 3; etc. Title of Article. *Journal Abbreviation* [Online] **Year**, *Volume*, Article Number or other identifying information.

· For monographs: Casy, A. F.; Parfitt, R. T. *Opioid Analgesics*; Plenum: New York, 1986.

· For edited books: Rall, T. W.; Schleifer, L. S. Drugs Effective in the Therapy of the Epilepsies. In *The Pharmacological Basis of Therapeutics*, 7th ed.; Gilman, A. G., Goodman, L. S., Rall, T. W., Murad, F., Eds.; Macmillan: New York, 1985; pp 446-472

List submitted manuscripts as “in press” only if formally accepted for publication. Manuscripts available on the Web with a DOI number are considered published. For manuscripts not accepted, use “unpublished results” after the names of authors. Incorporate notes in the correct numerical sequence with the references. Footnotes are not used.

2.2.8 Tables. Tabulation of experimental results is encouraged when this leads to more effective presentation or to more economical use of space. Tables should be numbered consecutively in order of citation in the text with Arabic numerals. Footnotes in tables should be given italic lowercase letter designations and cited in the tables as superscripts. The sequence of letters should proceed by row rather than by column. If a reference is cited in both table and text, insert a lettered footnote in the table to refer to the numbered reference in the text. Each table must be provided with a descriptive title that, together with column headings, should make the table self-explanatory. Titles and footnotes should be on the same page as the table. Tables may be created using a word processor’s text mode or table format feature. The table format feature is preferred. Ensure each data entry is in its own table cell. If the text mode is used, separate columns with a single tab and use a return at the end of each row. Tables may be inserted in the text where first mentioned or may be grouped after the references.

2.2.9 Figures, Schemes/Structures, and Charts. The use of illustrations to convey or clarify information is encouraged. Structures should be produced with the use of a drawing program such as ChemDraw. Authors using other drawing packages should, in as far as possible, modify their program's parameters so that they conform to ChemDraw preferences. Remove all color from illustrations, except for those you would like published in color. Illustrations may be inserted into the text where mentioned or may be consolidated at the end of the manuscript. If consolidated, legends should be grouped on a separate page(s). Include as part of the manuscript file.

To facilitate the publication process, please submit manuscript graphics using the following guidelines:

1. The preferred submission procedure is to embed graphic files in a Word document. It may help to print the manuscript on a laser printer to ensure all artwork is clear and legible.
2. Additional acceptable file formats are: TIFF, PDF, EPS (vector artwork) or CDX (ChemDraw file). If submitting individual graphic files in addition to them being embedded in a Word document, ensure the files are named based on graphic function (i.e. Scheme 1, Figure 2, Chart 3), not the scientific name. Labeling of all figure parts should be present and the parts should be assembled into a single graphic.

EPS files: Ensure that all fonts are converted to outlines or embedded in the graphic file. The document settings should be in RGB mode. **NOTE:** While EPS files are accepted, the vector-based graphics will be rasterized for production. Please see below for TIFF file production resolutions.

3. TIFF files (either embedded in a Word doc or submitted as individual files) should have the following resolution requirements:

- Black & White line art: 1200 dpi
 - Grayscale art (a monochromatic image containing shades of gray): 600 dpi
 - Color art (RGB color mode): 300 dpi
- The RGB and resolution requirements are essential for producing high-quality graphics within the published manuscript. Graphics submitted in CMYK or at lower resolutions may be used; however, the colors may not be consistent and graphics of poor quality may not be able to be improved.
 - Most graphic programs provide an option for changing the resolution when you are saving the image. Best practice is to save the graphic file at the final

resolution and size using the program used to create the graphic.

4. Graphics should be sized at the final production size when possible. Single column graphics are preferred and can be sized up to 240 points wide (8.38 cm.). Double column graphics must be sized between 300 and 504 points (10.584 and 17.78 cm's). All graphics have a maximum depth of 660 points (23.28 cm.) including the caption (please allow 12 points for each line of caption text).

Consistently sizing letters and labels in graphics throughout your manuscript will help ensure consistent graphic presentation for publication.

2.2.10 Image Manipulation. Images should be free from misleading manipulation. Images included in an account of research performed or in the data collection as part of the research require an accurate description of how the images were generated and produced. Apply digital processing uniformly to images, with both samples and controls. Cropping must be reported in the figure legend. For gels and blots, use of positive and negative controls is highly recommended. Avoid high contrast settings to avoid overexposure of gels and blots. For microscopy, apply color adjustment to entire image and note in the legend. When necessary, authors should include a section on equipment and settings to describe all image acquisition tools, techniques and settings, and software used. All final images must have resolutions of 300 dpi or higher. Authors should retain unprocessed data in the event that the Editors request them.

2.3 Specialized Data

2.3.1 Biological Data. Quantitative biological data are required for all tested compounds. Biological test methods must be referenced or described in sufficient detail to permit the experiments to be repeated by others. Detailed descriptions of biological methods should be placed in the experimental section. Standard compounds or established drugs should be tested in the same system for comparison. Data may be presented as numerical expressions or in graphical form; biological data for extensive series of compounds should be presented in tabular form.

Active compounds obtained from combinatorial syntheses should be resynthesized and retested to verify that the biology conforms to the initial observation. Statistical limits (statistical significance) for the biological data are usually required. If statistical limits cannot be provided, the number of determinations and some indication of the variability and reliability of the results should be given. References to statistical methods of calculation should be included.

Doses and concentrations should be expressed as molar quantities (e.g., mol/kg, $\mu\text{mol/kg}$, M, mM). The routes of administration of test compounds and vehicles used should be indicated, and any salt forms used (hydrochlorides, sulfates, etc.) should be noted. The physical state of the compound dosed (crystalline, amorphous; solution, suspension) and the formulation for dosing (micronized, jet-milled, nanoparticles) should be indicated. For those compounds found to be inactive, the highest concentration (in vitro) or dose level (in vivo) tested should be indicated.

If human cell lines are used, authors are strongly encouraged to include the following information in their manuscript:

- the cell line source, including when and from where it was obtained;
- whether the cell line has recently been authenticated and by what method;
- whether the cell line has recently been tested for mycoplasma contamination.

2.3.2 Purity of Tested Compounds.

Methods: All scientifically established methods of establishing purity are acceptable. If the target compounds are solvated, the quantity of solvent should be included in the compound formulas. No documentation is required unless asked by the editors.

Purity Percentage: All tested compounds, whether synthesized or purchased, should possess a purity of at least 95%. Target compounds must have a purity of at least 95%. In exceptional cases, authors can request a waiver when compounds are less than 95% pure. For solids, the melting point or melting point range should be reported as an indicator of purity.

Elemental analysis: Found values for carbon, hydrogen, and nitrogen (if present) should be within 0.4% of the calculated values for the proposed formula.

2.3.3 Confirmation of Structure. Adequate evidence to establish structural identity must accompany all new compounds that appear in the experimental section. Sufficient spectral data should be presented in the experimental section to allow for the identification of the same compound by comparison. Generally, a listing of ^1H or ^{13}C NMR peaks is sufficient. However, when the NMR data are used as a basis of structural identification, the peaks must be assigned.

List only infrared absorptions that are diagnostic for key functional groups. If a series contains very closely related compounds, it may be appropriate merely to list the spectral data for a single representative member when they share a common major structural component that has identical or very similar spectral features.

3. Submitting the Manuscript

3.1 Communication and log in to Author's Module All submissions to Acta Pharmaceutica Scientia should be made by using e-Collittera (Online Article Acceptance and Evaluation) system on the journal main page (www.actapharmsci.com)

3.2 Registration to System It is required to register into the e-Collittera system for the first time while entering by clicking "Create Account" button on the registration screen and the fill the opening form with real information. Some of the information required in form is absolutely necessary and the registration will not work if these fields are not completely filled.

After the registration, a "Welcome" mail is sent to the user by the system automatically reminding user name and password. Authors are expected to return to the entry screen and log on with their user name and password for the submission. Please use only English characters while determining your username and password.

If you already registered into the e-Collittera system and forget your password, you should click on "Forgot My Password" button and your user name and password will be mailed to your e-mail in a short while.

3.3 Submitting A New Article The main page of author module consists of various parts showing the situation of manuscripts in process. By clicking the New Manuscript button, authors create the beginning of new submission, a process with a total of 9 consecutive levels. In first 7 levels, information such as the article's kind, institutions, authors, title, summary, keywords etc. are asked respectively as entered. Authors can move back and forth while the information is saved automatically. If the transaction is discontinued, the system move the new submission to "Partially Submitted Manuscripts" part and the transaction can be continued from here.

3.1.1 Sort of Article Authors should first select the type of article from the drop down menu.

Warning. If "Return to Main Page" button is clicked after this level, the article automatically assigned as "Partially Submitted Manuscripts".

3.2.2 Institutions Authors should give their institutional information during submission.

3.2.3 Authors The authors' surnames, names, institutional information appear as entered order in the previous page. Filling all e-mail addresses are re-

quired. Institutional information is available in **Manuscript Details** table at the top of the screen. After filling all required fields, you may click the **Continue** button.

3.2.4 Title should be English, explaining the significance of the study. If the title includes some special characters such as alpha, beta, pi or gamma, they can easily be added by using the **Title** window. You may add the character by clicking the relevant button and the system will automatically add the required character to the text.

Warning. No additions to cornered parenthesis are allowed. Otherwise the system will not be able to show the special characters.

3.2.5 Abstract The summary of the article should be entered to **Abstract** window at this level. There must be an English summary for all articles and the quantity of words must be not more than 150. If special characters such as alpha, beta, pi or gamma are used in summary, they can be added by **Abstract** window. You may add the character by clicking the relevant button and the system will automatically add the required character to the text. The abstract of the articles are accessible for arbitrators; so you should not add any information related to the institutions and authors in this summary part. Otherwise the article will returned without evaluation. Authors will be required to comply with the rules.

Warning. No additions to cornered parenthesis are allowed. Otherwise the system will not be able to show the special characters.

3.2.6 Keywords There must be five words to define the article at the keywords window, which will diverged with commas. Authors should pay attention to use words, which are appropriate for “*Medical Subjects Headings*” list by National Library of Medicine (NLM).

3.2.7 Cover Letter If the submitting article was published as thesis and/or presented in a congress or elsewhere, all information of thesis, presented congress or elsewhere should be delivered to the editor and must be mentioned by the “Cover Letter” field.

3.3.1 Adding Article This process consists four different steps beginning with the loading of the article in to system. **Browse** button is used to reach the article file, under the **Choose a file to upload** tab. After finding the article you may click to **Choose File** and file will be attached.

Second step is to select the file category. Options are: Main Document, Black and White Figure, Color Figure and Video.

The explanation of the files (E.g., Figure 1, Full Text Word File, supplements etc.) should be added on third step and the last step is submitting the prepared article into the system. Therefore, **Download** button under the **Send your file by clicking on download button** tab is clicked.

Reminder If the prepared article includes more than one file (such as main document, black and white figure, video), the transaction will be continued by starting from the first step. The image files must be in previously defined format. After all required files were added, **Continue** button should be clicked. All details and features of the article might be reached from the **Article Information** page.

This page is the last step of the transaction which ensures that entered information is controlled.

3.3.2 Your Files After adding the article you may find all information related to article under **Your Files** window.

File Information This window includes file names, sizes, forming dates, categories, order numbers and explanations of files. The details about the files can be reached by clicking on **Information** button.

If you click on **Name of File**, the file download window will be opened to reach the copy of the file in system.

File Download This window submits two alternatives, one of them is to ensure the file to be opened in valid site and the second one is to ensure to download submitted file into the computer.

Opening the Category part on fourth column can change the category of the file.

Opening the Order column on fifth column can change the order of file.

The file can be deleted by clicking on **Delete** button on the last column. Before deleting, system will ask the user again if it's appropriate or not.

3.3.3 Sending Article Last level is submitting the article and the files into the system. Before continuing the transaction, **Article Information** window must be controlled where it is possible to return back; by using **Previous** button and required corrections can be made. If not, clicking the **Send the Article** button completes transaction.

3.3.4 Page to Follow The Article The Main Page of Author ensures possibility to follow the article. This page consists three different parts; some infor-

mation and bridges related to the sent articles, revision required articles and the articles that are not completed to be sent.

3.3.4.1 Articles Not Completed to be Sent After the sending transaction was started, if article is not able to continue until the ninth step or could not be sent due to technical problems shown at this part. Here you can find the information such as the article's number which is assigned by system, title and formation date. You may delete the articles by using **Delete** button on the right column, if the article is not considered to send into the system.

3.3.4.2 Articles That Require Revision Articles, which were evaluated by the referee and accepted by the editor with revision, continues to **Waiting for Revision** table.

The required revisions can be seen in “**Notes**” part by clicking the articles title.

In order to send any revision, **Submit Revision** button on the last column should be clicked. This connection will take the author to the first level of **Adding Article** and the author can complete the revision transaction by carrying out the steps one by one. All changes must be made in the registered file and this changed file must be resent. Author's most efficacious replies relating to the changes must be typed in “Cover Letter” part.

If the is transaction is discontinued, the system move the revised article to **Submitted Manuscripts** part and the transaction can be continued from here.

After the transaction was completed, the system moves the revised article to “Submitted Manuscripts” part.

3.3.5 Submitted Manuscripts Information related to articles can be followed through the **Submitted Manuscripts** line. Here you can find the information such as the article's number assigned by system, title, sending date and transaction situation. The **Manuscript Details** and summary files can be reached by clicking the title of the article and the **Processing Status** part makes it possible to follow the evaluation process of the article.

ORIGINAL ARTICLES

Synthesis, Characterization and Evaluation of the Anti-cancer Activity of Silver Nanoparticles by Natural Organic Compounds Extracted from *Cyperus sp.* rhizomes

Rasim Farraj Muslim¹, Mustafa Nadhim Owaid^{1,2*}

¹ Department of Ecology, College of Applied Sciences-Hit, University of Anbar, Hit, Anbar 31007, Iraq.

² Department of Heet Education, General Directorate of Education in Anbar, Ministry of Education, Hit, Anbar 31007, Iraq.

ABSTRACT

The object of this work is biosynthesizing AgNPs from extracts of *Cyperus sp.* galingale rhizomes, studying their characteristics using UV-visible spectroscopy, AFM, SEM, FTIR, and EDX analyses and testing their anticancer activity (*in vitro*) against L20B cell line. Biosynthesizing AgNPs using various plants is considered eco-friendly, cheap, energy saving and reproducible compared with non-green methods. UV-Visible spectrum checked the surface plasmon resonance of AgNPs at 410-420 nm. FT-IR exhibited that the presence of carbonyl and hydroxyl groups in the extract of *Cyperus sp.* can reduce and stabilize AgNPs. EDX, SEM, and AFM analyses were applied to confirm the nature, morphology and topography of the biosynthesized AgNPs. AgNPs are spherical or irregular in shape with the average diameter of hot extract-AgNPs is 56.31 nm in comparison with cold extract-AgNPs is 92.53 nm. The hot extract-AgNPs paly a suitable role against mouse cell line (L20B) which have receptors for polioviruses better than the cold extract-AgNPs.

Keywords: SEM, EDS, Green nanotechnology, Galingale, L20B.

INTRODUCTION

The synthesis of metallic nanoparticles has become an important issue in recent decades due to their various beneficial and unique properties and biomedical and industrial applications ¹. Nanotechnology is seeking to synthesize nanoparticles have substantial biomedical applications because of their unique characteristics and their green nature due to using some medicinal plants as

*Corresponding Author: Mustafa Nadhim Owaid, email: mustafanowaid@gmail.com

Rasim Farraj Muslim ORCID Number: 0000-0002-8273-2429

Mustafa Nadhim Owaid ORCID Number: 0000-0001-9005-4368

(Received 26 November 2018, accepted 30 December 2018)

a reducer agent in the biosynthesis of metallic nanoparticles ². Silver nanoparticles are considering famous nanoparticles compared with other metallic nanoparticles because of their antibiotic activity against viruses ³, bacteria ^{4,5}, fungi ⁶, cancers ^{7,8}, and parasites ⁹.

Green synthesis of AgNPs was successfully done in simple, rapid, eco-friendly and a cheaper method using plant leaves extracts like *Azadirachta indica* ¹⁰rapid, simple approach was applied for synthesis of silver nanoparticles using *Azadirachta indica* aqueous leaf extract. The plant extract acts both as reducing agent as well as capping agent. To identify the compounds responsible for reduction of silver ions, the functional groups present in plant extract were investigated by FTIR. Various techniques used to characterize synthesized nanoparticles are DLS, photoluminescence, TEM and UV-Visible spectrophotometer. UV-Visible spectrophotometer showed absorbance peak in range of 436–446 nm. The silver nanoparticles showed antibacterial activities against both gram positive (*Staphylococcus aureus*, *Panax ginseng* ⁸, *Tridax procumbens* ¹¹, *Ziziphus nummularia* ¹², *Thevetia peruviana* ¹³, olive (*Olea europaea*) ¹⁴, *Cleome viscosa*, ⁴ and fenugreek (*Trigonella foenum-graecum* L.) ¹⁵, and applying them in medicine as a green drug against bacteria, fungi and tumors.

Galingale *Cyperus rotundus* belongs to Cyperaceae (sedge family). *C. rotundus* L., purple nutsedge as a common name, is a perennial weed with slender, scaly creeping rhizomes, and arising singly from the rhizomes which are about 1-3 cm. its rhizomes are externally blackish in color and white inside with a characteristic odor ^{16,17}. Watery and ethanol crude extracts of *C. rotundus* rhizomes showed significant effects against gram-negative ¹⁸ and gram-positive bacteria, *Candida albicans* ^{19,20} and fungal pathogens ²¹. On the other hand, aqueous extract of *C. longous* has activity against parasitic worms ²².

Recently, rhizomes of *Cyperus rotundus* had anticancer effects in a recent Iraqi study ⁷, and no studies of *Cyperus* rhizomes extracts that have been reported in synthesizing silver nanoparticles. Thus we selected these galingale plant rhizomes to biosynthesize AgNPs to arise the value of inhibitory effect of *Cyperus* sp. toward human cancers *in vitro*.

However, silver nanoparticles have been biosynthesized from cold and hot extracts of *Cyperus* sp. galingale rhizomes and studied the nature and characteristics of these nanoparticles using UV-Visible spectroscopy, AFM, SEM, FT-IR and EDX analyses and evaluation of their anticancer activity (*in vitro*) against L20B cell line is a receptor for human poliovirus.

METHODOLOGY

Rhizomes samples

Fresh rhizomes of *Cyperus* sp. galingale were collected from gardens of Al-Baghdadi district west of Hit, Iraq on October 2017. The plant has identified in College of Applied Sciences-Hit using identification keys as mentioned in ^{16,17}.

Aqueous extraction of *Cyperus* sp. (galingale) rhizomes

The cold extraction method

The fresh rhizomes of galingale were cleaned from the soil and residues of roots and washed with tap water and then by distilled water (D.W) as in figure 1. The rhizomes were peeled to remove the black cortex and then extracted. For extraction achievement, 10 g of the freshly peeled rhizomes of *Cyperus* sp. was crushed in 100 mL D.W using a mortar and stored in a freezer for 48 hr. The iced extract was slowly dissolved in the room temperature. The whitish aqueous extract was filtered using gauze and then by filter paper Whatman No.1 and centrifuged at 4000 rpm for 10 min. The supernatant was collected by a micropipette and named as cold extract solution (C). The residue was emitted. FT-IR spectrum of the crude extract was achieved to characterize and to compare with AgNPs which are formed later ⁶.

The hot extraction method

The fresh rhizomes were cleaned from the soil and residues of roots and washed with tap water and then by distilled water (D.W) as in figure 1. The rhizomes were peeled to remove the black cortex and then extracted. For extraction achievement, 10 g of the freshly peeled rhizomes of *Cyperus* sp. galingale was crushed in 100 mL D.W using a mortar and boiled in the magnetic stirrer hotplate for 15 min. The whitish aqueous extract was filtered using gauze and centrifuged at 4000 rpm for 15 min twice. The clear supernatant was collected by a micropipette and named as a hot extract solution (H). The residue was emitted. FT-IR spectra of the crude extract (cold and hot extracts) were done to determine the functional groups comparison with FT-IR spectra of their AgNPs which are formed later ⁶.

Biosynthesis of silver nanoparticles

Only 33.8 μg of AgNO_3 (its purity 99.9%, AFCO For Metal, China) was dissolved in 200 mL distilled water (D.W) using the magnetic stirrer hotplate until the completion dissolving was observed to get the final concentration 10^{-3} M. Five milliliters of series concentrations of cold and hot galingale extracts (20%, 40%, 60%, 80%, and 100%) were separately mixed with 5 mL of 10^{-3} M AgNO_3

solution in 10-mL test tubes and darkly kept at 25 °C for three days ⁶. From another hand, the second method to biosynthesize AgNPs by heating of 30 mL each crude galingale extract [cold extract (C) and hot extract (H)] was separately added drop by drop into two 500mL-flask containing 100 mL of 10⁻³ M AgNO₃ solution using magnetic stirrer hotplate at 60 °C for 1 hr. The change in the mixture color was checked and recorded each 15 min.

Characterization of AgNPs

Galingale-mediated synthesis of silver nanoparticles (AgNPs) using its cold and hot extracts were characterized using changes in color of the mixture, UV-Visible spectroscopy (by spectroscopy: EMC-LAB V-1100 Digital, 325-1000 nm, Germany), FT-IR (Fourier Transform Infrared) spectra, SEM (Scanning Electron Microscope), EDX, AFM (Atomic Force Microscope), and SPM (Scanning Probe Microscope) analyses.

Anticancer efficacy

The anticancer activity of two types of AgNPs against L20B tumor cell line was evaluated. The colorimetric cell viability MTT assay was used as mentioned by ²³ and ²⁴. Firstly, 100 µL/well of L20B cells (10⁶ cell/mL) were cultured in a 96-wells tissue culture plate. Three concentrations of colloid AgNPs (50%, 75% and 100%) were applied in this test. Moreover, then 100 µL of each concentration was added within each well and incubated at 37 °C for 48 hr. after that, 10 µL of MTT solution (5 mg/mL) was added to each well and reincubated at 37 °C for 4 hr. Finally, 50 µL DMSO (dimethyl sulfoxide) was added to each well and incubated for 10 min. L20B cells were cultured in complete medium without AgNPs or the extract of *Cyperus* sp. solution as a control. The absorbance was measured for each well at 620 nm using ELISA reader. The inhibition percentage was calculated according to the equation below:

$$\text{Growth inhibition percentage} = \frac{(\text{OD of control wells} - \text{OD of test wells})}{\text{OD of control wells}} \times 100$$

Statistical Analysis

Triplicates of growth inhibition percentage were analyzed by one-way analysis of variance using ANOVA table by SAS program version 9 (SAS Institute Inc., USA). The significance of differences was calculated using Duncan's Multiple Range Test (DMRT). Probability value least than 5% was considered to be statistically significant.

RESULTS AND DISCUSSION

The change in color for the mixture of AgNO_3 and the *Cyperus* rhizomes extract from milky (hot extraction) and bright yellow (cold extraction) to the brown color was exhibited as seen in figure 1. The previous figure also is showing adsorption peaks at 410-420 nm in comparison with the crude extracts of the peeled rhizomes. Hot extract-AgNPs are showing the widest adsorption (2068 cm^{-1}) than cold extract-AgNPs (1800 cm^{-1}).

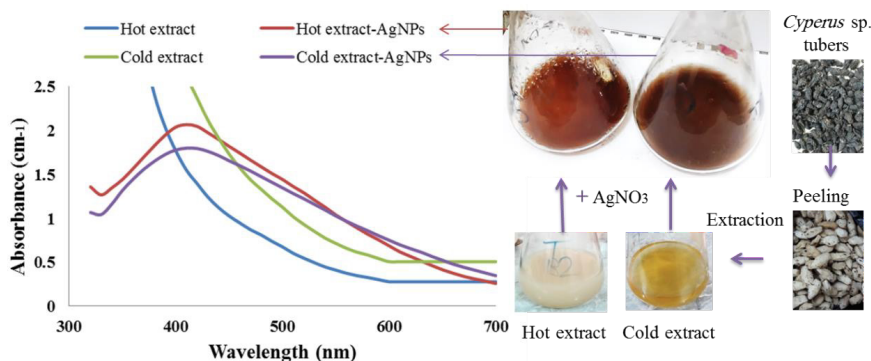


Figure 1. Change in color and UV-Visible spectrum of the biosynthesized AgNPs from *Cyperus* rhizomes extract

SEM images (figure 2) exhibited the morphology of AgNPs which ranged from spherical to irregular particles. The 3D and 2D images of AFM showed the topography of the nanoparticle's surfaces (Figure 3). However, AFM has the advantageousness of probing the surface topography deeply. The AFM image displays the surface morphology of silver nanoparticles synthesized by *Cyperus* rhizome extracts which reveal the appearance of spherical or irregular and needle-like nanoparticles for the cold extract-AgNPs and the hot extract-AgNPs respectively. Also, roughness average is 7.65 nm and 7.11 nm ; the surface area ratio is $15.3:1$ and $22.5:1$ and the density of summits $258 \mu^{-2}$ and $386 \mu^{-2}$ for the cold extract-AgNPs and the hot extract-AgNPs respectively.

Histogram of particle size distribution (SPM) showed the granularity distribution, volumes and averages of diameters of AgNPs (figure 3). This parameter is affirming the results of AFM images which appears smallness size of the hot extract-AgNPs comparing to the cold ones. The average diameter of the cold extract-AgNPs is 92.53 nm in comparison with the hot extract-AgNPs is 56.31 nm . Histogram of the particle size distribution of the two AgNPs was presented

in figure 4 was clear evidence for the formation of silver particles by the percentages of Ag particles in the two treatments.

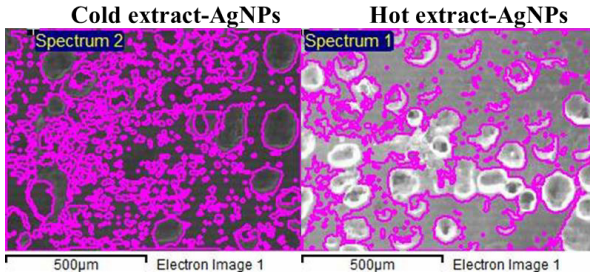


Figure 2. SEM of the biosynthesized silver nanoparticles

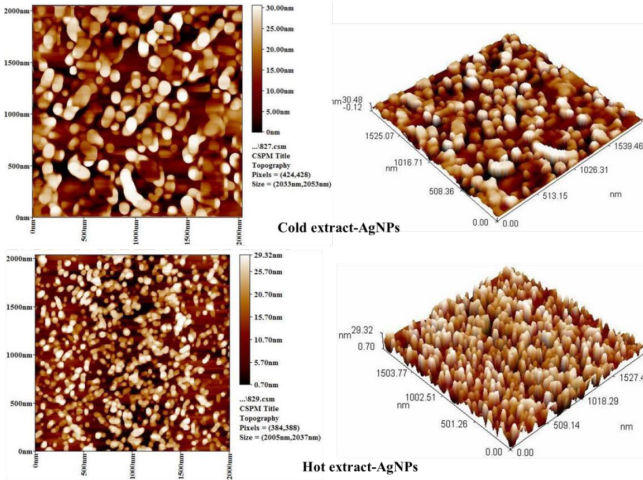


Figure 3. AFM of the colloid silver nanoparticles

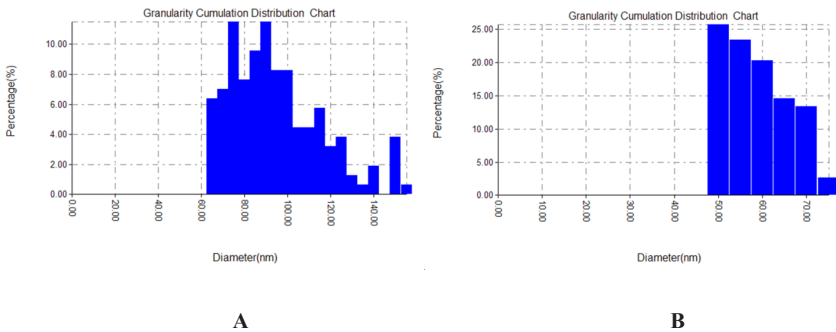


Figure 4. Histogram of the particle size distribution of the biosynthesized silver nanoparticles including the cold extract-AgNPs (A) and the hot extract-AgNPs (B)

The FT-IR spectrum the cold extract (figure 5A) and the hot extract (figure 5B) showed the peak 771 cm^{-1} is due to the covalent bonding between carbon and silicon (Si-C) and other peaks 1105 cm^{-1} and 1108 cm^{-1} for cold and hot extracts respectively. These are evidence of linkage of oxygen with silicon in (Si-O). Both spectra also showed two absorption bands at 1384 cm^{-1} and 1417 cm^{-1} belong to vibrations of homogeneous and heterogeneous bends of methylene group ($-\text{CH}_2$) or methyl group ($-\text{CH}_3$) and two absorption bands at 2891 cm^{-1} and 2894 cm^{-1} for cold and hot extracts respectively, and at 2935 cm^{-1} for cold and hot extracts too. All the mentioned absorption bands belong to the previous groups which presented in the composition of amino acids, peptides or proteins. There were absorption bands at 1053 cm^{-1} and 1062 cm^{-1} proved the protein structures for cold and hot extracts respectively belong to the single bond (C-C). The spectra showed absorption bands at 1631 cm^{-1} and 1633 cm^{-1} for cold and hot extracts respectively go back to vibrations of stretching of C=C group. On another hand, the presence of C-H-containing compounds (C-H) is evidenced by the presence of two bands at 3109 and 3130 cm^{-1} for cold and hot extracts, respectively. It is confirmed that flavonoids, amino acids, peptides, proteins, polyphenols and sugars are present in the presence of a long stretching vibration of the absorption peak at 3396 and 3458 cm^{-1} for cold and hot extracts respectively. As well as two bending vibration bands at 1384 cm^{-1} for the cold extract and 1388 cm^{-1} for the cold extract belong to the hydroxyl groups ($-\text{OH}$); and the absorption band at 1417 cm^{-1} belongs to the group (C-O).

There are two bands at 1749 , 1726 cm^{-1} for cold and hot extracts respectively, although weak. The cause of weakness is probably the multiplicity in these groups and the possibility of a succession that changes this group into a single carbon-oxygen bond. These bands go back to Carbonyl group (C=O) and this is evidence that the extracts contain flavonoids, mersatin and camphorol.

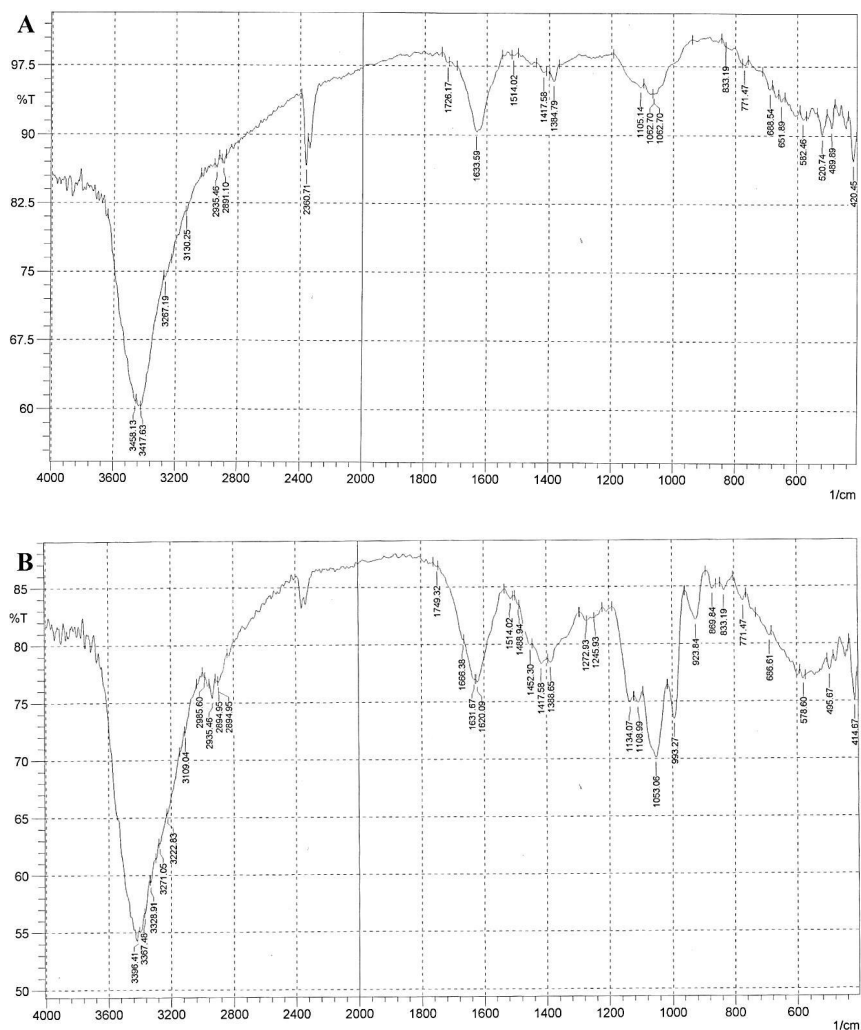


Figure 5. FT-IR of the cold extract (A) and the hot extract (B)

As for the FT-IR spectroscopy of silver nanoparticles of the hot and cold extracts, Figures 6A and 6B. The absorption bands at 1132 cm^{-1} and 1120 cm^{-1} , the two bands at 1382 cm^{-1} and 1388 cm^{-1} , the two bands at 1421 cm^{-1} and 1419 cm^{-1} , and the two bands at 1622 cm^{-1} and 1623 cm^{-1} for the AgNPs of cold and hot extracts respectively are clear evidence of the presence of silver nanoparticles in the synthesis of the samples. These two spectra are very similar to the infrared spectrum of cold and hot extracts (figure 5) and therefore the composition is not but the insulation, clarity and beam width are better in the infrared spectrum of the nanostructures.

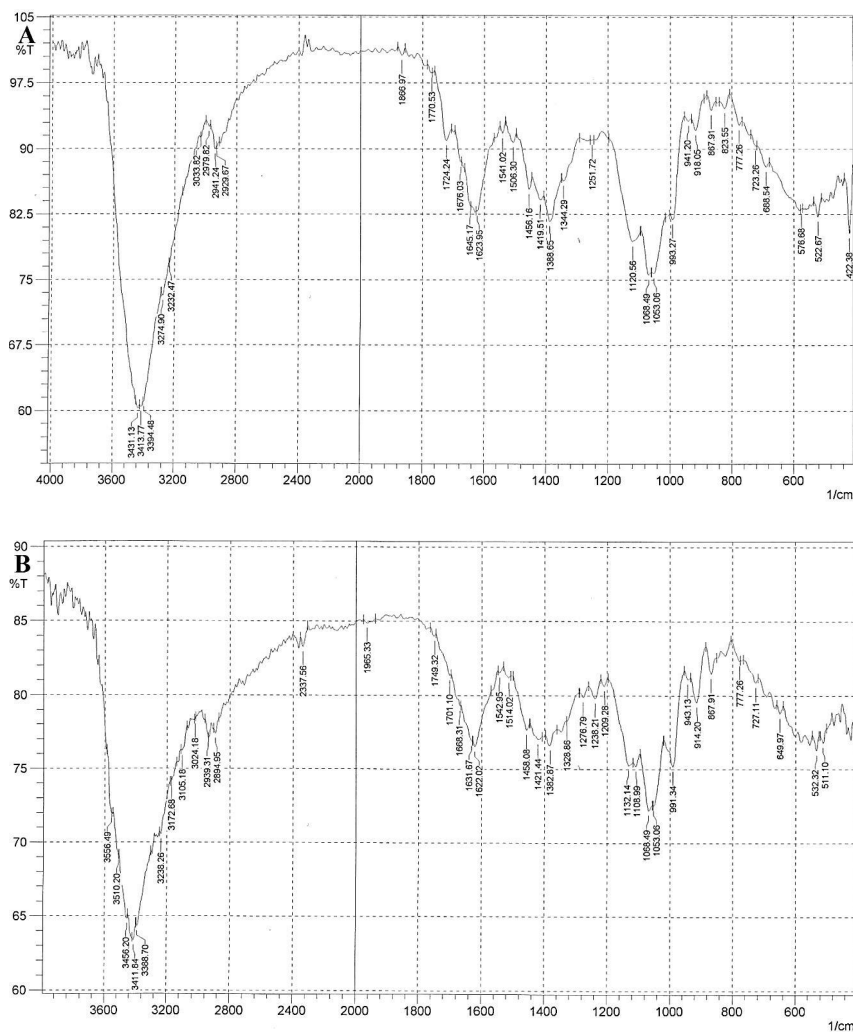
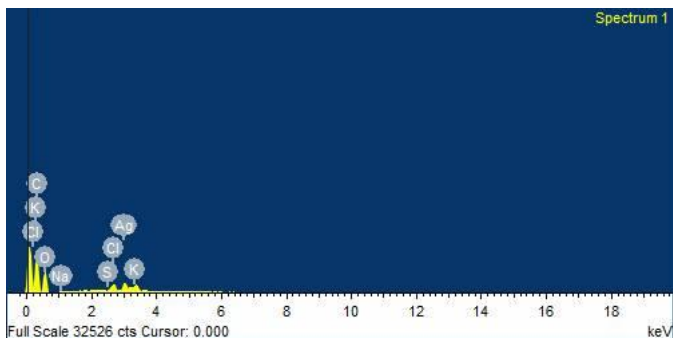
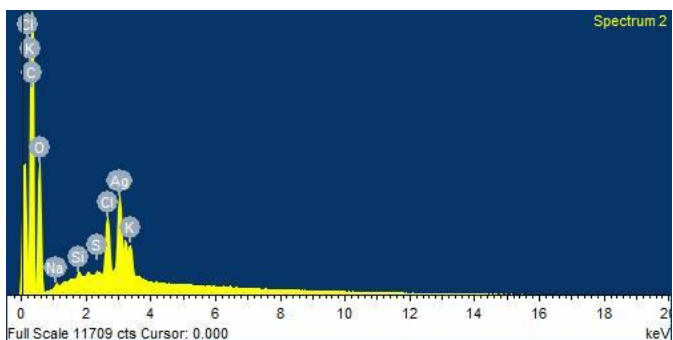


Figure 6. FT-IR of silver nanoparticles of the cold extract (A) and AgNPs of the hot extract (B)

The EDX spectrum of the biosynthesized AgNPs (figure 7) shows finding silver element as an indicator for the formation of silver nanoparticles from the hot extract better than the cold extract. Also, it exhibits the C, O, Cl, Si, and K elements have been presented in the used sample.



A



B

Figure 7. EDX images of the colloid AgNPs formed from the hot extract (A) and the cold one (B)

Both the cold extract-AgNPs and the hot-AgNPs were investigated against cell line of murine fibroblast cells have receptors for human polioviruses (L20B) *in vitro*. Figure 8 exhibited the anticancer activity of the colloid AgNPs synthesized from aqueous extracts of the peeled Galingale rhizomes. The hot-AgNPs gave better growth inhibition than the cold extract-AgNPs. The best inhibition showed by the concentration 100% of the hot-AgNPs 35.3% significantly ($p < 0.01$) followed by 22.5% by the concentration of 75% of the hot-AgNPs. The concentration 100% of the cold-AgNPs exhibited 22.4% then decreased to 17.9% by the concentration of 75% of the cold-AgNPs. The concentration 50% did not show any inhibitory effects as in the crude extracts of *Cyperus* rhizomes.

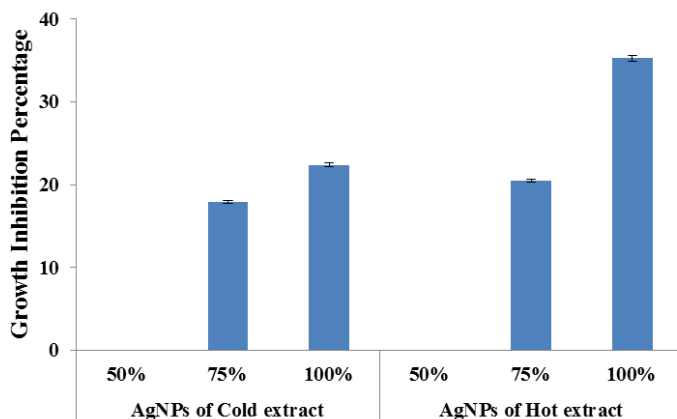


Figure 8. Anticancer activity of the colloid AgNPs synthesized from aqueous extracts of the peeled Galingale rhizomes

The change in color for the mixture of AgNO_3 and the *Cyperus* rhizomes extract from milky (hot extraction) bright yellow (cold extraction) to the brown color is a sign for the formation silver nanoparticles ⁶ as seen in figure 1. The density of brown color is due to excitation of surface plasmon vibrations in the silver nanoparticles ²⁵, and that is confirmed using UV-Visible spectra. Hot extract-AgNPs are showing the widest adsorption (2068 cm^{-1}) than cold extract-AgNPs (1800 cm^{-1}), because of the resonance wavelength of silver nanoparticles has strong depending on Ag atoms, size and morphology of particles ²⁶.

SEM, AFM and Histogram of particle size distribution (SPM) were used to confirm the nature, topography, morphology of the silver nanoparticles. SEM images (figure 2) exhibited the morphology of AgNPs which ranged from spherical to irregular particles. The shape of silver nanoparticles agreed with many recent studies ²⁷. The 3D and 2D images of AFM showed the topography of the nanoparticles surfaces (figure 3). Atomic Force Microscope is a useful tool to study different morphological parameters. AFM images as in figure 3 show high-resolution topography and the silver nanoparticles can be visualized under the dry condition ²⁸.

However, AFM has the advantageousness of probing the surface topography deeply due to its lateral and trial dimensions in nanometer scale resolution ²⁹. The AFM image displays the surface morphology of silver nanoparticles synthesized by *Cyperus* rhizome extracts which reveal the appearance of spherical or irregular and needle-like nanoparticles for the cold extract-AgNPs and

the hot extract-AgNPs respectively. Also, roughness average, the surface area ratio and the density of summits are evidence to form the smallest nanoparticles for AgNPs formed from the hot extract of *Cyperus* rhizome and more summits by high surface area ratio.

Histogram of particle size distribution (SPM) showed the granularity distribution, volumes and averages of diameters of AgNPs (figure 3). This parameter is affirming the results of AFM images which appears smallness size of the hot extract-AgNPs comparing to the cold ones. The average diameter of the cold extract-AgNPs is 92.53 nm in comparison with the hot extract-AgNPs is 56.31 nm. The reason for this phenomenon is related to the extraction technique which means the heating process during preparation of the herbal extracts leads to destroying active ingredients³⁰. Then the interaction of the finer biomolecules with silver ions leads to synthesize finer nanoparticles. Histogram of the particle size distribution of the two AgNPs was presented in Figure 4 was clear evidence for the formation of silver particles by the percentages of Ag particles in the two treatments. All sizes of the biosynthesized AgNPs in the colloids are lesser than 100 nm which is considered a definite proof for the formation of AgNPs³¹.

Fourier Transform Infrared spectrum (FT-IR) was used to determine the chemical structure and the functional groups. In cold and hot extracts, the similarities were observed in the peak sites. The FT-IR spectrum the cold extract (figure 5A) and the hot extract (figure 5B) confirms the presence of compensated aromatic rings all of which go back to the amino acids, peptides and proteins³², amintoflavone and flavonoids³³ see figure 9, poly hydroxyl compounds such as myristin, albicaine, camphorol³⁴ see figure 10, alkene compounds such as lemons, cocaine and mirentol³⁵ see figure 11.

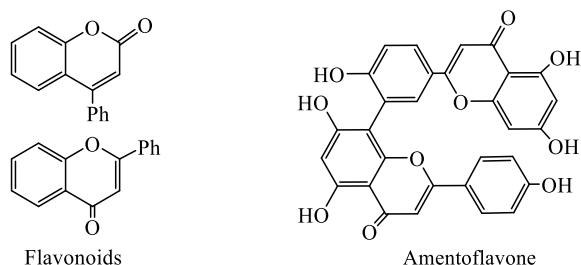


Figure 9. Structures of amintoflavone and flavonoids compounds in *Cyperus* sp. rhizomes

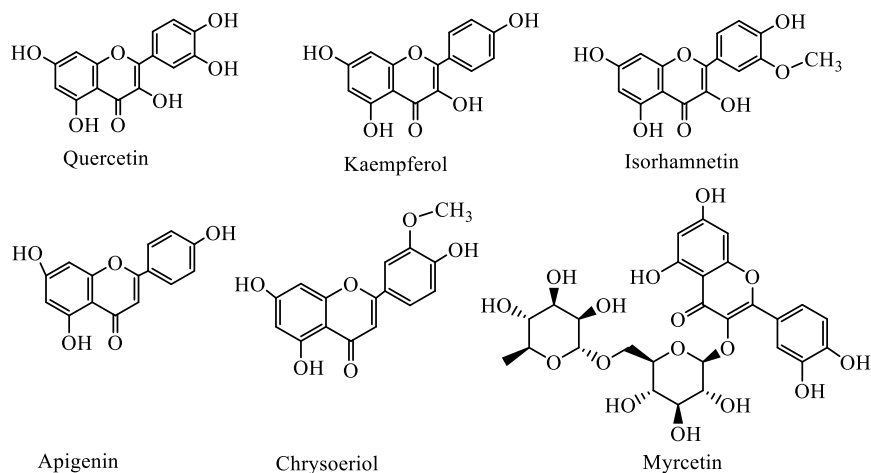


Figure 10. Structures of poly hydroxyl compounds in *Cyperus* sp. rhizomes

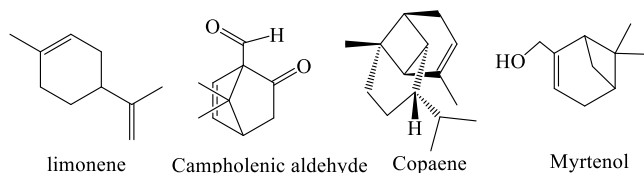


Figure 11. Structures of alkene compounds in *Cyperus* sp. rhizomes

The absorption bands at 2891 cm^{-1} and 2894 cm^{-1} for cold and hot extracts respectively, and at 2935 cm^{-1} for cold and hot extracts also belong to vibrations of homogeneous and heterogeneous stretching of a methylene group ($-\text{CH}_2$) or a methyl group ($-\text{CH}_3$)³⁶. This research includes synthesis of new heterocyclic derivatives of disubstituted 1,3-oxazepine-5-one. Azomethine compounds (N1-N5). The spectra showed absorption bands at 1631 cm^{-1} and 1633 cm^{-1} for cold and hot extracts respectively go back to vibrations of stretching of $\text{C}=\text{C}$ group belongs to the alkene compounds and the successive double bonds in the benzene ring in the aromatic structures³⁷. As well as two bending vibration bands at 1384 cm^{-1} for the cold extract and 1388 cm^{-1} for the cold extract belong to the hydroxyl groups ($-\text{OH}$); and the absorption band at 1417 cm^{-1} due to the stretching vibration of the group ($\text{C}-\text{O}$)³⁸. The absorption bands $582\text{--}578\text{ cm}^{-1}$ and $688\text{--}686\text{ cm}^{-1}$ for the cold and hot extracts respectively indicate to the amide group ($\text{O}=\text{C}-\text{N}-\text{H}$), which binds two consecutive amino acids in the synthesis of peptides or proteins. The bands at $3267\text{--}3271\text{ cm}^{-1}$ and $3417\text{--}3367\text{ cm}^{-1}$ indicate for the presence of the amine group ($-\text{NH}_2$) in the synthesis of amino acids, peptides and proteins for cold and hot extracts respectively^{32,39}. The presence of the carboxylic group in

amino acids, peptides and proteins are the appearance of the wide absorption range (2400-3600 cm^{-1}) for both extracts and maybe the presence of a carboxylic group (-COOH) in mono acidic saccharides compounds such as glucuronic acid ⁴⁰⁻⁴³3-oxazepin-5(1H see figure 12.

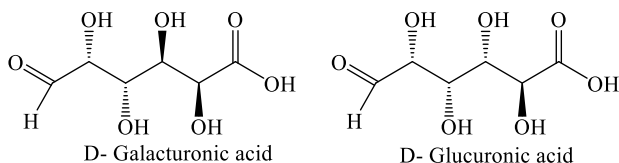


Figure 12. Structures of mono acidic saccharides compounds in *Cyperus sp.* rhizomes

The FT-IR spectra of silver nanoparticles of the hot and cold extracts (Figures 6A and 6B) showed clear evidence of the presence of silver nanoparticles in the synthesis of the samples because in a study on mushroom found that the silver nanostructure binds with the hydrocarbon's compounds. It shows four packages located nearby and within the ranges listed ⁴⁴. These two spectra are very similar to the infrared spectrum of cold and hot extracts and therefore the composition is not, but the insulation, clarity and beam width are better in the infrared spectrum of the nanostructures. The spectrum of silver nanoparticles (Figure 6B) was observed to be similar to Figure 5B regarding the sites of the functional groups, but the appearance of the bands was more apparent and better. That may be due to the presence of silver atoms with a high surface area that allows all the atoms with negative electrical and containing pairs of electrons not involved as in the mushroom extract to participate in the silver nanoparticles sample containing the atoms of silver spread well. It is known that the silver atoms contain 47 electrons, so contain in its fifth shell one electron in the second level 5s. Thus, the other secondary levels are 5p containing three orbitals, 5d containing five orbitals and 4f containing seven empty orbitals and can accommodate electronic pairs coming from atoms with good negative electrical. The oxygen atom found in the formation of mono crystalline polysaccharides in the form of (-OH) in acid sugars or in the form of (C=O) or in the form of carbonyl (C=O) in male compounds previously, the link is as follows (Ag-OR) where R is mono crystalline or polyunsaturated sugar or amino acid or Peptide, protein, phenols or flavonoids. Another example of good electrolyte atom is the atom of nitrogen in the form of (=NH) in arginine or the form of (-NH₂) or (-NH-C=O) in peptides and proteins. The association is as follows (Ag-NR) (R) is an amino acid, peptide or protein,

and the other electrolytic atom is the sulfur atom found in the synthesis of amino acids, peptides and proteins in the form of (-S-) and in the form of (-SH) (Ag-SR) where R is an amino acid or peptide or protein. FT-IR exhibited that the presence of carbonyl (C=O) and hydroxyl groups (-OH) in the extract of *Cyperus* sp. can reduce and stabilize silver nanoparticles¹³.

Carbon and oxygen are presented in the EDX graph (Figure 7) due to the organic molecules which found in the extract of the mushroom. These biomolecules may be amino acids or proteins or polysaccharides or polyphenols which capped the silver nanoparticles as capping and stabilizing agents. The presence of the elemental Ag can be seen in the EDX graph (figure 7) that indicates the reduction of Ag ions to elemental silver⁴⁵. Further, Chlorine is also observed due to the unreacted precursors of AgNO₃⁴⁶.

The silver nanoparticles formed from these rhizomes are exhibiting unique physicochemical and biological activities¹³ thus they have the inhibitory role. The reason of the high inhibitory effects of the hot extract-AgNPs returns to smallness the average of size of these AgNPs (56.31 nm in diameter) in comparison to the average of size of the cold extract-AgNPs (92.53 nm) as in Figure 4 that lead to increase the surface area ratio of the hot extract-AgNPs as AFM in Figure 3.

This study proved the rhizome-mediated synthesis of AgNPs using the cold and hot watery rhizomes extracts of *Cyperus* sp. FT-IR exhibited that the presence of carbonyl and hydroxyl groups in the extract of *Cyperus* sp. can reduce and stabilize silver nanoparticles. EDX, SEM, and AFM analyses were confirmed that the biosynthesized silver nanoparticles were spherical or irregular in shape with the average diameter of the hot extract-AgNPs is 56.31 nm in comparison with the cold extract-AgNPs is 92.53 nm. EDX images indicate to form silver nanoparticles from the hot extract better than the cold one. The synthesized silver nanoparticles were tested against cancer cell line L20B. The hot extract-AgNPs plays a suitable role against mouse cell line (L20B) which have receptors for polioviruses better than the cold extract-AgNPs. The best inhibition showed by the concentration 100% of the hot-AgNPs 35.3% significantly ($p < 0.01$).

ACKNOWLEDGEMENTS

The author and co-author are thanking the staff of Department of Ecology, College of Applied Sciences-Hit in University of Anbar to complete project No. 3/122 on 15 Oct 2017. Special thanks to President of the University Prof. Dr. Khalid Battal Najim and Dean of the College, Prof. Dr. Tahseen Ali Zaidan for their continuous support in publishing the research in the certified international journal. Another thank is introducing to the University of Baghdad for achieving the AFM nanophotographic.

REFERENCES

1. Rao, C. N. R.; Kulkarni G. U.; Thomas, P. J.; Edwards, P. P. Metal Nanoparticles and Their Assemblies. *Chem. Soc. Rev.* **2000**, *29*, 27–35.
2. Karthiga P.; Soranam, R.; Annadurai, G. Alpha-Mangostin, the Major Compound from *Garcinia mangostana* Linn. Responsible for Synthesis of Ag Nanoparticles: Its Characterization and Evaluation Studies. *Nanosci. Nanotechnol.* **2012**, *2*, 46–57.
3. Elechiguerra, J. L.; Burt, J. L.; Morones, J. R.; Camacho-Bragado, A.; Gao, X.; Lara, H. H.; Yacaman, M. J. Interaction of Silver Nanoparticles with HIV-1. *J. Nanobiotechnology* **2005**, *3*, 6.
4. Lakshmanan, G.; Sathiyaseelan, A.; Kalaichelvan, P. T.; Murugesan, K. Plant-Mediated Synthesis of Silver Nanoparticles Using Fruit Extract of *Cleome viscosa* L.: Assessment of Their Antibacterial and Anticancer Activity. *Karbala Int. J. Mod. Sci.* **2018**, *4*, 61–68.
5. Owaid, M. N.; Muslim, R. F.; Hamad, H. A. Mycosynthesis of Silver Nanoparticles Using *Terminia* sp. Desert Truffle, Pezizaceae, and Their Antibacterial Activity. *Jordan J. Biol. Sci.* **2018**, *11*, 401–405.
6. Owaid, M. N.; Raman, J.; Lakshmanan, H.; Al-Saedi, S. S. S.; Sabaratnam V.; Ali, I. A. Mycosynthesis of Silver Nanoparticles by *Pleurotus cornucopiae* var. *citrinopileatus* and Its Inhibitory Effects against *Candida* sp. *Mater Lett* **2015**, *153*, 186–190.
7. Al-Hilli, Z. A.; Al-Jumaily, E. F.; Yaseen, N. Y. Role of Volatile Oils Fraction of *Cyperus rotundus* L. in Induction of Apoptosis on Cancer. *Iraqi J. Biotech.* **2010**, *9*, 286–298.
8. Castro-Aceituno, V.; Ahn, S.; Simu, S. Y.; Singh, P.; Mathiyalagan, R.; Lee, H. A.; Yang, D. C. Anticancer Activity of Silver Nanoparticles from *Panax ginseng* Fresh Leaves in Human Cancer Cells. *Biomed Pharmacother.* **2016**, *84*, 158–165.
9. Kalangi, S. K.; Dayakar, A.; Gangappa, D.; Sathyavathi, R.; Maurya, R. S.; Rao, D. N. Bio-compatible Silver Nanoparticles Reduced from *Anethum graveolens* Leaf Extract Augments the Antileishmanial Efficacy of Miltefosine. *Exp Parasitol.* **2016**, *170*, 184–192.
10. Ahmed, S.; Saifullah; Ahmad, M.; Swami, B. L.; Ikram, S. Green Synthesis of Silver Nanoparticles Using *Azadirachta indica* Aqueous Leaf Extract. *J. Radiat. Res. Appl. Sci.* **2016**, *9*, 1–7.
11. Sangeetha, R.; Niranjana P.; Dhanalakshmi, N. Characterization of Silver Nanoparticles Synthesized Using the Extract of the Leaves of *Tridax procumbens*. *Res. J. Med. Plant* **2016**, *10*, 159–166.
12. Khan, F. A.; Zahoor, M.; Jalal, A.; Rahman, A. U. Green Synthesis of Silver Nanoparticles by Using *Ziziphus nummularia* Leaves Aqueous Extract and Their Biological Activities. *J. Nanomater.* **2016**, *2016*, 8.
13. Oluwaniyi, O. O.; Adegoke, H. I.; Adesuji, E. T.; Alabi, A. B.; Bodede, S. O.; Labulo, A. H.; Oseghale, C. O. Biosynthesis of Silver Nanoparticles Using Aqueous Leaf Extract of *Thevetia peruviana* Juss and its Antimicrobial Activities. *Appl. Nanosci.* **2016**, *6*, 903–912.
14. Nasir, G. A.; Mohammed, A. K.; Samir, H. F. Biosynthesis and Characterization of Silver Nanoparticles Using Olive Leaves Extract and Sorbitol. *Iraqi J. Biotechnol.* **2016**, *15*, 22–32.
15. Jasim, B.; Thomas, R.; Mathew J.; Radhakrishnan, E. K. Plant Growth and Diosgenin Enhancement Effect of Silver Nanoparticles in Fenugreek (*Trigonella foenum-graecum* L.). *Saudi Pharm. J.* **2017**, *25*, 443–447.

16. Kassab, N. H. Antifungal Effect of Some Agents on *Candida albicans* Growth on Acrylic Resin Denture Base Surface (*in vitro* Study), University of Mosul, **2002**.
17. Chakravarty, H. L. *Plant Growth of Iraq (Adictionary of Economic Plants)*; Botany Directorate, Ministry of Agriculture and Agrarian Reform: Baghdad, **1976**.
18. Abdul-Rahman, G. Y.; Rasoul, A. H. Evaluation of the Antibacterial Activity of *Cyperus rotundus* Extract (an *in vitro* Study). *J. Edu. Sci.* **2006**, *18*, 59–63.
19. Najah, A. M. *In Vitro* Inhibitory Effect of *Cyperus rotundus* L. Crude Extracts on Mouth Isolates *Streptococcus mutans* and *Candida albicans*. *AJPS* **2012**, *11*, 85–91.
20. Ali, M. R.; Hussin, M. S.; Kadum, M. M.; Kadum, Y. A.; Hamza, E. H. *In-Vitro* Antimicrobial Activities of *Myrtus communis* L. and *Cyperus rotundus* L. Extracts. *Al-Mustansiriya J Sci* **2009**, *20*, 1–13.
21. Özdemir, Z.; Erincik, Ö. Antimicrobial Activities of Extracts of *Cyperus rotundus* L. Rhizomes against Some Bacterial and Fungal Pathogens of Strawberry and Tomato. *Arch Phyto-pathol Plant Prot* **2015**, *48*, 850–861.
22. Mustafa, F. A. J. The Aqueous and Alcoholic Extracts of *Cyperus longous* (Cyperaceae) and Two Drugs (Tinidazole and Praziquantel) on Killing the Protoscolices of *Echinococcus granulosus* *in vitro*. *Bas J Vet Res* **2009**, *8*, 148–160.
23. Chih, P. L.; Wei, J. T.; Yuang, L. L.; Yuh, C. K. The Extracts from *Nelumbonucifera* Suppress Cell Cycle Progression, Cytokine Genes Expression, and Cell Proliferation in Human Peripheral Blood Mononuclear Cells. *Life Sci* **2004**, *75*, 699–716.
24. Freshney, R. I. *Culture of Animal Cell*, 6th ed.; Wiley-Liss: New York, **2012**.
25. Shankar, S. S.; Ahmad, A.; Sastry, M. Geranium Leaf Assisted Biosynthesis of Silver Nanoparticles. *Biotechnol. Prog.* **2003**, *19*, 1627–1631.
26. Xia, Y.; Halas, N. Shape-Controlled Synthesis and Surface Plasmonic Properties of Metallic Nanostructures. *MRS Bull* **2005**, *30*, 338–344.
27. Owaid, M. N.; Ibraheem, I. J. Mycosynthesis of Nanoparticles Using Edible and Medicinal Mushrooms. *Eur J Nanomedicine* **2017**, *9*, 5–23.
28. Rani, P. U.; Rajasekharreddy, P. Plants : The Green Factories for Synthesis of Nanomaterials. In *Nanotechnology Vol. 6: Energy and Environment*; Govil, J. N., Ed.; Studium Press LLC, USA, **2013**; pp 51–78.
29. Farhadi, S.; Ajerloo, B.; Mohammadi, A. Green Biosynthesis of Spherical Silver Nanoparticles by Using Date Palm (*Phoenix dactylifera*) Fruit Extract and Study of Their Antibacterial and Catalytic Activities. *Acta Chim Slov* **2017**, *64*, 129–143.
30. Sasidharan, S.; Chen, Y.; Saravanan, D.; Sundram, K. M.; Yoga Latha, L. Extraction, Isolation and Characterization of Bioactive Compounds from Plants' Extracts. *African J Tradit Complement Altern Med* **2011**, *8*, 1–10.
31. Vo-Dinh, T. Protein Nanotechnology, Protocols, Instrumentation, and Applications. In *Methods in Molecular Biology*; Humana Press Inc.: Totowa, NJ, **2005**; pp 1–7.
32. Mistry, B. D. *A Handbook of Spectroscopic Data CHEMISTRY (UV, JR, PMR, JJCNMNMR and Mass Spectroscopy)*, 2009th ed.; Oxford Book Company, **2009**.
33. Ju, Y.; Xiao, B. Chemical Constituents of *Cyperus rotundus* L. and Their Inhibitory Ef-

fects on Uterine Fibroids. *Afr Health Sci* **2016**, *16*, 1000–1006.

34. Al-Daody, A. C.; Al-Hyaly, A. M.; Al-Soultany, A. A. Chromatographic Identification of Some FlavonoidS Compounds From “*Cyperus rotundas*” Growing in Iraq. *Tikrit J Pure Sci* **2010**, *15*, 218–222.

35. Richa, T.; Suneet, K. Chemical Constituents of the Essential Oil of *Cyperus rotundus* Linn. *Int J Drug Dev Res* **2014**, *6*, 57–60.

36. Muslim, R. F.; Tawfeeq, H. M.; Owaid, M. N.; Abid, O. H. Synthesis, Characterization and Evaluation of Antifungal Activity of Seven-Membered Heterocycles. *Acta Pharm Sci* **2018**, *56*, 39–57.

37. Abid, O. H.; Muslim, R. F.; Mohammed, K. M. Synthesis and Characterization of Novel 1,3-Oxazepin-4-Ones Derivatives via Schiff Bases Reactions with Phthalide. *J Univ Anbar Pure Sci* **2016**, *10*, 1–9.

38. Abid, O. H.; Muslim, R. F.; Mohammed, K. M. Synthesis and Characterization of Novel 1,3,4,9a-Tetrahydrobenzo[e][1,3]Oxazepin- 5(5aH)-One Derivatives via Cycloaddition Reactions of Schiff Bases. *J Univ Al-Anbar Pure Sci* **2016**, *10*, 8–18.

39. Silverstein, R.; Webster, F.; Kiemle, D. *Spectrometric Identification of Organic Compounds*, 7th ed.; John Wiley and sons, Inc.: London, UK, **2005**.

40. Nakamoto, K. *Infrared and Raman Spectra of Inorganic and Coordination Compounds Part A: Theory and Applications in Inorganic Chemistry*, 6th ed.; A John Wiley and Sons, Inc., **2009**.

41. Field, L. D.; Sternhell, S. Kalman, J. R. *Organic Structures from Spectra*, 4th ed.; John Wiley and Sons Ltd, **2008**.

42. Abid, O. H.; Tawfeeq, H. M.; Muslim, R. F. Synthesis and Characterization of Novel 1,3-Oxazepin-5(1H)-One Derivatives via Reaction of Imine Compounds with Isobenzofuran-1(3H)-One. *Acta Pharm Sci* **2017**, *55*, 43–55.

43. Simek, J. *Organic Chemistry*, 8th ed.; Pearson education, Inc., **2013**.

44. Sujatha, S.; Tamilselvi, S.; Subha, K.; Panneerselvam, A. Studies on Biosynthesis of Silver Nanoparticles Using Mushroom and Its Antibacterial Activities. *Int J Curr Microbiol App Sci* **2013**, *2*, 605–614.

45. Al-Bahrani, R.M.; Abdel Majeed, S.M.; Owaid M.N.; Mohammed, A.B.; Rheem, D.A. Phyto-fabrication, characteristics and anti-candidal effects of silver nanoparticles from leaves of *Ziziphus mauritiana* Lam. *Acta Pharm Sci* **2018**, *56*, 85–92.

46. Kathiravan, V.; Ravi, S.; Ashokkumar, S. Synthesis of Silver Nanoparticles from *Melia dubia* Leaf Extract and Their *in vitro* Anticancer Activity. *Spectrochim Acta Part A Mol Biomol Spectrosc* **2014**, *130*, 116–121.

Anti-inflammatory and Analgesic Potential of Acetone Leaf Extract of *Combretum Sordidum* and its Fractions

Babatunde B. Samuel^{1*}, Olayinka A. Oridupa², Fisayo Gbadegesin¹

¹ Department of Pharmaceutical Chemistry, Faculty of Pharmacy, University of Ibadan.

² Department of Veterinary Pharmacology and Toxicology, Faculty of Veterinary Medicine, University of Ibadan.

ABSTRACT

Combretum species are traditionally used in treatment of arthritis, fungal and bacterial infections. This study investigated anti-inflammatory activity of *C. sordidum* acetone extract in egg albumen-induced paw oedema and formalin paw lick test in rats, while analgesic activity was determined by acetic acid-induced abdominal writhing test in mouse. Bioactivity guided analgesic effect were also carried out on solvent-solvent partitioned and chromatographic fractions. Rats administered with extract progressively showed significant reduction in oedema formation 60 minutes post-induction. Dose-dependent inhibition of formalin-induced paw lick was observed at early and late phases of the experiment compared to indometacin. Abdominal writhing was significantly inhibited with 400mg/kg extract effect (73.1%) comparable to aspirin (75.9%). Most active chromatographic fraction identified as F7 (79.5%) showed significant analgesic activity, higher than aspirin (55.0%). Results established anti-inflammatory and analgesic of *C. sordidum*. Further studies are on-going to identify and characterize the bioactive principle responsible for these pharmacological effects.

Keywords: *Combretum sordidum*, Anti-inflammatory, Analgesic, Bioactivity-guided separation

INTRODUCTION

In recent years, the search for phytochemicals with antioxidant, anti-inflammatory and analgesic properties have been on the rise due to their potential use in the therapy of various chronic and infectious diseases.^{1,2} Many diseases originate from uncontrolled or unregulated inflammatory process in the body.³ Inf-

*Corresponding Author: Babatunde B. Samuel, e-mail: tundebsamuel@gmail.com

Babatunde B. Samuel ORCID Number: 0000-0002-1834-9548

Olayinka A. Oridupa ORCID Number: 0000-0002-6435-6925

Fisayo Gbadegesin ORCID Number: 0000-0003-1322-679X

(Received 10 September 2018, accepted 15 January 2019)

lammation is a localized protective reaction of cells/tissues of the body to allergic or chemical irritation, injury and/or infections.⁴ Inflammation is characterized by pain, heat, redness, swelling and loss of function resulting from vasodilation and leading to an increased blood supply with increased influx of leukocytes, protein and fluids into intercellular spaces of the inflamed regions.⁵ Inflammatory responses occur as the body recognizes injury and prepare to repair the damage, but uncontrolled inflammation leads to development and progression of diseases and disorders which are manifested as exacerbated symptoms of inflammation.^{6,7,8}

Since antiquity, medicinal plants such as plants in genus *Combretum* have been employed for treatment of inflammation, pain and related diseases. One of plants in the genus, *Combretum sordidum* Exell (Combretaceae) is so employed as traditional remedy of infectious and non-infectious ailments.⁹ *C. sordidum* a scandent shrub or a creeper with white flowers and easily recognized by the small red scales on the under-surface of the leaves.¹⁰ They are widely distributed throughout South and West Africa.¹¹ This plant and other members of the genus from different regions of Africa are traditionally used by local healers for treatment of diseases of inflammatory origin including conjunctivitis, abdominal disorders, backache, toothache, diabetes.^{12,13} It has been scientifically proven to have antiasthmatic, antimicrobial and antiplasmodic effects.¹⁴ Another member of the genus, *C. molle* R.Brex was reported to have cardiocascular effect¹⁵, anti-inflammatory and inhibitory effect on haematopoietic prostaglandin D2 synthase; while *Combretum woodii* have shown significant anti-infective activities.^{16,17,18}

Despite the use of *C. sordidum* in traditional medicine, there is a dearth of knowledge on the medicinal and ethnopharmacological uses of *C. sordidum* in literature. This current study investigated the anti-inflammatory and analgesic potential of the acetone extract of *Combretum sordidum*. Its constituent fractions which were separated by solvent-solvent partitioning using n-hexane, ethyl acetate and methanol were also assessed for their analgesic effect and bioassay guided purification of the most potent fraction was carried out to isolate the bioactive compound responsible for its analgesic effect.

METHODOLOGY

Preparation of plant extract

Fresh leaves of *Combretum sordidum* were collected from Federal Research Institute of Nigeria (FRIN), Ibadan, Oyo state (Voucher No: 109923). The leaves were air dried and then pulverized. Acetone extract of the pulverized plant material was obtained by extracting 1kg of the plant using a soxhlet extractor (hot extraction), after which it was concentrated using Buchi® rotary evaporator at 40°C.

Experimental Animal Model

Wistar rats weighing 120-160g and mice weighing 15-20g were obtained and housed at the Experimental Animal Unit of Department of Veterinary Pharmacology and Toxicology, University of Ibadan. The rats were fed with standard pellets and allowed access to water *ad libitum*. The animals were divided into groups of five rats each and were fasted overnight before commencement of each experiment.

Anti-inflammatory Activity of the crude extract

Egg albumen –induced Paw oedema in Rats

In this model, following an overnight fasting, three doses *C. sordidum* leaf extracts (100mg/kg, 200mg/kg and 400mg/kg) were orally administered to rats in three different treatment groups, and simultaneously, indomethacin (10mg/kg) was administered to animals in the reference group. Control animals received distilled water (10ml/kg) only.

An hour after the treatment, egg albumen (0.2ml) was injected into the right paw of each rat under the sub plantar region. The paw sizes were measured before and at interval of 30mins, 60mins and 90mins after egg albumen injection by using the cotton thread method. The cotton thread was wrapped around the paw and the circumference was measured with a meter rule. Oedema formation was determined as indicator of inflammatory response in the injected paw.

The inhibition of oedema formation was calculated according to the formula;

$$\% \text{ inhibition} = [(C_1 - C_0)_{\text{control}} - (C_1 - C_0)_{\text{test}}] / (C_1 - C_0)_{\text{control}} \times 100$$

Where C_0 = Paw size at time zero minute

C_1 = Paw size at time t minutes.

Formalin Paw lick Test in Rats

Following an overnight fast, the rats were also grouped and treated with the extracts were as in the experiment above. Thirty minutes after treatment, 25 μ l of 2.5% formalin was injected into the sub-planar surface of the rat paw. Responses were measured between 0 to 5 minutes after injection of formalin for the first phase response; while the second phase response was observed between 15 to 30 minutes after the injection. The licking of the paw by the rat is indicative of pain and the duration was counted in seconds as the response to inflammatory pain.

Analgesic Activity of the crude extract

Acetic acid- induced abdominal writhing test was used to determine the analgesic property of the crude extract in mice. Five groups of mice were pre-treatment with saline, extract (100, 200, 400 mg/kg), aspirin at 15mg/kg and injected intraperitoneally with 0.01ml of 0.6% acetic acid solution 60 minutes post-treatment. Five minutes post- injection of acetic acid, the number of writhing was observed and counted for the next twenty minutes and recorded. The inhibition of acetic acid- induced abdominal contractions is indicative of analgesic effect.

% inhibition = (Mean No. of writhing) control – (Mean No. of writhing) test / Mean No of writhing) control X 100

Solvent-solvent partitioning of the crude extract

To carry out the solvent–solvent partitioning of the extract, 17g of the crude extract was dissolved in 250ml of a mixture of solvents (15% of methanol in water) in a Separating funnel. The dissolved extract in the separating funnel was partitioned with equal volume of hexane. After the collection of the hexane fraction; the methanol-water fraction was further fractionated with ethyl acetate to obtain the ethyl acetate fraction. Three major fractions were obtained which are hexane, ethyl acetate and water/methanol fractions. The analgesic activities of the three fractions were conducted at doses of 20mg/kg and 50mg/kg using Acetic acid- induced abdominal writhing test as described above. The result was compared to that of mice treated with aspirin (15mg/kg).

Column Chromatography of Hexane Fraction of *C. sordidum*

Column chromatographic separation of the hexane fraction was carried out on silica gel stationary phase using the following order of mobile phases: hexane 100% followed by hexane: ethyl acetate (97.5:2.5), (95:5), (92.5:7.5), (90:10), (85:15), (80:20), (70:30), (60:40), (50:50), (40:60), (30:70), (20:80), (10:90), ethyl acetate 100% and methanol 100%. A total of 175 fractions (30mL) were collected and combined on the basis of TLC fingerprint. Seven (7) major fractions labeled F1-F7 were obtained. The analgesic activity of the seven fractions was carried out at 10mg/kg and 15mg/kg to identify the compound responsible for the activity. The result was also compared to that obtained for mice administered with aspirin at 15mg/kg.

Statistical Analysis

All values are expressed as mean \pm S.E.M. Data was analyzed by one- way analysis of variance and two- way analysis of variance (ANOVA) followed by

Dunnet and Tukey's multiple comparison tests using Graphpad prism (6) software. Differences of mean were considered at $p < 0.05$.

RESULTS AND DISCUSSION

Anti-inflammatory and Analgesic Activities of the crude extract

The initial change in paw size observed at 0 minute was primarily due to the volume of egg albumen injected into the rat paw. The rats administered with the acetone extract showed a dose-dependent inhibition of the paw oedema induced by the egg albumen. The inflammatory response in paw of rats administered with the extract at doses of 100mg/kg (0.54 ± 0.02 cm and 0.56 ± 0.05 cm), 200mg/kg (0.84 ± 0.12 cm and 0.44 ± 0.11 cm) and 400mg/kg (0.84 ± 0.12 cm and 0.52 ± 0.07 cm) were reduced compared to that of indomethacin (1.04 ± 0.3 cm and 0.86 ± 0.08 cm) at 30 minutes and 60 minutes post-injection, but the extract at 200mg/kg dose inhibited (0.26 ± 0.11 cm) oedema formation more significantly ($p < 0.05$) compared to indomethacin (0.42 ± 0.1 cm) at 90 minutes post-injection (Table 1).

Rats pretreated with the plant extract showed lesser response to pain at both phases of formalin paw lick model in a dose-dependent manner. Inhibition of the response to pain in rats administered with all the extract doses was comparable to that observed for rats administered with indomethacin in the early phase. At the late phase, rats treated with 200mg/kg and 400mg/kg doses showed significantly inhibition of response to pain (62% and 64% respectively) compared to rats administered with indomethacin (37.3%) (Table 2).

A dose-dependent inhibition of abdominal writhes was observed in mice administered with doses of the extract. The inhibition of abdominal writhing observed in mice administered 400mg/kg (11.75 ± 1.19) was comparable to mice administered aspirin (10.5 ± 0.83). Pain expressed as abdominal writhes were significantly ($p < 0.05$) inhibited in all mice administered with the crude extract when compared to the negative control (untreated mice) (Table 3).

Solvent-solvent partitioned fractions and analgesic activity

Three different fractions were obtained from the solvent partitioned crude extract; hexane, ethyl acetate and methanol/water which gave 5.151, 4.793 and 5.468g respectively. The fractions significantly inhibited abdominal writhes compared to the control mice, and the level of inhibition of the writhes was compared with aspirin at 15mg/kg (42.8%). Lower doses of the fractions (20mg/kg) showed better inhibition of abdominal writhes, with mice administered with hexane fraction (20mg/kg) showed the highest percentage inhibiti-

on (44.4%) (Table 4). The analgesic activity of column fractions of the hexane extract at 10mg/kg showed F1- 46.09%, F2- 48.45%, F3- 43.94%, F4- 43.94%, F5- 57.88%, F6- 74.89%, F7- 79.51%, hexane fraction- 63.88%, while aspirin at 15mg/kg had 54.99% (Fig 1).

Table 1. Paw size (cm) and percentage oedema formation in rat paw injected with Egg albumen and pre-treated with *Combretum sordidum* extract

Group	0 minute	30 minutes	60 minutes	90 minutes	120 minutes
Control	0.36±0.05 (0%)	0.62±0.12 (72.2%)	0.68±0.07 (88.9%)	0.82±0.09 (127.8%)	0.88±0.09 (144.4%)
CS 100mg/kg	0.46±0.06 (0%)	0.54±0.02 (17.4%)	0.56±0.05 (21.7%)	0.50±0.07 (8.7%)	0.50±0.07 (8.7%)
CS 200mg/kg	0.38±0.06 (0%)	0.84±0.12 (121.1%)	0.44±0.11 (15.8%)	0.26±0.11 (-31.6%)	0.20±0.10 (-47.4%)
CS 400mg/kg	0.34±0.04 (0%)	0.84±0.12 (147.1%)	0.52±0.07 (52.9%)	0.46±0.08 (35.3%)	0.20±0.09 (-41.2%)
Indomethacin 10mg/kg	0.56±0.1 (0%)	1.04±0.3 (85.7%)	0.86±0.08 (53.6%)	0.42±0.1 (-25%)	0.38±0.08 (-32.1%)

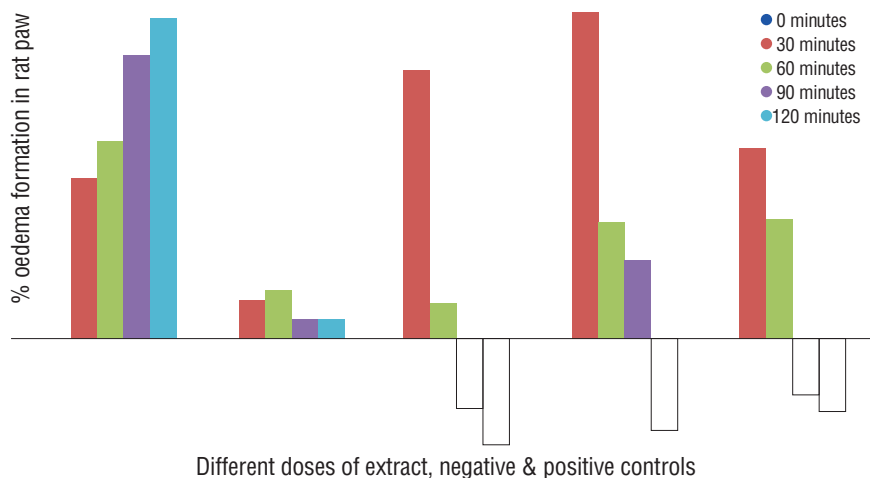


Figure 1: Paw size (cm) and percentage oedema formation in rat paw injected with Egg albumen and pre-treated with *Combretum sordidum* extract

Table 2. Number of paw licks (and percentage inhibition of licks) in rats administered with formalin and pretreated with *Combretum sordidum* extract

Groups	Number of Licks	
	Early Phase (5 minutes)	Late Phase (20-25minutes)
Control	107.5±17.07 (0%)	75.0±5.37 (0%)
CS 100mg/kg	90.3±15.09 (16.1%)	68.25±6.73 (9%)
CS 200mg/kg	91.3±8.08 (17.8%)	28.5±6.38 (62%)
CS 400mg/kg	81.8±3.89 (23.95%)	27.0±9.57 (64%)
Indomethacin 10mg/kg	88.5±1.03 (17.7%)	47.0±7.50 (37.3%)

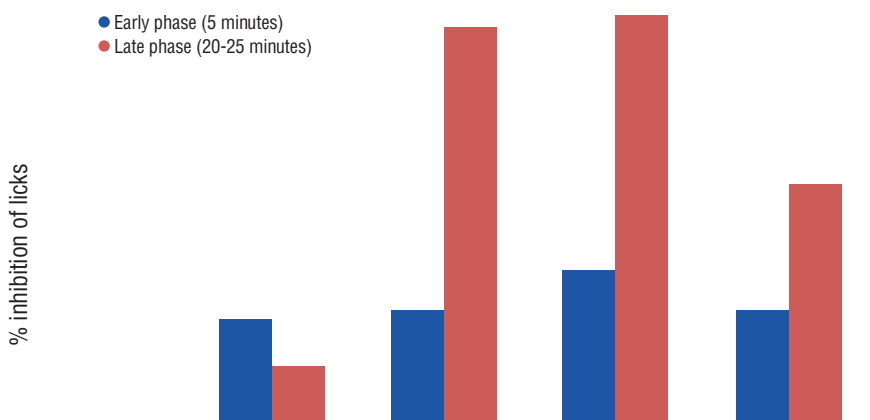


Figure 2. Number of paw licks (and percentage inhibition of licks) in rats administered with formalin and pretreated with *Combretum sordidum* extract

Table 3. Abdominal writhing in mice intraperitoneally injected with acetic acid and pre-treated with *Combretum sordidum*

Group	Number of Writhes	Inhibition (%)
Control	43.6±2.22	0
CS 100mg/kg	37.6±3.41	13.76
CS 200mg/kg	25.3±4.90	42.09
CS 400mg/kg	11.8±1.19	73.05
Indomethacin 10mg/kg	10.5±0.83	75.9

Figure 3. Abdominal writhing in mice intraperitoneally injected with acetic acid and pre-treated with *Combretum sordidum*

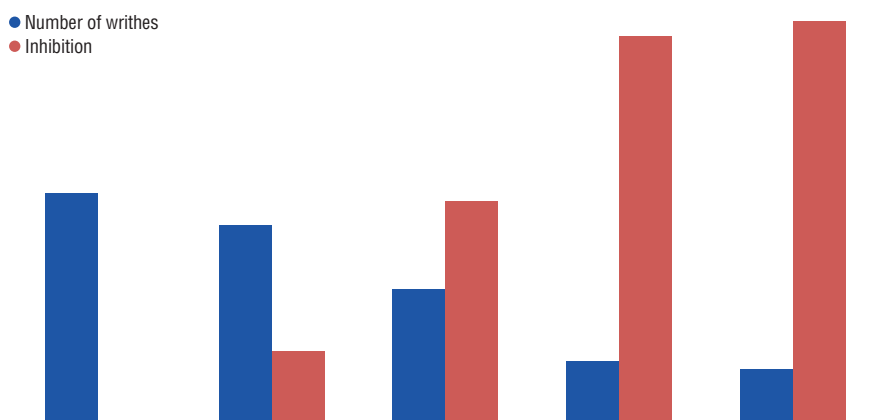


Table 4. Effect of Methanol-water, ethyl acetate, and Hexane fractions on acetic acid- induced abdominal writhing in mice

Group	Number of writhes	Inhibition (%)
Control	62.6 ± 1.25	0
Aspirin 15mg/kg	35.8 ± 4.31	42.8
MeOH 20mg/kg	39.0 ± 3.53	37.7
MeOH 50mg/kg	46.5 ± 2.97	25.7
EA 20mg/kg	35.4 ± 1.67	43.5
EA 50mg/kg	43.0 ± 4.10	31.3
Hex 20mg/kg	34.8 ± 4.14	44.4
Hex 50mg/kg	46.0 ± 3.65	26.5

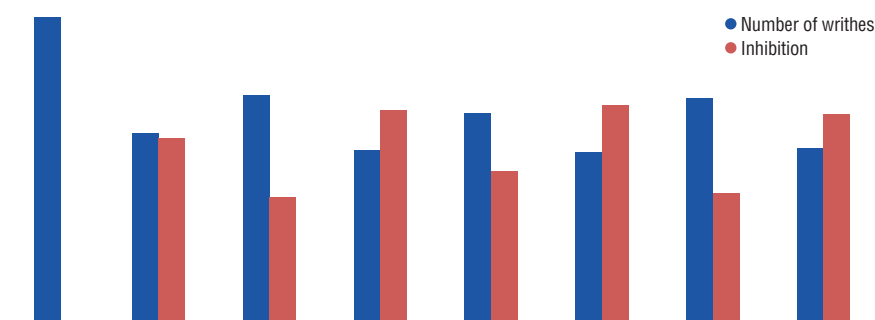


Figure 4. Effect of Methanol-water, ethyl acetate, and Hexane fractions on acetic acid- induced abdominal writhing in mice

In this study, acetone extract of *C. sordidum* demonstrated anti-inflammatory activities by inhibition of paw oedema formation after exposure to egg albumen and paw licking as a response to formalin-induced pain in rats. The anti-inflammatory response was comparable to that of indomethacin, a non-steroidal anti-inflammatory drug used for treatment of arthritis, gout, bursitis.¹⁸ Egg albumen-induced paw oedema is an animal model of inflammation used to detect anti-inflammatory agents with activity in the acute phase of inflammation.¹⁹ This study demonstrated the anti-inflammatory effect of *C. sordidum* was significantly established by 60 minutes post-injection of albumen. This suggests anti-inflammation with activity in acute inflammatory phase. Findings from the formalin-induced paw lick model also corroborated the anti-inflammatory effect of *C. sordidum*. It further established a more marked anti-inflammatory activity in the late phase of inflammation, with significantly more profound anti-inflammatory action compared to the same indomethacin.

Formalin-induced paw lick model of inflammation demonstrates the interrelation of inflammation and nociception with distinct responses in the early

and late phases of inflammation but mediated via different inflammatory pathways.²⁰ The early phase is correlated with direct effect on peripheral nociceptors with minimal influence of prostaglandins. This stimulation in the early phase culminates in centrally mediated pain accompanied by release of substance P.^{21,22} The late phase is characterized by release of mediators of inflammation; histamine, prostaglandins, serotonin and bradykinin.^{23,24} The anti-inflammatory activity of *C. sordidum* is suggested to be mediated via the peripheral and central mechanisms of inflammatory pathways, and may involve inhibition of cyclooxygenase enzymes which are active players in the model. Centrally acting drugs such as opioids inhibit both phases equally but peripherally acting drugs such as cyclooxygenase inhibitors and corticosteroids only inhibit the late phase.²⁵

The acetone extract of *Combretum sordidum* was also found to possess analgesic activities in this study with the significant inhibition of abdominal writhing in the pretreated mice. Acetic acid- induced writhing in mice is a commonly used model of analgesia in experimental animals for establishment of peripherally acting analgesic drugs which may involve stimulation of local peritoneal receptors.^{26,27} The crude extract of *C. sordidum* showed a dose-dependent and significant analgesic action when compared to the reference drugs, indomethacin and aspirin. Acetic acid causes pain by liberating endogenous substances that excite pain nerve endings.²⁸

Pain sensation in acetic acid-induced writhing method is elicited by triggering localized inflammatory response resulting in release of free arachidonic acid from tissue phospholipids via cyclooxygenase (COX) and prostaglandin (PG) biosynthesis.^{29,30} The acetic acid – induced writhing has been specifically associated with increased level of PGE₂ and PGE₂α in peritoneal fluids as well as lipooxygenase products.³¹ The increase in prostaglandin levels within the peritoneal cavity then enhances inflammatory pain by increasing capillary permeability. The acetic acid- induced writhing method is effective to evaluate peripherally active analgesics. Agents which reduce the number of writhes will render analgesic effect probably by inhibition of prostaglandin synthesis, a peripheral mechanism of pain inhibition.³² Therefore, the result of this study shows that the extract possesses strong peripheral analgesic effect. Some of the phytoconstituents of this plant such as flavonoids, saponins, and tannins have been demonstrated to have significant pharmacological activities.³³

Solvent partitioned fractions of *C. sordidum* extract (hexane, ethyl acetate and methanol-water fractions) demonstrated potent analgesic effect in acetic acid-induced writhing test in mice, with the hexane fraction showing the highest

activity at 20mg/kg body weight. Further purification of the hexane fraction yielded 7 fractions with fractions 6 and 7 showing marked inhibition of abdominal writhing, almost 2-folds of that observed in aspirin.

Extract of *C. sordidum* at all doses showed anti-inflammatory and analgesic activities which are comparable to that exhibited by indomethacin or aspirin. This study suggested that the anti-inflammatory effect of *C. sordidum* may be mediated via both peripheral and central mechanisms of inflammation. The solvent partitioned fractions showed hexane fraction had the most potent analgesic activity and further purification yielded 7 fractions. Fractions 6 and 7 showed remarkable analgesic effect with almost 2-folds of that observed for aspirin. The peripheral pathway for mediation of the analgesic effect of the extract, solvent-partitioned fractions and column fractions of hexane fractions was established also. This is a report of preliminary anti-inflammatory and analgesic activities of *C. sordidum*. Further studies are going on to purify, characterize and completely elucidate the structure of the bioactive compound in this extract, particularly bioactive compounds responsible for the remarkable analgesic activity of the fractions.

REFERENCES

1. Miguel, M. G. Antioxidant and Anti-Inflammatory Activities of Essential Oils: A short review. *Molecules*. **2010**, *15*, 9252-9287
2. Kusuma, I. W.; Kuspradini, H.; Arung, E. T.; Aryani, F.; Min, Y. H.; Kim, J. S.; Kim, Y. Biological Activity and Phytochemical Analysis of Three Indonesian Medicinal Plants, *Murraya koenigii*, *Syzygium polyanthum* and *Zingiber purpurea*. *J. Acupunct. Meridian Stud.* **2011**, *4*, 75-79.
3. Iwalewa, E. O.; McGaw, L. J.; Naidoo, V.; Eloff, J. N. Inflammation: the foundation of diseases and disorders. A review of phytomedicines of South African origin used to treat pain and inflammatory conditions. *Afr. J. Biotechnol.* **2007**, *6*, 2868-2885.
4. Plytycz, B.; Seijelid, R. From inflammation to sickness: historical perspective. *Arch. Immunol. Ther. Exp.* **2003**, *51*, 105-109.
5. Parham, C.; Chirica, M.; Timans, J.; Vaisberg, E.; Travis, M.; Cheung, J. Pflanz, S.; Zhang, R.; Singh, K. P.; Vega, F.; To, W.; Wagner, J.; O'Farrell, A. M.; McClanahan, T.; Zurawski, S.; Hannum, C.; Gorman, D.; Rennick, D. M.; Kastelein, R. A.; De Waal Malefyt, R.; Moore, K. W. A receptor for the heterodimeric cytokine IL-23 is composed of IL-12Rbeta1 and a novel cytokine receptor subunit, IL-23R. *J. Immunol.* **2002**, *168*, 5699-5708.
6. Gao, H. M.; Hong, J. S. Why neurodegenerative diseases are progressive: uncontrolled inflammation drives disease progression. *Trends Immunol.* **2008**, *29*, 357-365.
7. Teresita Guardia, Alejandra Ester Rotelli, Ame´rico Osvaldo Juarez, Lilian Eugenia Pelzer (2001) Anti-inflammatory properties of plant flavonoids. Effects of rutin, quercetin and hesperidin on adjuvant arthritis in rat. *Farmaco.* **2001**, *56*, 683-687.
8. Baricevic, D. S.; Sosa, R.; Della Loggia, A.; Tubaro, B.; Simonovska, A.; Krasna, A.; Zupan-

cic A. Topical anti-inflammatory activity of *Salvia officinalis* L. leaves: the relevance of ursolic acid. *J. Ethnopharmacol.* **2001**, *75*, 125–132.

9. Olaoluwa, O.; Ogunbor, F. Phytochemical screening, antimicrobial properties and essential oil constituents of *Combretum sordidum* Exell. *Int. J. Pharm. Sci. Res.* **2015**, *6*, 1176–1180.

10. Beaudelaire K. P.; Luciano, B.; Remy, B. T.; Marius, M.; Télésphore, B. N.; Hee-Juhn, P.; Kyung-Tae, L.; Leon, A. T. Polyhydroxyoleanane-type triterpenoids from *Combretum molle* and their antiinflammatory activity. *Phytochem. Lett.* **2008**, *1*, 183–187.

11. Teshome, T. D.; Ayana, A.; Sileshi, N.; Tadesse, W. Savanna land use and its effect on woody plant species diversity in Borana, Southern Ethiopia. *Sci. Technol. Arts Res. J.* **2012**, *1*, 43–52.

12. Eloff, J. N.; Katerere, D. R.; McGaw, L. J. The biological activity and chemistry of the southern African *Combretaceae*. *J. Ethnopharmacol.* **2008**, *119*, 686–699.

13. Aroke S. A.; Lyndy, J. M.; Esameldin, E. E.; Vinasan, N.; Jacobus, N. E. Polarity of extracts and fractions of four *Combretum* (*Combretaceae*) species used to treat infections and gastrointestinal disorders in southern African traditional medicine has a major effect on different relevant in vitro activities. *J. Ethnopharmacol.* **2014**, *154*, 339–350.

14. Magwenzi, R.; Nyakunu, C.; Mukanganyama, S. The Effect of Selected *Combretum* species from Zimbabwe on the growth and drug efflux systems of *Mycobacterium aurum* and *Mycobacterium smegmatis*. *J. Micr. Biochem. Technol.* **2014**, *S3*, 003.

15. Moyo, R.; Chimponda, T.; Mukanganyama, S. Inhibition of hematopoietic prostaglandin D2 synthase (H-PGDS) by an alkaloid extract from *Combretum molle*. *BMC Complement. Altern. Med.* **2014**, *14*, 221.

16. Ojewole, J. A. Cardiovascular effects of mollic acid glucoside, a 1 α -hydroxycycloartenoid saponin extractive from *Combretum molle* R Br ex G Don (*Combretaceae*) leaf. *Cardiovasc. J. Afr.* **2008**, *19*, 128–134.

17. Eloff, J. N.; Famakin, J. O.; Katerere, D. R. P. *Combretum woodii* (*Combretaceae*) leaf extracts have high activity against Gram-negative and Gram-positive bacteria. *Afr. J. Biotechnol.* **2005**, *4*, 1161–1166.

18. Rubin, B. R.; Burton, R.; Navarra, S.; Antigua, J.; Londoño, J.; Pryhuber, K. G.; Lund, M.; Chen, E.; Najarian, D. K.; Petruschke, R. A.; Ozturk, Z. E.; Geba, G. P. Efficacy and safety profile of treatment with etoricoxib 120 mg once daily compared with indomethacin 50 mg three times daily in acute gout: A randomized controlled trial. *Arthritis Rheum.* **2004**, *50*, 598–606.

19. Amos, S. B.; Chindo, I.; Edmond, P. A.; Wambebe, C.; Gamaniel, K. Anti-inflammatory and anti-nociceptive effects of *Ficus platyphylla* in rats and mice. *J. Herbs Spices Med. Plants.* **2002**, *9*, 47–53.

20. Oyebanji, B. O.; Saba, A. B.; Oridupa, O. A. Anti-nociceptive and anti-inflammatory activities of methanol extract of the leaves of *Cajanus cajan*. *Niger. J. Physiol. Sci.* **2014**, *29*, 183–188

21. Shah, B. N.; Seth, A. K.; Maheshwari, K. M. A review on medicinal plants as a source of anti-inflammatory agents. *Res. J. Med. Plants.* **2011**, *5*, 101–115.

22. Oridupa, O. A.; Saba, A. B. Relative anti-inflammatory and analgesic activities of the who-

le fruit, fruit bark, pulp and seed of *Lagenaria breviflora* Roberty. *J. Pharm. Toxicol.* **2012**, 7, 288-297.

23. Zeashana, H.; Amresha, G.; Raoa, C. V.; Singh, S. Antinociceptive activity of *Amaranthus spinosus* in experimental animals. *J. Ethnopharmacol.* **2009**, 122, 492-496.

24. Alam, M. B.; Hossain, M. S.; Chowdhury, N. S.; Asadujjaman, M.; Zahan, R.; Islam, M. M.; Mazumder, M. E. H.; Haque, M. E.; Islam, A. Antioxidant, anti-inflammatory and antioyretic activities of *Trichosanthes dioica* Roxb. Fruits. *J. Pharm. Toxicol.* **2011**, 6, 440-453.

25. Amanlou, M.; Dadkhah, F.; Salehnia A.; Farsam H.; Dehpour A. R. An anti-inflammatory and anti-nociceptive effect of hydroalcoholic extract of saturejakhuzistanicajamzad extract. *J. Pharm. Sci.* **2005**, 8, 102-106.

26. Hasan, S. M. R; Hossain, M. M.; Akter, R.; Jamila, M.; Mazumder, M. E. H.; Alam, M. A.; Faruque, A.; Rana, S.; Rahman, S. Analgesic activity of the different fractions of the aerial parts of *Commelina benghalensis* Linn. *Int. J. Pharmacol.* **2010**, 6, 63-67.

27. Ullah, M.; Showkat, N. U.; Ahmed, S. Evaluation of *Momordica charantia* L fruit extract for analgesic and anti-inflammatory activities using *in vivo* assay. *Res. J. Med. Plant.* **2011**, 6, 236-244.

28. Duarte, I. D. G.; Nakamura, M.; Ferreira, S. H. Participation of the sympathetic system in acetic acid-induced writhing in mice. *Braz. J. Med. Biol. Res.* **1988**, 21, 341-343.

29. Ahmed, F.; Hossain, M. H.; Rahman, A. A.; Shahid, I. Z. Antinociceptive and sedative effects of the bark of *Cerberaodollam* Gaertn. *Orient. Pharm. Exp. Med.* **2006**, 6, 344-348.

30. Derardt, R.; Jougney, S.; Delevalcece, F.; Falhout, M. Release of prostaglandins E and F in an algogenic reaction and its inhibition. *Eur. J. Pharmacol.* **1980**, 51, 17-24.

31. Zakaria, Z. A.; Abdul Gani, Z. D. F. Antinociceptive, anti-inflammatory, and antipyretic properties of an aqueous extract of *Dicranopteris linearis* leaves in experimental animal models. *J. Nat. Med.* **2008**, 62, 179-187.

32. Ferdous, M.; Rouf, R.; Shilpi, J. A.; Uddin, S. J. Antinociceptive activity of the ethanolic extract of *Ficus racemosa* Linn. (Moraceae). *Orient. Pharm. Exp. Med.* **2008**, 8, 93-96.

33. Egharevba, H. O.; Odigwe, A. C.; Abdullahi, M. S.; Okwute, S. K.; Okogun, J. I: Phytochemical analysis and broad-spectrum antimicrobial activity of *Cassia Occidentalis* (whole plant). *N. Y. Sci. J.* **2010**, 3, 74-81.

Combination of Cumulative Area Pre-Processing and Partial Least Squares for Handling Intensely Overlapping Binary and Ternary Drug Systems

Yahya S Al-Degs^{1*}, Amjad H. El-Sheikh¹, Eman A. Abu Saaleek¹, Reema A. Omeir¹, Musab A. Al-Ghodran¹

¹ Chemistry Department, The Hashemite University, P. O. Box 150459 Zarqa 13115 Jordan

ABSTRACT

The analytical performance of cumulative area pre-processing (CAP), a recently developed signal filtering method, along with multivariate calibration for quantification of spectrally overlying drugs was outlined. The drug combinations containing high level of paracetamol (PAR) in the presence of caffeine (CAF), chlorpheniramine maleate (CHL), pseudoephedrine hydrochloride (PSE), phenylephrine hydrochloride (PHE), and diphenhydramine hydrochloride (DPH). The tested formulations were: PAR-CAF-PHE, PAR-CAF-PHE, and PAR-DRH. Based on net-analyte signal calculations, the formulations exhibited intense overlapping 53-68% for PAR-PSE-CHL, 55-95% for PAR-CAF-PHE, and 44% for PAR-DRH. For each system, PLS latent variables were estimated using cross-validation technique and more factors were needed for highly overlapping systems. PLS-CAP was found applicable for drugs quantification in all systems with excellent performance regardless the size of spectral overlapping and ratios of components in the formulation. For PAR-PSE-CHL (ratio 300:30:2 mg/tablet), the ingredients were quantified by CAP-PLS with satisfactorily recoveries (RSD, $n = 3$) 89.9% (3.1%), 104.6% (2.7%), and 99.0% (1.5%) for PAR, PSE, and CHL, respectively. Both PLS and CAP-PLS were demonstrated the same performance for binary system of modest overlapping and no component available in low concentration.

Keywords: Signal Pre-processing; Spectral overlapping; Binary and Ternary Drug Formulations; PLS calibration

*Corresponding Author: Dr. Yahya Al-Degs, e-mail: yahyaaldeqs@yahoo.com
Yahya S. Al-Degs ORCID Number: 0000-0002-9555-7594
Amjad H. El-Sheikh ORCID Number: 0000-0001-8321-3236
Eman A. Abu Saaleek ORCID Number: 0000-0003-3163-2919
Reema A. Omeir ORCID Number: 0000-0002-3508-5927
Musab A. Al-Ghodran ORCID Number: 0000-0002-4766-0730
(Received 29 December 2018, accepted 24 January 2019)

INTRODUCTION

Commercial drug formulations often contain more than one activates pharmaceutical ingredients (APIs) that present in variable levels to achieve the best pharmacological performance¹. The spectral overlapping between the active ingredients is often moderate but intense overlapping is also possible. In addition to spectral overlapping and nonlinearity in the system, drug production stages like crystallization, drying, solid dosage form, added excipients, and tableting at different conditions can affect the spectral behavior of APIs^{1,2}. Accordingly, accurate analytical methods are always needed in this regard¹. The development and formulation of the pharmaceuticals brought a revolution in human health. These pharmaceuticals would help their intent only if they are free from impurities and are administered in an appropriate quantity. Hence, there are many challenges and it can be reduced by effective use of excipients, which permits formulators to overcome these challenges. It becomes necessary to develop new analytical methods because sometimes the dosage form contains other substances which potentially interfere in the assay and, if not corrected, may impart a systematic error to the assay¹. Multi-component formulations have gained a lot of attention nowadays due to greater patient acceptability, increased potency, multiple action, quick relief and fewer side effects^{1,2}. Market is flooded with combination of drugs in various dosage form. One of such combination is paracetamol (PAR) with other drugs including caffeine (CAF), diphenhydramine hydrochloride (DPH), chlorpheniramine maleate (CHL), pseudoephedrine hydrochloride (PSE), phenylephrine hydrochloride (PHE). For example, PAR and DPH are co-formulated in pharmaceutical product for temporary relief of pain when associated with sleeping difficulty²⁻⁷. The combination PAR-CHL-PSE has been recently introduced in the market to treat the symptoms of most flues⁵⁻⁷. The combination PAR-CAF-PHE was also formulated to relief from major cold and flu symptoms and applied at day time as it doesn't cause drowsiness.

Various chemical and instrumental methods were developed to make drugs serve their purpose at regular intervals which are involved in the estimation of drugs. These pharmaceuticals may develop impurities at various steps of their development, transportation and storage, which makes the pharmaceutical risky to be administered. Thus, they must be identified and quantified. Hence, analytical instrumentation and methods play an important role. Thus, the review highlights a variety of analytical, chromatographic and instrumental method developed such as; High Performance Liquid Chromatography (HPLC), High Performance Thin Layer Chromatography (HPTLC), and Gas Chroma-

tography (GC) have wide application in assuring the quality and quantity of pharmaceutical products and these instrumental methods are simple, precise, rapid, and reproducible and have been applied in the analysis of pharmaceuticals for assessing the quality of the drugs⁸⁻¹⁰.

Recently, multivariate calibration methods have been intensively employed for analyzing pharmaceutical formulations and detection of released drugs in urine and plasma⁵⁻⁷. Particularly speaking, PAR and CAF have been quantified in drug formulations using first-order multivariate calibration methods with high accuracy and without implementing any chromatographic procedure^{6,7}. Compared to liquid chromatography, assaying drug formulations by multivariate calibration required less solvent consumption and avoids using tedious chromatographic instruments²⁻³. First order multivariate calibration methods includes multilinear regression (MLR), principal component regression (PCR), partial least-squares (PLS-1), and many others¹¹. In a recent study, both PAR and PHE were quantified in four-drug formulations using PLS1 calibration^{5,6}. PHE was quantified in the presence of PAR in tablet form with excellent recovery⁷. In another study, novel application of PCR and PLS was developed for determination of PAR, CAF, and CHL in real formulations containing other medicines^{6,7}. In the drug formulation, the recovery and RSD values were 99.91% (1.69%), 100.15%(1.35%) and 100.49%(1.66%) for PAR, CAF and CHL, respectively. In the second method PLS was applied to quantify four medicines in real formulation with high recoveries and RSD: 99.80% (1.67%), 100.19% (1.42%) and 100.45% (1.86%) for PAR, CAF and CHL, respectively⁷. There is no published literature dealing with simultaneous quantification of PAR and DPH in real formulations. Spectral overlapping between drugs was reported to have a negative influence on the performance of multivariate calibration methods¹¹. From the earlier studies, it is concluded that multivariate calibration is applicable for medicines determination in different commercial formulations including tablet and syrups.

Usually, the pre-processing methods are divided into three categories: a) filtering and de-noising, generally associated with the improvement of the signal-to-noise ratio. These methods are applied to the raw data before the construction of the multivariate model and reduce the influence of the random variance without altering that useful, b) spectral normalization and differentiation, such as the spectral derivation and the application of the Fourier transform. These procedures are also applied before the construction of the model, and c) selection of the variables and reduction of dimensionality of the data. These methods are applied by multivariate modeling and therefore involve both the

matrix X (independent variables) and the matrix Y (dependent variables). The most used method is orthogonal signal correction. There are a number of excellent review articles providing guidance for application of the pre-processing techniques to the analytical signals¹²⁻¹⁴. In some pharmaceutical formulations one or more components are present in very low concentrations, so as to be hidden by the components more concentrated or by the instrumental noise. This increases the difficulty of building a mathematical model able to predict in a satisfactory manner all the species present in the mixture. In these cases, the data pre-treatment should provide to amplify the analytical information due to the components at lower concentration and at the same time to minimize the spectral noise that can interfere with their determination.

In the current work, the application of newly proposed cumulative area pre-processing (CAP) will be evaluated for prior to PLS calibration for quantification of binary and ternary drugs systems. CAP was developed to amplify the spectral signals. CAP-PLS will be tested on the quantitative analysis of one binary and ternary pharmaceutical formulation. The common difficulty in analyzing these matrices was the presence of some components in much lower amount than other components. The binary formulation consisted of paracetamol-diphenhydramine hydrochloride (ratio 20:1), paracetamol-caffeine-phenylephrine hydrochloride (ratio 100:5:1 mg/tablet), and paracetamol-pseudoephedrine hydrochloride-chlorpheniramine maleate (ratio 150:15:1 mg/tablet). The analytical performance of CAP-PLS and PLS for drugs quantification will critically discussed. More attention will be paid on the influence spectral overlapping among drugs on their quantification by CAP-PLS. Influence of pH and spectral range on spectral analysis will be also considered.

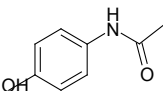
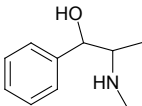
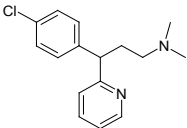
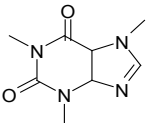
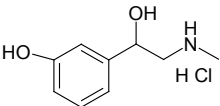
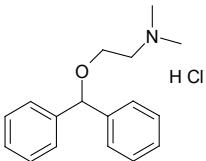
METHODOLOGY

Drugs and marketed formulations

The pharmaceuticals paracetamol (PAR), caffeine (CAF), diphenhydramine hydrochloride (DPH), phenylephrine hydrochloride (PHE), pseudoephedrine hydrochloride (PSE), and chlorpheniramine maleate (CHL) were kindly donated from Dar Al-Dawaa company (Dar Al-Dawaa, Naour, Amman, Jordan). Distilled water was used for preparation of standard solutions and dissolution of commercial tablets. The marketed drugs were Panadol cold and flu® (Active ingredients: PAR-PSE-CHL 500:30:2 mg/tablet; excipients Silicon dioxide, stearic acid, sodium benzoate, povidone, starch, maize starch, and talc, GlaxoSmithKline Dungarvan Ltd., Co. Waterford, Ireland), Panadol cold and flu Day® (Active ingredients: PAR-CAF-PHE 500:25:5 mg/tablet; excipients pre-gelatinised starch, maize starch, povidone, potassium sorbate, talc, stearic

acid, microcrystalline cellulose, sodium lauryl sulphate, sunset yellow, GlaxoSmithKline Dungarvan Ltd., Co. Waterford, Ireland), and Panadol night® (PAR-DPH 500:25 mg/tablet; excipients maize starch, pregelatinised starch, potassium sorbate, povidone, talc, and stearic acid, GlaxoSmithKline Dungarvan Ltd., Co. Waterford, Ireland) All other reagents were of the highest purity commercially available. Table 1 summaries some chemical parameters of the undertaken pharmaceuticals.

Table 1. Chemical properties of studied pharmaceuticals.

Name/short name	Formula	Structural formula	Medical action	pK _a
Paracetamol PAR	C ₈ H ₉ O ₂		Treat mild to moderate pains	9.5
Pseudoephedrine hydrochloride PSE	C ₁₀ H ₁₅ ON		Shrink blood vessels in the nasal passage (prevent stuffy nose)	10.3
Chlorpheniramine Maleate CHL	C ₁₅ H ₁₉ N ₂ Cl		Relieve symptoms of allergy	9.1
Caffeine CAF	C ₈ H ₁₀ N ₄ O ₂		Acts as central nervous system stimulant	14.0
Phenylephrine hydrochloride PHE	C ₉ H ₁₄ ClNO ₂		Sympathomimetic (descongestants)	9.07
Diphenhydramine Hydrochloride DPH	C ₁₇ H ₂₂ ClNO		Blocking the effects of histamine and causes drowsiness.	9.13

Standard solutions, calibration/validation mixtures

Stock solutions were separately prepared by dissolving in ethanol nearly 25.0 (± 0.0001 g) mg of each drug in 100 mL volumetric flasks. A first set of 9 binary calibration samples was built by combining five levels of PAR and DPH within the range 1.0–12.0 mg/L. A second calibration set of nine ternary mixture solutions was prepared for PAR-CAF-PHE and PAR-PSE-CHL systems. For PAR-CAF-PHE, drug ranges were 2.0–15.0 mg/L for PAR, 2.0–16.0 mg/L for CAF and 1.0–8.0 mg/L for PHE. For PAR-PSE-CHL, drug ranges were 1.0–16.0 mg/L for PAR, 1.0–8.0 mg/L for PSE, and 1.0–12.0 mg/L for CHL. Calibration set of the binary mixtures was created by following a full experimental design while calibration sets of binary systems selected according to Brereton's rule using three different concentration levels. To validate the PLS and CAP-PLS models, three independent external validation sets consisting of 7 solutions for binary and ternary systems were prepared. Marketed formulations were assayed by weighing four tablets for binary system and five tablets for ternary systems and grinding the tablets to a fine powder. The powder was suspended in water and diluted to a final volume of 100 mL. The suspension was sonicated for 10 min, filtered through a 0.45 μm filter, and properly diluted in preparation for spectral analysis.

Partial least squares and net-analyte signal calculations

A double beam UV-visible spectrophotometer (Thermo scientific. Genesys 10S UV-VIS (USA)) with quartz cuvette cell of 1.0 cm path length was employed. The spectral bandwidth was 1.0 nm with fast wavelength-scanning speed. Scans were carried out in the range of 200–300 nm at (1.0 nm step, 101 points/spectrum). The spectral data obtained for calibration mixtures are placed in matrix **A** (size 101 \times 9) and spectral data of validation set are placed matrix **B** (size 101 \times 7). On the other hand, concentration data are placed matrix **C** (size 9 \times 3 for ternary systems and size 9 \times 2 for binary system). Partial least squares PLS1 is an efficient tool for developing a quantitative relationship between several predictor variables **A** (spectral data) and a property of interest **c** (the independent variable or drugs content) as shown below^{11,15}:

$$\mathbf{c} = \mathbf{A}\mathbf{b} \quad (1)$$

Where **c** contains the concentrations of calibrated drug in calibration samples arranged in **a** vector and **b** is the calibration sensitivity which is necessary for estimating drugs content in the adsorption solutions^{11,16–18}:

$$\mathbf{b} = \mathbf{W}^t(\mathbf{P}\mathbf{W}^t)^{-1}\mathbf{q} \quad (2)$$

Where \mathbf{W} is the weights matrix for \mathbf{A} , \mathbf{P} is the loadings matrix of \mathbf{A} , \mathbf{q} is the loadings vector for \mathbf{c} , \mathbf{t} donates transpose operation, and -1 stands for inverse operation. Once \mathbf{b} is estimated, prediction of drug concentrations (\mathbf{c}_{un}) from the unknown spectrum \mathbf{a} is carried out as following^{11,16-18}:

$$\mathbf{c}_{un} = \mathbf{a}\mathbf{b} \quad (3)$$

Optimum number of PLS-latent variables were estimated using cross-validation method¹⁵. The predicted concentrations were compared with the known concentrations of the compounds in each calibration sample. The prediction error sum of square (PRESS) and the relative error of prediction (REP %) were calculated for drugs in calibration and validation samples as following^{17,19}:

$$PRESS = \sum_{i=1}^n (C_{i,actual} - C_{i,pred})^2 \quad (4)$$

$$\%REP = 100 \times \left(\frac{\sum_{i=1}^n (C_{i,pred} - C_{i,act})^2}{\sum_{i=1}^m (C_{i,act})^2} \right)^{1/2} \quad (5)$$

Where C_{actual} , C_{pred} and n , are actual concentration (mg/L), predicted concentration obtained by PLS (mg/L), and number of training samples (solutions), respectively. A unifying framework for calibration and prediction in multivariate calibration is shown based on the concept of the Net Analyte Signal (NAS). NAS is the part of the measured spectrum that the calculated model uses for prediction. The main equation that is needed to estimated figures of merit is^{15,20,21}:

$$s_k^* = [I - S_k S_k^+] s_k \quad (6)$$

Where S is the matrix of sensitivities collected for all other solutes, s_k is the sensitivity vector of the analyte, and s_k^* is the spectrum of pure analyte k measured at unite concentration (sensitivity factor). Sensitivity (SEN) value of analyte k is the norm ($\| \|$) of the net sensitivity vector, it was defined as the amount of *net* signal that, in prediction, corresponds to a concentration equal to unity²¹:

$$SEN = \| s_k^* \| \quad (7)$$

Selectivity (SEL) can be defined as the part of the measured signal unique to the analyte of interest. Based on NAS theory, the selectivity measures the extent of spectral overlapping. SEL can be expressed by the ratio between the norm of the NAS vector and the norm of the spectra. SEL values are extended

from zero (high overlap with other interferences) to unity (no overlap with other sample components). High values of SEN are an indication of high method accuracy for that analyte^{15,20,21}:

$$SEL = \frac{\|s_k^*\|}{\|s_k\|} \quad (8)$$

The limit of detection (LOD) obtained assumes that the prediction uncertainties are approximately constant. LOD gives the minimum detectable amount of k solute. A reasonable estimation to determine the LOD can be estimated as²¹:

$$LOD = 3 \frac{\|\varepsilon\|}{\|s_k^*\|} \quad (9)$$

Where $\|\varepsilon\|$ is a measurement of the instrumental noise, and s^* was defined above. Then the norms of blank readings ($\|NAS_{\text{blank}}\|$) are estimated and $\|\varepsilon\|$ is taken as the standard deviation of estimated norms²¹. The limit of quantification (LOQ) is the minimum quantifiable amount of the solute, is estimated as^{15,21}:

$$LOQ = 10 \frac{\|\varepsilon\|}{\|s_k^*\|} \quad (10)$$

All calculations were carried out using special matlab-codes under MATLAB®.

Cumulative area pre-processing of spectral data prior to PLS calibration

Data treatment by CAP transforms the original UV spectrum to a new curve using the area underlying the same spectrum. This elaboration is based on two mathematical steps. In the first step, the area a_{λ_i} binning of the two consecutive wavelengths (λ_i and λ_{i+1}) is calculated as⁷:

$$a_{\lambda_i} = \frac{ab_{\lambda_i} + ab_{\lambda_{i+1}}}{2} \quad (11)$$

Where ab is the absorbance value at a single wavelength. This calculation is repeated for all the wavelengths in the spectrum. In the second step, the cumulative sum of the single areas is computed, in such a way as the cumulative area at each wavelength A_{λ_i} resulted from the sums of all areas a_i of the preceding wavelengths. For a spectral region between λ_m and λ_n ($\lambda_m < \lambda_n$), the cumulative area $A_{\lambda_{m,n}}$ is estimated as⁷:

$$A_{\lambda_{m,n}} = \sum_{i=\lambda_m}^{\lambda_n} a_{\lambda_i} \quad (12)$$

Treatment of the original UV spectra using CAP (Eqs 11 and 12) offers many advantages including amplification of the analytical signals for all solutes and possible quantification

RESULTS AND DISCUSSION

Influence of solution pH on spectral behavior of pharmaceuticals

Influence of solution pH on spectral behavior was studied for all drugs at pH 3.0, 7.0, and 10.0 to cover all possible conditions. Among the drugs, identical spectral shapes over the range (230-280 nm) were observed for CHL and PSE and hence there was no need to present their profiles. On the other hand, the UV-absorption behavior of PAR (which present in all systems), CAF, PHE, and DPH were notably changed with solution pH as depicted in Fig 1.

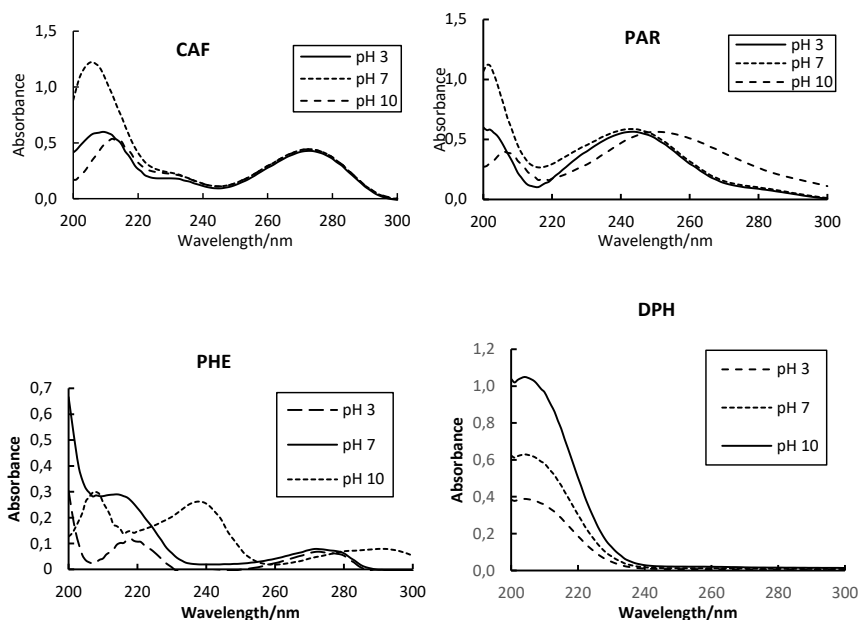


Figure 1. Influence of pH on spectral behavior of tested drugs (7.0 mg/Leach drug)

As shown in Fig 1, large variation was noted in the spectra of CAF at the studied pH and over the range (200-240 nm) and slight variations were observed over the rest of the domain. In the same time, the distinct wavelength positioned at 273 nm was not affected with solution pH. More variations were observed in the PAR spectra, the intensity was notably increased at pH over the range 200-220 nm while the main peak (243 nm) was shifted to 250 nm at pH 10.0. The most drastic

changes were reported for PHE as shown in Fig 1. It was highly possible that PHE underwent chemical reaction at the basic medium and this was deduced from the developed spectrum which has two wavelengths at 208 and 237 nm. To avoid PHE side-reaction, it was practical to run UV measurements at pH 7.0. As can be noted from the earlier discussion, the optimum pH for spectral analysis is 7.0 which maintain stable structure and high UV absorption for all drugs. For DPH, there was a significant light absorption with pH over the range (200-230 nm), while, pH has no effect on the spectrum over the rest of the domain. pH 7.0 seems to be a good choice to run spectral measurement for this drug. In fact, protonation, hydrolysis, and internal-arrangement of drug molecules are highly possible at acidic or basic solutions and this affects their spectral properties. Accordingly, solution pH should be adjusted to get unique spectral characteristics of the measured drug.

Spectral behavior of pharmaceuticals and spectral overlapping

In fact, intense spectral overlapping among pharmaceuticals would retard their quantification in solution and in real formulation^{11,15}. Accordingly, the spectral behavior of pharmaceuticals and extent of overlapping were evaluated before running multivariate calibration. The UV spectra of the studied systems are presented in Fig. 2

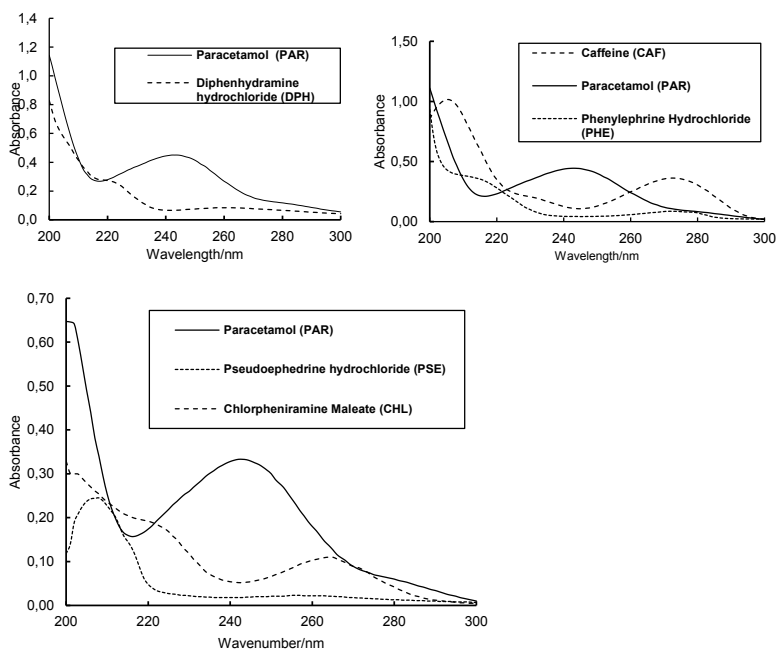


Figure 2. UV Spectra of the binary and ternary drug systems. Top PAR–DPH (6.0 mg/L and pH 7.0), Middle CAF–PAR–PHE (7.0 mg/L and pH 7.0) Bottom PAR–PSE–CHL (5.0 mg/L and pH 7.0)

As indicated in Fig. 2, all drugs exhibited strong light absorption over the range (200–300 nm) in addition to intense overlapping among the signals. For PAR-DPH, a large spectral overlap was observed between both compounds and particularly over the range 220–280 nm. In addition to intense overlapping, PAR has better UV absorption compared to DPH and would make their quantification by simple spectrometry (especially DPH) a hard task. The intense absorption of PAR at 243 nm was mainly attributed to the $n\rightarrow\pi^*$. One more point on this PAR-DPH is the presence of DPH in much lower amount compared to PAR in real formulation and this added more analytical obstacles on their accurate quantification. For the ternary system CAF–PAR–PHE, the solutes were actively absorbing over the region this was attributed to their chemical structure which contains many active functional groups. The spectra of the drugs indicated the following distinct absorption wavelengths at 243, 273, and (215 and 272 nm) for PAR, CAF and PHE, respectively. The reported absorption wavelengths were mainly attributed to $n\rightarrow\pi^*$ and $\pi\rightarrow\pi^*$ electronic transitions in the molecules. In fact, the longer maximum wavelength of absorption observed for CAF (273 nm) was attributed to the conjugated system as indicated from the chemical structures of the drugs (Table 1). Generally, PHE showed weaker absorption compared to other drugs and absorb near the lower end of the spectral range (220 nm). The spectral overlap between drugs is high over the entire spectral range. Within the spectral regions 250–270, an intense overlapping between PAR and CAF was observed and this would affect their quantification in real formulations. Moreover, PHE absorbs over the entire range. In this ternary system, PHE should be added in much lower levels and this negatively reflected on its quantification in real formulations. For PAR–PSE–CHL, the solutes were active in UV region and this is attributed to their chemical structure which contains aromatic parts substituted with functional groups (Table 1). The spectra of drugs indicated the following special absorption wavelengths 210, 242, and 265 nm for PSE, PAR and CHL, respectively. The observed bands were mainly attributed to $n\rightarrow\pi^*$ and $\pi\rightarrow\pi^*$ electronic transitions. Generally, PSE has a poor UV absorption compared to two drugs and absorb near the extreme of the applied spectral domain. In fact, the spectral overlap between drugs is high over the entire spectral range. Within the spectral regions 220–240 and 260–280 nm, an intense overlapping between PAR and CHL was observed (Fig. 1). Moreover, PSE absorbs over the entire range. Practically, PAR and PSE are added in much higher levels compared to CHL and this would make quantification of the later drug a hard-analytical task. For each system, the extent of spectral overlapping between drugs was estimated using net-analyte signal calculations (Eq. 8) and the results are provided in Table 2.

Table 2. Extent of spectral overlapping in the drug systems using NAS calculations^a

Total spectral overlapping with other drugs%	
PAR–PSE–CHL	
PAR	53
PSE	55
CHL	68
CAF–PAR–PHE	
CAF	68
PAR	85
PHE	79
PAR–DPH	
PAR	38
DPH	62

^aFor PAR–PSE–CHL, NAS calculations were carried out at 5.0 mg/L, pH 7.0, and spectral range 200–300 nm. For CAF–PAR–PHE, calculations were carried out at 7.0 mg/L, pH 7.0 and 200–300 nm. For PAR–DPH, 6.0 mg/L, pH 7.0 and 200–300 nm.

As indicated in Table 2, a significant overlapping among drugs was reported and the intense overlapping was in the ternary system (CAF–PAR–PHE) which extended from 68% to 85%. For the earlier ternary system, PAR exhibited an intense overlapping with CAF and PHE which may negatively reflect on its accurate quantification in solution or in real extracts. In fact, PAR is added many-folds higher than other two drugs in the formulation which may not affect its final measurements. On the other hand, the high overlapping of CAF and PHE (68%–79%) is negatively affect their final quantification taking into account their lower levels compared to CAF in real formulations. This ternary system represented a real challenge for multivariate calibration methods due to the intense spectral overlapping. The same discussion is holding true for other systems. The most problematic issue in the ternary system CAF–PAR–PHE is the intense overlapping of PHE with other drugs (79%) while being present in very little amount compared to the rest of drugs. The same is true for CAF as it added in modest amounts compared to PAR which added in much higher dosages. In the same manner, accurate quantification of DPH (spectral overlapping 62% with PAR) in real formulations may not be a straightforward analytical job. In addition to spectral overlapping, the presence of un-calibrated excipients in the extra will add more interference on analysis and hence reduce the performance of multivariate calibration methods^{11,16,17}.

Pre-processing of the UV spectral data by CAP: Signal amplification

For better assessment on signal preprocessing before PLS calibration, UV spectra of all drugs and their mixtures (binary and ternary) were recorded at the ratios identical to the real formulations along with CAP spectral transformation. The results are shown in Fig 3.

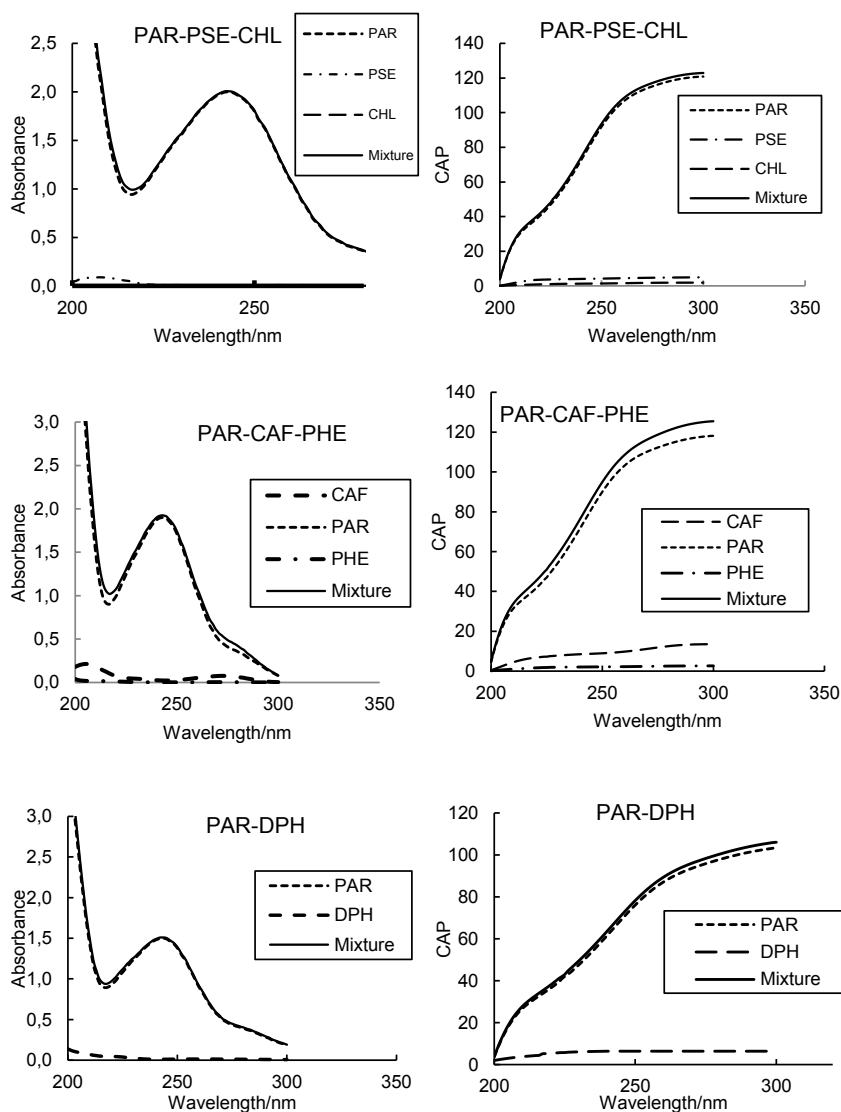


Figure 3. UV spectra and CAP transformation of drugs and their mixtures recorded at the same ratios as in real formulations.

In the three systems, UV spectra indicated a strong absorption signal of PAR due its higher concentration. For PAR-PSE-CHL, PAR was added in excess than CHL and CHL by 150 and 10 times, respectively. While for PAR-CAF-PHE, PAR was 100 and 20 times higher than PHE and CAF, respectively. For the binary system, PAR was 20-times higher than the other drug. The high level of PAR in the systems would explain the similarity between PAR and the spectrum of the mixture in all cases. The difficulty in analyzing the mixtures was increased by the fact that the absorptivity values of CAF, CHL, PSE and DPH in the respective formulations were much lower than the other PAR over the entire spectral domain, making their accurate determination a hard-analytical task unless the components are separated before detection. This difficulty drastically reduced the chance to apply classical spectroscopic methods which often adopted discrete wavelengths for detection. In these cases, multivariate calibration methods seem more suitable because they use simultaneously a large number of signals per spectrum. However, considering the difficulty in solving this type of mixtures, an appropriate pre-processing of the analytical data seemed necessary in order to minimize any instrumental interference and at the same time select the most useful information to emphasize the contribution of substances of low concentration.

As outlined earlier, CAP treatment transforms the original UV spectrum into a new curve created by using the area underlying the spectrum. This treatment is based on two mathematical steps as outlined earlier. Indeed, the conversion of original UV spectra through the CAP method provided many advantages among which the amplification of the analytical signals. Fig 3 shows the outputs of CAP treatment of the spectral of the three systems where drugs recorded at their actual ratios. The major differences in comparing the original absorbance curves with CAP plots are: a) the magnitudes on the y -axis indicated a high amplification of the signal and this supposed to increase the sensitivity of the quantitative measurements and help in quantifying the components even at trace levels (like PSE, CHL, CAF and DPH in the presence of PAR), b) CAP was able to magnify the weak signals of PSE, CHL, CAF and DPH and over the whole spectrum and this option is rather fundamental when applying multivariate techniques which utilize the full spectrum to extract the maximum analytical information, and c) Unlike UV signal, the values of CAP signal were stabilize at constant value and this was reported for all drugs. This stable value, in fact, is due to the additive contribution of all intensities at all wavelengths. It was reported that CAP filtering would end up with accurate quantification of drugs when present at trace levels⁷. The analytical matrices were built on the spectral data. In the matrix **A** (dependent variables) each sample was described by n

variables, corresponding to the wavelengths and to the respective absorbance values; in the matrix **C** (independent variables) the samples were described by the concentrations of each component. Two data matrices for each drug-system were created; the first matrix contained the untreated spectral data while the other matrix contained the spectral data upon CAP. The calibration curves relative to the binary (PAR-DPH) and ternary systems (PAR-PSE-CHL and PAR-CAF-PHE) along with CAP transformation are presented in Figure 4.

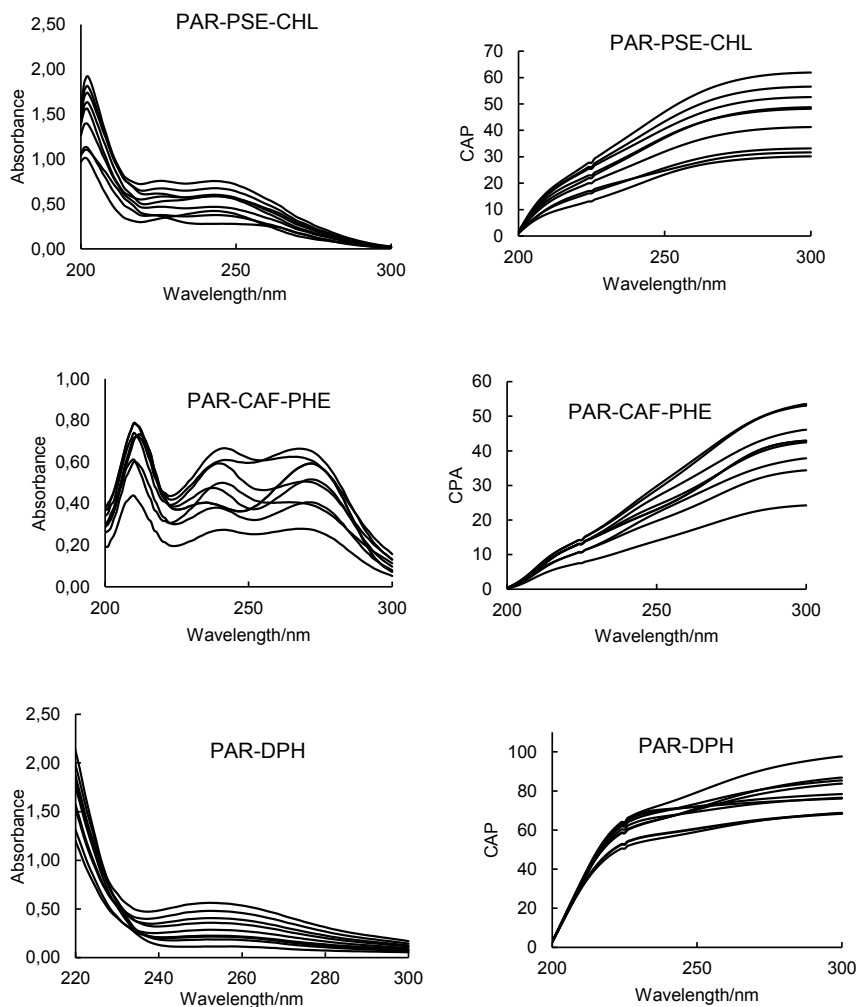


Figure 4. UV spectra of PAR-DPH, CAF-PAR-PHE and PAR-PSE-CHL calibration samples and plots after CAP transformation.

Determination of pharmaceuticals in binary and ternary drugs systems by PLS

PLS and CAP-PLS can be created and applied to predict drugs without previous knowledge on calibrated solutes. However, intense overlapping between drugs and strong influence of excipients would affect the prediction power of PLS^{15,16}. The performance of before and after signal filtering drugs prediction in validation set is provided in Table 3.

Table 3. External prediction of drugs in different systems.

Drug	PLS ^a			CAP-PLS ^b		
	PRESS	REP%	Rec%	PRESS	REP%	Rec%
PAR-PSE-CHL						
PAR	0.32	3.9	96.3 (4)	0.06	1.7	98.0 (3)
PSE	2.95	12.6	95.2 (5)	0.13	3.1	97.7 (4)
CHL	2.32	11.2	94.0 (5)	0.15	2.5	97.7 (4)
PAR-CAF-PHE						
PAR	3.41	14.0	106.8 (5)	0.82	5.8	99.2 (3)
CAF	2.93	10.0	97.4 (4)	0.45	4.3	103.6 (3)
PHE	1.54	8.0	95.8 (4)	0.18	2.1	101.4 (3)
PAR-DPH						
PAR	0.45	3.4	96.9 (3)	0.14	2.1	98.5 (2)
DPH	0.64	4.9	95.7 (5)	0.19	3.0	97.0 (4)

^aSpectral range 200-300 nm (101 point/spectrum). Calibration and prediction steps were carried out using Eqs 1-3. Calibration and validation sets are provided in Table 1. PLS variables were provided between brackets for each system.

^bPrior to PLS calibration, spectral data were filtered using cumulative area pre-processing method (Eqs 11 & 12) and PLS variables were provided between brackets for each system.

As shown in Table 3, PLS was workable to predict PAR-PSE-CHL and the best prediction observed for PAR with a REP value 3.9%. In general, PLS was not so-effective for predicting PSE in the mixtures with a high REP 12.6% which may not acceptable for pharmaceutical analysis. The modest prediction of PSE was mainly attributed to the intense spectral-overlapping with other drugs (Table 2). Accordingly, application of PLS for PSE and CHL may not be workable taking into account the negative influence of excipients in real cases. As indicated in Table 3, the performance of CAP-PLS was very promising with

REP values of 1.7%, 2.5%, and 3.1% for PAR, CHL, and PSE, respectively, and this reflected the high closeness between nominal and predicted values. The earlier results showed that CAP-PLS outperformed PLS for predicting PSE and CHL in ternary systems. In general, CAP-PLS was excellent for predicting all drugs with PRESS values less than 1.0 in all cases. The same results were noted for PAR-CAF-PHE where CAP-PLS outperformed PLS for drugs quantification with final REP 2.1-5.8%. The best prediction was reported for PHE down to 1.0 mg/L in mixtures rich with PAR and CAF. Due to the lesser spectral overlapping, both PLA and CAP-PLS were both of comparable performance for PAR-DPH quantification, REP was all lower than 5% for both methods. The superiority of CAP-PLS was mainly attribute to the effective signal filtering prior to PLS calibration which improved final prediction⁷.

Quantification of drugs in real formulations

The real testing of the proposed CAP-PLS method will be assessed by analyzing binary and ternary systems in the commercial formulations. Direct analysis of drugs in commercial tablets is not an easy task due to the presence of drugs in unequal quantities and also the presence of excipients that did not involve while constructing calibration mixtures. In addition to the above, the drugs are often placed at concentrations far higher than the calibration solutions. Therefore, all the ingredients should be properly diluted to be measured with acceptable sensitivity. In this case, signal filtering/enhancing will be essential before running classical PLS calibration. It is rather essential to mention that matrix-cleaning methods may be adopted to eliminate/reduce the influence of interferences before running analysis²²⁻²⁴. It was necessary to evaluate the effect of dilutions on drugs quantification. The spectral shapes of the systems and at variable dilutions are provided in Figure 5. Drugs quantification in real formulations is provided in Table 4 and the PLS outputs are provided for comparison purposes.

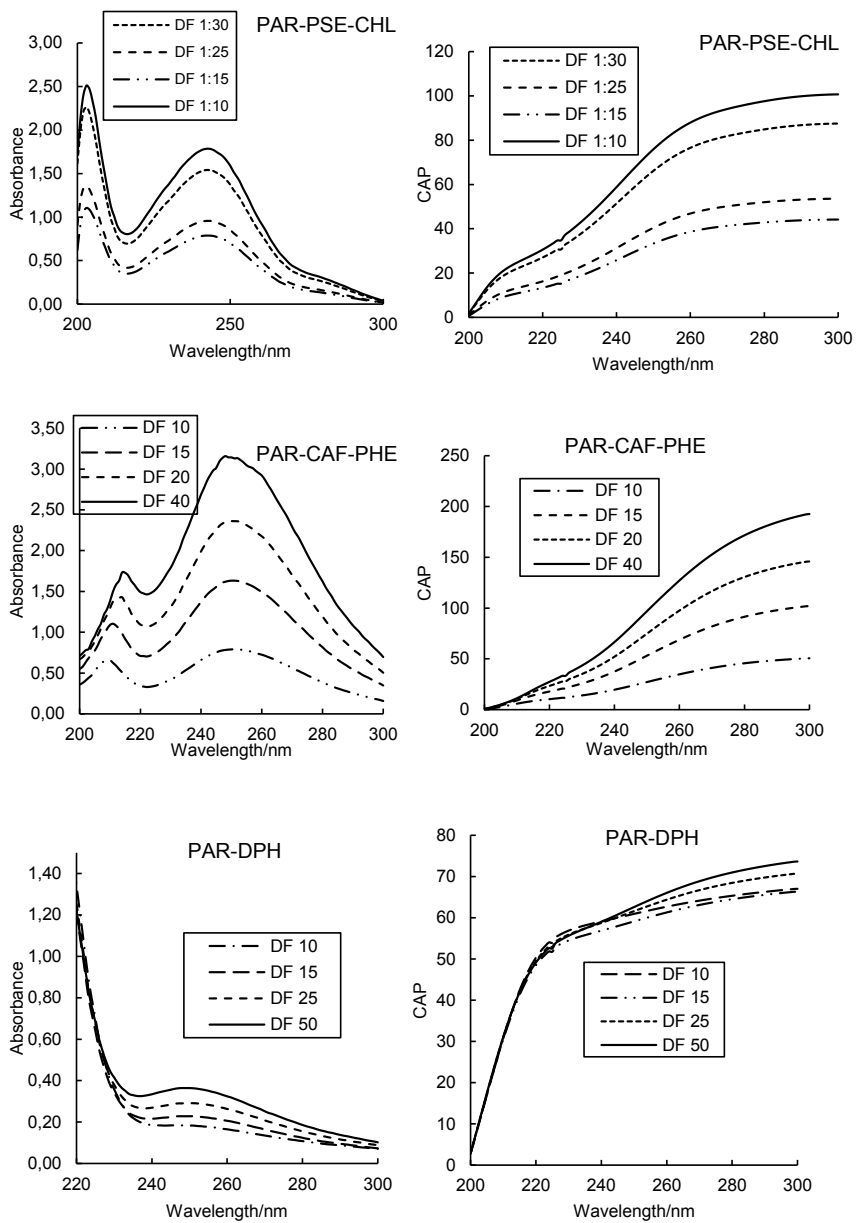


Figure 5. UV spectra of marketed formulations after extraction and dilution with distilled water and CAP plots.

Table 4. Implementation of PLS and CAP-PLS for drugs quantification on different systems.

System	Claimed (mg/tablet)	PLS			CAP-PLS		
		Predicted (mg/tablet) ^a	Mean Recovery % (n=3)	Precision (n=3, RSD%)	Predicted (mg/tablet)	Mean Recovery % (n=3)	Precision (n=3, RSD%)
PAR-CAF-PHE							
PAR	500	503.0	100.6	8.4	501.0	102.6	2.1
CAF	25	26.0	104.0	6.5	24.7	103.0	3.1
PHE	5	4.5	90.0	7.3	5.1	94.3	4.2
PAR-PSE-CHL							
PAR	300	508.0	99.0	5.0	504.0	98.9	3.1
PSE	30	28.7	102.0	7.0	25.2	104.6	2.7
CHL	2	1.8	99.0	4.6	2.1	99.0	1.5
PAR-DPH							
PAR	500	503	101.2	2.1	502	104.2	0.8
DPH	25	28	105.3	3.1	24	106.3	1.0

As indicated in Fig 5, identical UV spectra and CAP signals were observed for the systems. Higher intensities (for CAP signals) were observed at lower dilutions (DF 10 and 15). Initial analysis indicated that running PLS or CAP-PLS using signals recorded at DF 10 or 15 ended up with high prediction errors. In fact, at lower DF the content of drugs is much higher than those used in calibration mixtures making external prediction is not valid. As already known, the external prediction of solutes is often dependent on the ranges selected in the calibration mixtures. In the current systems, the best prediction in real formulations was achieved at DF 15, 20, and 25 for PAR-DPH, PAR-CAF-PHE, and PAR-PSE-CHL, respectively. Both models were used to assay drugs in real formulations which based the same composition of the calibration mixtures. The results, provided in Table 4, indicated the high performance of CAP-PLS for accurate quantification of drugs in binary and ternary systems. For ternary mixtures, CAP-PLS manifested better accuracy than PLS with recoveries 94.3%-102.6% and precisions (RSD) 2.1-3.1% for PAR-CAF-PHE and 98.9%-104.6% and 1.5-3.1 for PAR-PSE-CHL. It seems that signal filtering by CAP has passively reflected on the final PLS performance. For the other binary system, a good agreement was observed between experimental and nominal levels (obtained by both models) of the commercial formulation. Again, PLS calibration created using CAP-filtered-data generated the best results and may properly handed the negative influence of excipients present in the dosage forms.

UV-signal filtering by CAP prior to PLS was found more effective than PLS when handling ternary drug mixtures. The proposed CAP-PLS can handle systems in which one component present at lower levels in the formulation. CAP simply estimated the cumulative sum of the areas under curve between two consecutive wavelengths which improved the analytical signal. The proposed CAP-PLS was effective to predict two ternary systems (PAR-CAF-PHE and PAR-PSE-CHL) of intense overlapping and containing one ingredient available at lower concentration. For binary system, application of CAP-PLS was as good as classical PLS along with raw UV signals. CAP, as an appropriate pretreatment method, have been succeeded for accurate and simultaneous quantification of commercial pharmaceutical formulations in which the ratio between the components is highly variable.

ACKNOWLEDGEMENTS

The authors thank Deanship of Graduate Studies (The Hashemite University, Jordan) and for the financial support to this research. The researchers also thank all the technical staffs at chemistry department for their continued help.

List of abbreviations

CAF	Caffeine
CHL	Chlorpheniramine Maleate
CAP	Cumulative Area Pre-Processing
DPH	Diphenhydramine Hydrochloride
LOD	Limit of Detection
LOQ	Limit of Quantification
NAS	Net Analyte Signal
PLS	Partial Least Squares
PRESS	Prediction Error Sum of Square
PSE	Pseudoephedrine Hydrochloride
REP%	Relative Error of Prediction
SEL	Selectivity
SEN	Sensitivity

REFERENCES

1. Shaikh, K.; Devkhile, A. Simultaneous determination of aceclofenac, paracetamol, and chlorzoxazone by RP-HPLC in pharmaceutical dosage form. *J. Chroma. Sci.* **2008**, *46*, 649-652.
2. Ali, N.; Zaazaa, H.; Abedelkawy, M.; Magdy, M. Simultaneous determination of paracetamol and diphenhydramine hydrochloride in presence of paracetamol degradation product. *J. Pharm. Anal. Acta.* **2011**, *2*, 9.
3. Dou, Y.; Sun, Y.; Ren, Y.; Ren, Y. Artificial neural network for simultaneous determination of two components of compound paracetamol and diphenhydramine hydrochloride powder on NIR spectroscopy. *Anal. Chim. Acta.* **2005**, *528*, 55-61.
4. Goicoechea, H.; Olivieri, A. Simultaneous multivariate spectrophotometric analysis of paracetamol and minor components (diphenhydramine phenylpropanolamine) in tablet preparations. *J. Pharm. Biomed. Anal.* **1999**, *20*, 255-261.
5. Hegazy, M.; Abbas, S.; Zaazaa, H. Resolution of overlapped quaternary spectral bands by net analyte signal based methods; an application to different combinations in tablets and capsules. *J. Anal. Chem.* **2015**, *70*, 450-458.
6. De Luca, M.; Ioele, G.; Spatari, C.; Ragno, G. Optimization of wavelength range and data interval in chemometric analysis of complex pharmaceutical mixtures. *J. Pharm. Anal.* **2016**, *6*, 64-69.
7. De Luca, M.; Ioele, G.; Ragno, G. Cumulative area pre-processing (CAP): A new treatment of UV data for the analysis of complex pharmaceutical mixtures. *J. Pharm. Biomed. Anal.* **2014**, *90*, 45-51.
8. Singh, V.; Daharwal, S.; Suresh, P. A review of instrumental analytical methods to assay active ingredients in multicomponent pharmaceutical formulations. *Columb. J. Pharm. Sci.* **2014**, *1*, 27-39.
9. Qi, M.; Wang, P.; Zhou, L.; Sun, Y. Simultaneous determination of four active components in a compound formulation by liquid chromatography. *Chromatographia.* **2003**, *58*, 183-186.
10. Belal, T.; Abdel-Hay, K.; Clark, R. Selective determination of dimenhydrinate in presence of six of its related substances and potential impurities using a direct GC/MS method. *J. Adv. Res.* **2016**, *7*, 53-58.
11. Gergov, G.; Alin, A.; Doychinova, M.; De Luca, M.; Simeonov, V.; Al-Degs, Y. Assessment of different PLS algorithms for quantification of three spectrally overlapping drugs. *Bull. Chem. Comm.* **2017**, *49*, 410-421.
12. Khajehsharifi, H.; Sadeghi, M.; Pourbasheer, E. Spectrophotometric simultaneous determination of ceratine, creatinine, and uric acid in real samples by orthogonal signal correction-partial least squares regression. *Chemical Monthly.* **2009**, *140*, 685-691.
13. Gabrielsson, J.; Jonsson, H.; Airiau, C.; Schmidt, B.; Escott, R.; Trygg, J. OPLS methodology for analysis of pre-processing effects on spectroscopic data. *Chemom. Intell. Lab. Syst.* **2006**, *84*, 153-158.
14. Svensson, O.; Kourti, T.; MacGregor, J. An investigation of orthogonal signal correction algorithms and their characteristics. *J. Chemomet.* **2002**, *16*, 176-188

15. Al-Degs, Y.; El-Sheik, A.; Issa, A.; Al-Ghouthi, M.; Sunjuk, M. A simple and accurate analytical method for determination of three commercial dyes in different water systems using partial least squares regression. *Wat. Sci. Technol.* **2012**, *66*, 1647-1655.
16. Goicoechea, H.; Olivieri, A. Simultaneous determination of phenobarbital and phenytoin in tablet preparations by multivariate spectrophotometric calibration. *Talanta.* **1998**, *47*, 103-108
17. Haaland, D.; Thomas, E. Partial least-squares methods for spectral analyses. 1. Relation to other quantitative calibration methods and the extraction of qualitative information. *Anal. Chem.* **1988**, *60*, 1193-1202.
18. Andersson, M. A comparison of nine PLS1 algorithms. *J. Chemomet.* **2009**, *23*, 518-529
19. Noor, P.; Khanmohammadi, M.; Roozbehani, B.; Garmarudi, A. Evaluation of ATR-FTIR spectrometry in the fingerprint region combined with chemometrics for simultaneous determination of benzene, toluene, and xylenes in complex hydrocarbon mixtures. *Chem. Month.* **2018**, *149*, 1341-1347.
20. Lorber, A.; Faber, K.; Kowalski, B. Net analyte signal calculation in multivariate calibration. *Anal. Chem.* **1997**, *69*, 1620-1626.
21. Yousefinejad, S.; Hemmateenejad, B. Simultaneous spectrophotometric determination of paracetamol and para-aminophenol in pharmaceutical dosage forms using two novel multivariate standard addition methods based on net analyte signal and rank annihilation factor analysis. *Drug test. Anal.* **2012**, *4*, 507-514.
22. El-Sheikh, A.; Al-Jafari, M.; Sweileh, J. Solid phase extraction and uptake properties of multi-walled carbon nanotubes of different dimensions towards some nitro-phenols and chloro-phenols from water, *Int. J. Env. Anal. Chem.* **2012**, *92*, 190-209.
23. El-Sheikh, A.; Sweileh, J.; Saleh, M. Partially-pyrolyzed olive pomace sorbent of high permeability for preconcentration of metals from environmental waters, *J. Hazard. Mat.* **2009**, *169*, 58-64.
24. Al-Hashimi, N.; Aleih, H.; Fafous, I.; AlKhatib, H. Multi-Walled Carbon Nanotubes as Efficient Sorbent for the Solid Bar Microextraction of non-Steroidal Anti-Inflammatory Drugs from Human Urine Samples. *Curr. Pharm. Anal.* **2018**, *14*, 239-246.

Chemical Composition and Comparative Antibacterial Properties of Basil Essential Oil against Clinical and Standard Strains of *Campylobacter* spp.

Aysegul Mutlu-Ingok^{1,2*}, Burcu Firtin¹, Funda Karbancioglu-Guler¹

¹ Istanbul Technical University, Faculty of Chemical and Metallurgical Engineering, Department of Food Engineering, Istanbul, Turkey.

² Duzce University, Akcakoca Vocational School, Food Technology Department, Duzce, Turkey.

ABSTRACT

This study has aimed to evaluate comparative antibacterial activity of basil essential oil against clinical and standard isolates of *Campylobacter* spp. by different methods as agar well diffusion, agar and broth dilution methods. Gas Chromatography (GC) and Gas Chromatography/Mass Spectrometry (GC/MS) analysis were also examined to determine the chemical composition of the tested essential oil. GC/MS analysis showed that, basil essential oil was predominated by methyl chavicol (86.6%) followed by 1,8-cineole (2.8%) and α -bergamotene (2.4%). Although, inhibition zone diameters were in the range of 10.9 ± 0.8 to 21.8 ± 1.4 mm, higher MIC values were obtained against clinical strains compared with standard ones. Due to the differences in antimicrobial resistance of the clinical and standard strains, antimicrobial activity tests should be carried out with isolates from different sources.

Keywords: Basil essential oil, Chemical composition, Agar well diffusion, Broth microdilution, Agar dilution.

INTRODUCTION

Campylobacter spp. is considered to be the most common bacterial cause of human gastroenteritis in the world¹. Food-borne *Campylobacter* infections are considered to be caused by animal origin foods, mainly poultry and poultry products. Besides poultry, raw milk, pork, beef, lamb and seafood are responsible of *Campylobacter* infections². The antimicrobial resistance of

*Corresponding Author: Aysegul Mutlu-Ingok, e-mail: aysegulmutlu@duzce.edu.tr

Aysegul Mutlu-Ingok ORCID Number: 0000-0001-9571-0053

Burcu Firtin ORCID Number: 0000-0002-4633-9582

Funda Karbancioglu-Guler ORCID Number: 0000-0001-6576-0084

(Received 15 January 2019, accepted 23 February 2019)

thermophilic campylobacters, including *Campylobacter jejuni* and *C. coli* has been identified especially to tetracyclines and fluoroquinolones at important levels in many different parts of the world¹⁻³. Using chemical compounds have limits because of their carcinogenic effects, acute toxicity, and environmental hazard potential⁴. Increasing resistance to currently used antimicrobials and consumer concerns about using chemical preservatives lead to investigation of alternative strategies to prevent and control these microorganisms. Despite the high number of studies on the antimicrobial effects of essential oils (EOs), most studies have focused on pathogenic bacteria like *Staphylococcus aureus*, *Escherichia coli*, and *Bacillus cereus*⁵.

Essential oils which were synthesized naturally in different plant parts are complex volatile compounds. They can be extracted from medicinal aromatic plants and have strong antimicrobial activity against various bacterial, fungal, and viral pathogens. In addition to their antibacterial properties, they have antiviral, antimycotic, antitoxigenic, antiparasitic, insecticidal, antimutagenicity, cytoprotective, moderation of insulin secretion analgesic, neuroprotective, antioxidant, antiproliferative proapoptotic anxiolytic-like activities⁶. Their wide range of antimicrobial activity was a result of different types of aldehydes, phenolics, terpenes, and other antimicrobial compounds⁴. Mechanism of antimicrobial action is still lacking although a few studies have been elucidated⁷.

Basil is the common name for the culinary herb *Ocimum basilicum* of the family Lamiaceae (Labiatae). Although the basil essential oil's antibacterial activity is associated with its high content in linalool and estragole, antimicrobial spectrum is restricted to specific bacteria other than *Campylobacter* spp.⁸ Although in few studies antimicrobial activity of basil essential oil against *Campylobacter* spp. has been mentioned^{9,10}, our literature review revealed that the differences of antimicrobial effects against clinical and standard *Campylobacter* isolates were not discussed.

In this study, it was aimed to evaluate comparative antibacterial activity of basil essential oil against clinical and standard isolates of *Campylobacter jejuni* and *Campylobacter coli* by different methods as agar well diffusion, agar and broth dilution methods. Gas Chromatography (GC) and Gas Chromatography/Mass Spectrometry (GC/MS) analyses also examined the chemical composition of the tested EO.

METHODOLOGY

Bacterial culture and essential oils

The antimicrobial activity of the cold pressed basil essential oil was tested

against clinical *Campylobacter jejuni*, *Campylobacter coli* identified by Matrix-Assisted Laser Desorption/Ionization time-of-flight Mass Spectrometry (MALDI TOF MS)¹¹ and standard *Campylobacter jejuni* (ATCC 33660), *Campylobacter coli* (NCTC 12525). Basil essential oil was obtained in food grade form from “International Flavors & Fragrances (IFF)”, Gebze, Kocaeli (Turkey). Dilutions were made in 10% dimethyl sulfoxide (DMSO, Merck). Before analysis, basil essential oil was sterilized by filtration through 0.22 µm filters (Minisart® Syringe Filter, Sartorius Stedim Biotech GmbH, Germany) and stored in dark at 4 °C.

Gas Chromatography (GC)

Essential oils were analyzed by GC-FID using an Agilent 7890B GC (Agilent, Palo Alto, CA) with a flame ionization detector (FID). The chromatographic separation was accomplished using an Agilent HP- Innowax column (60 m x 0.25 mm Ø, with 0.25 µm film thickness) with a helium as a carrier gas (0.7 mL/ minute). GC oven temperature was kept at 60 °C for 10 min and programmed to 220 °C at a rate of 4 °C/ minute and then kept constant at 220 °C for 10 min and programmed to 240 °C at a rate of 1 °C/ minute. The injector and flame ionization detector temperatures were adjusted to 250 °C. The relative percentage amounts of the separated compounds were calculated from FID chromatograms.

Gas Chromatography-Mass Spectrometry (GC/MS)

The essential oils were analyzed by GC/MS using an Agilent 7890B GC coupled with a 5977B MSD (Agilent, Palo Alto, CA). The same column and analytical conditions were used for both GC/MS and GC/FID. The mass range was recorded from m/z 35 to 425. The injector temperature was adjusted to 250 °C. MS were recorded at 70 eV. Alkanes were used as reference points in the calculation of relative retention indices (RRI). The components of EOs were identified by using Wiley 9- Nist 11 Mass Spectral Database and standard Alkan series (C7-C40).

Agar-well diffusion assay

Inhibition zone diameters were determined using previously described method with slight modifications¹². Bacterial inoculum was prepared in Mueller-Hinton Broth (MHB, Merck, Darmsdat, Germany) for standard isolate and MHB with 5% horse blood for clinical isolate and incubated at 42 °C for 48 h under microaerophilic conditions created by Anaerocult® C (Merck, Darmsdat, Germany). Concentrations of bacterial suspensions were adjusted to approximately 10⁸ cfu/mL and 100 µL of culture suspension was spreaded on *Camp-*

ylobacter Blood-Free Selective Agar Base medium (modified CCDA, Merck, Darmsdat, Germany) for standard isolate, Mueller-Hinton Agar (MHA, Merck, Darmsdat, Germany) medium with 5% horse blood for clinical isolate. Three wells were cut out of agar and filled with 5 μ L, 10 μ L and 20 μ L of basil EO. The inoculated plates were incubated at 42 °C for 48 h under microaerophilic conditions. After incubation, inhibition zone diameters were measured. All experiments were performed in triplicate. Zones of inhibition (including the 6 mm of the well) were expressed as mean values with \pm standard deviation.

Broth microdilution assay

Broth microdilution method was used to determine the minimum inhibition concentrations (MICs), which was described previously by Wiegand et al.¹³. Stock solution was prepared in 10% DMSO and two-fold serial dilutions of EO were prepared. After sub-culturing in MHB, bacterial concentration was adjusted to approximately 10^8 cfu/mL. The 96-well plates were prepared by dispensing, into each well, 95 μ L of MHB, 100 μ L of EO and 5 μ L of the inoculants. The final volume in each well was 200 μ L. The microplates were incubated at 42 °C for 24 h under microaerophilic conditions. MIC values were determined spectrophotometrically by measuring the optical density at an absorbance of 600 nm (Synergy HT, BioTek Instruments Inc., Winooski, VT, USA). Negative controls (involving 195 μ L of MHB and 5 μ L of inoculum but no EO) for each microorganism and sterility controls (involving 100 μ L MHB and 100 μ L EO but no inoculum) for each EO concentrations were prepared.

Agar dilution method

For clinical strains, to determine minimum inhibitory concentrations (MICs), agar dilution method according to Stepanović et al.¹⁴ was used with slight modifications. This method based on preparation of MHA with 5% horse blood with the additions of 1% Tween 20 and different concentration of essential oils after sterilization of agar. Test plates were prepared with 19 mL of MHA, and 1 mL of two-fold dilutions of essential oils. After adjusting bacterial concentration approximately to 10^8 cfu/mL, 10 μ L of culture suspension was inoculated to agar plates. Plates were incubated for 48 h at 42 °C in microaerophilic conditions. The MICs were defined as the lowest concentration of essential oils that inhibited visible growth of microorganisms.¹⁴

RESULTS AND DISCUSSION

The chemical composition of the basil EO determined with GC/MS is given in Table 1. The main compound identified in the basil essential oil was methyl chavicol (86.6%). These results are consistent with those reported in the lite-

perature. Differences of constituents and their amounts may be related with the geographical origin of the plant, different parts of plants, extraction method and season of harvest¹⁵.

Table 1. Chemical compositions of basil essential oil.

No	Compound	RI ^a	Peak area (%) ^b
1	1,8-Cineole	1220	2.8
2	α-Bergamotene	1605	2.4
3	Methyl chavicol	1701	86.6
Total			91.8

^a: Retention index was calculated for all volatile constituents using a homologous series of n-alkanes C7- C40, b: Peak area obtained by GC-FID.

Although different chemical profiles of basil essential oil were reported in literature, methyl chavicol with high citral contents (methyl chavicol/citral) was previously detected as a “new chemo type” in the Turkish basil¹⁶. In addition to geological origin, chemical constituents varied with different seasons¹⁷. Generally, the chemical composition profile of basil essential oil confirms previous studies. Methyl chavicol was reported as major constituent in India (78.3%)¹⁸. In another study, three chemotypes of *Ocimum basilicum* (*O. basilicum*) were identified as a major methyl chavicol-rich type (>65%), a methyl chavicol (55%)-linalool (20–30%) type, a linalool (42–45%) and eugenol (15%) type¹⁹. For this respect, *O. basilicum* used in this study was in methyl chavicol-rich type with 86.6% methyl chavicol. High content of methyl chavicol was also confirmed by Vieira and Simon²⁰ with 47% methyl chavicol content.

The inhibition zone diameters measured ranged from 12.3±1.6 to 21.8±1.4 mm and 10.9±0.8 to 20.4±2.4 mm for clinical and standard *Campylobacter* isolates, respectively (Table 2). Considering the all results, mean inhibition zone diameter was 15.94±1.55 mm. Similar to current study, mean zone diameters were reported as 12.48 mm and 13.2 mm against gram positive and gram negative bacteria, respectively²¹. Smaller inhibition zones were also reported by Predoi et al.²² as 7–10 mm against *Escherichia coli*, *Staphylococcus aureus* and methicillin-resistant *Staphylococcus aureus*. In literature, inhibition zone diameters were varied depending on different extracts. It was reported that although methanol extracts showed inhibition zones against *Pseudomonas aeruginosa*, *Shigella* sp., *Listeria monocytogenes*, *Staphylococcus aureus* and two different strains of *Escherichia coli*, chloroform and acetone extracts of *O. basilicum* had no effect²³.

Poor solubility and high volatility of essential oils limit the usage of diffusion tests. It is suggested to use agar or broth dilution methods for true antimicrobial activity evaluation²⁴. With this respect, in this study, *in vitro* antimicrobial activity of basil essential oil was not tested only by agar diffusion method but also dilution methods against clinical and standard isolates of *Campylobacter* spp. (Table 2). It was reported that both agar dilution and broth microdilution methods were equally suitable against *Campylobacter* spp. and highly correlated²⁵. In this study, since broth microdilution method did not give any results against clinical strains, agar dilution method was used by taking this perspective into consideration. Tested essential oil displayed varying degree of antibacterial activity with MIC values ranging from 105.16 to 1787.7 µg/mL. Interestingly, MIC values against clinical ones were higher than standard isolates. Higher MIC values indicate that clinical strains are more resistant than standard strains against basil essential oil.

Table 2. Antimicrobial activity of basil essential oil against *Campylobacter* spp.

Isolate	Amount (µL)			MIC (µg/mL)
	5 µL	10 µL	20 µL	
	Inhibition zone diameter (mm)			
<i>C. jejuni</i> (Clinical)	NA ^a	13.0±2.2	20.1±1.6	1787.7
Streptomycin ^b	38.0±1.8	40.0±2.4	45.0±1.4	NT ^c
<i>C. coli</i> (Clinical)	NA	12.3±1.6	21.8±1.4	889.08
Streptomycin	32.0±1.4	38.0±1.4	40.0±1.3	NT
<i>C. jejuni</i> (ATCC 33560)	NA	10.9±0.8	20.4±2.4	105.16
Streptomycin	21.3±2.1	24.7±1.5	30.0±1.3	NT
<i>C. coli</i> (NCTC 12525)	NA	11.8±1.1	17.2±1.3	219.88
Streptomycin	21.7±1.6	24.8±0.7	28.8±1.3	NT

^aNA: No activity, ^b: Standard antibiotic, ^c: Not tested

Although the same MIC values were reported for essential oils against different strains in literature, in this study differences in MIC values were found against the clinical and standard strains of *Campylobacter*. In literature, different MIC values were reported. Antibacterial and antifungal activities of essential oils of twelve *Ocimum basilicum* L. cultivars which were grown in Serbia were investigated by Beatovic et al.²⁶. However, lower MIC values than current study were reported, they were ranging from 0.009-11.74 µg/mL. Silveira et al.²⁷, reported MIC values from 0.075 to 2.5 µg/mL against *S. aureus*, *L. monocytogenes*, *B. cereus*, *Yersinia enterocolitica*, *E. coli* and *S. typhimurium*. In another study, mean MIC values were detected as 0.75 and 0.73 µg/mL against 6 gram positive and 12 gram negative bacteria respectively²¹. Higher MIC values were also repor-

ted for gram positive bacteria as 18-36 µg/mL, and for gram-negative bacteria as 9-18 µg/mL²⁸. By the existence of different EO components with respect to harvesting season differences as well as extraction method, different antimicrobial activity levels can be obtained. These differences may be due to this fact¹⁵.

Antimicrobial spectrum of basil essential oil was reported as restricted to specific bacteria as *Staphylococcus* spp., *Enterococcus* spp., *E. coli*, *P. aeruginosa*, *Acinetobacter baumannii*, *Aeromonas hydrophila*, *B. cereus*, *Bacillus subtilis*, *Enterobacter* spp., *Listeria* spp., *Proteus* spp., *Salmonella* spp., *Serratia marcescens*, and *Y. enterocolitica* and fungi as *Candida* spp., *Rhodotorula* spp., and *Saccharomyces cerevisiae*⁸. Although basil essential oil has restricted antimicrobial activity, in current study it has also been proven that it has antimicrobial activity against *Campylobacter* spp.

This study described antibacterial efficiency differences of basil essential oil against clinical and standard isolates of *Campylobacter* spp., as well as the chemical composition of corresponding essential oil. The results indicated that tested EO has varying degree of antibacterial efficiency against both *C. jejuni* and *C. coli* isolates. However, with *in vitro* experiments, *in vivo* studies are also required because antimicrobial effect showed differences even between clinical and standard strains. In addition, optimum essential oil concentration should be determined to ensure antimicrobial activity and acceptable sensorial properties.

ACKNOWLEDGEMENTS

The authors wish to thank Anadolu University, Medicinal Plants, Drugs and Scientific Research Center for GC and GC-MS analyses of basil essential oil. This research was supported by Istanbul Technical University, Scientific Research Projects (Project no, 38819).

REFERENCES

1. WHO. The Global View of Campylobacteriosis, Report of an expert Consultation. Utrecht, Netherlands, **2002**.
2. Nachamkin, I.; Szymanski, C. M.; Blaser M. J. *Campylobacter* (No. Ed. 3). ASM Press. ProQuest Ebook Central, **2008**, 54.
3. Moore J. E; Barton, M. D., Blair, I. S., Corcoran, D., Dooley, J. S., Fanning S., Kempf, I.; Lastovica, A. J.; Lowery, C. J.; Matsuda, M.; McDowell, D.A.; McMahon, A.; Millar, B. C.; Rao, J. R.; Rooney, P. J.; Seal, B. S.; Snelling, W. J.; Tolba, O. The epidemiology of antibiotic resistance in *Campylobacter*. *Microbes Infect*, **2006**, 8, 1955-1966.
4. Swamy, M. K.; Akhtar, M. S.; Sinniah, U. R. Antimicrobial properties of plant essential oils against human pathogens and their mode of action: an updated review. *Evid Based Complement Alternat Med*, **2016**, 3012462.

5. Mutlu-Ingok, A.; Karbancioglu-Guler, F. Cardamom, Cumin, and Dill Weed Essential Oils: Chemical Compositions, Antimicrobial Activities, and Mechanisms of Action against *Campylobacter* spp. *Molecules*, **2017**, *22*, 1191.
6. Joshi, R. K. Role of Natural Products against Microorganisms. *Am J Clin Microbiol Antimicrob.*, **2018**, *1*, 1005.
7. Chouhan, S.; Sharma, K.; Guleria, S. Antimicrobial Activity of Some Essential Oils—Present Status and Future Perspectives. *Medicines*, **2017**, *4*, 58.
8. Sakkas, H.; Papadopoulou, C. Antimicrobial Activity of Basil, Oregano, and Thyme Essential Oils. *J Microbiol Biotechnol*, **2017**, *28*, 429-438.
9. Smith-Palmer, A.; Stewart, J.; Fyfe, L. Antimicrobial properties of plant essential oils and essences against five important food-borne pathogens. *Lett Appl Microbiol*, **1998**, *26*, 118–122.
10. Friedman, M.; Henika, P. R.; Mandrell, R. E. Bactericidal activities of plant essential oils and some of their isolated constituents against *Campylobacter jejuni*, *Escherichia coli*, *Listeria monocytogenes*, and *Salmonella enterica*. *J Food Protect*, **2002**, *65*, 1545–1560.
11. Şamlı, A.; Ayaş, R.; Ülger, N. Akut bakteriyel gastroenterit etkenleri arasında *Campylobacter* türlerinin yeri ve antibiyotiklere duyarlılıkları. ‘Ulusal Klinik Mikrobiyoloji Kongresi, **2013**, 408.
12. Deans, S.; Ritchie, G. Antimicrobial properties of plant essential oils. *Int J Food Microbiol*, **1987**, *5*, 165-180.
13. Wiegand, I.; Hilpert, K.; Hancock, R. E. W. Agar and broth dilution methods to determine the minimal inhibitory concentration (MIC) of antimicrobial substances. *Nat. Protoc.* **2008**, *3*, 163–175.
14. Stepanović, S.; Antić, N.; Dakić, I.; Švabić-Vlahović, M. In vitro antimicrobial activity of propolis and synergism between propolis and antimicrobial drugs. *Microbiol Res*, **2003**, *158*, 353-357.
15. Burt, S. Essential oils: Their antibacterial properties and potential applications in foods—a review. *Int J Food Microbiol*, **2004**, *94*, 223–253.
16. Telci, I.; Bayram, E.; Yılmaz, G.; Avcı, B. Variability in essential oil composition of Turkish basils (*Ocimum basilicum* L.). *Biochem. Syst. Ecol.*, **2006**, *34*, 489-497.
17. Hussain, A. I.; Anwar, F.; Sherazi, S. T. H.; Przybylski, R. Chemical composition, antioxidant and antimicrobial activities of basil (*Ocimum basilicum*) essential oils depends on seasonal variations. *Food Chem.*, **2008**, *108*, 986-995.
18. Chowdhury, J. U.; Bhuiyan, M. N. H.; Saha, G. C.; Nada, K.; Rahim, M. Compositions of the essential oils from two types of *ocimum basilicum* introduced in Bangladesh. *Bangladesh J Sci Ind Res*, **2013**, *48*, 217-220.
19. Yayi, E.; Moudachirou, M.; Chalchat, J. C. Chemotyping of three *Ocimum* species from Benin: *O. basilicum*, *O. canum* and *O. gratissimum*. *J Essent Oil Res.*, **2001**, *13*, 13-17.
20. Vieira, R. F.; Simon, J. E. Chemical characterization of basil (*Ocimum* spp.) found in the markets and used in traditional medicine in Brazil. *Econ Bot.*, **2000**, *54*, 207-216.
21. Gaio, I.; Saggiorato, A. G.; Treichel, H.; Cichoski, A. J.; Astolfi, V.; Cardoso, R. I.; ... &

Cansian, R. L. Antibacterial activity of basil essential oil (*Ocimum basilicum* L.) in Italian-type sausage. *J Verbrauch Lebensm*, **2015**, *10*, 323-329.

22. Predoi, D.; Iconaru, S. L.; Buton, N.; Badea, M. L.; Marutescu, L. Antimicrobial Activity of New Materials Based on Lavender and Basil Essential Oils and Hydroxyapatite. *Nanomaterials*, **2018**, *8*, 291.

23. Kaya, I.; Yigit, N.; Benli, M. Antimicrobial activity of various extracts of *Ocimum basilicum* L. and observation of the inhibition effect on bacterial cells by use of scanning electron microscopy. *Afr J Tradit Complement Altern Med.*, **2008**, *5*, 363-369.

24. Suppakul, P.; Miltz, J.; Sonneveld, K.; Bigger, S. W. Antimicrobial properties of basil and its possible application in food packaging. *J. Agric. Food Chem.*, **2003**, *51*, 3197-3207.

25. Luber, P.; Bartelt, E.; Genschow, E.; Wagner, J.; Hahn, H. Comparison of broth microdilution, E Test, and agar dilution methods for antibiotic susceptibility testing of *Campylobacter jejuni* and *Campylobacter coli*. *J. Clin. Microbiol.*, **2003**, *41*, 1062-1068.

26. Beatovic, D.; Krstic-Milosevic, D.; Trifunovic, S.; Siljegovic, J.; Glamoclija, J.; Ristic, M.; Jelacic, S. Chemical composition, antioxidant and antimicrobial activities of the essential oils of twelve *Ocimum basilicum* L. cultivars grown in Serbia. *Records of Natural Products*, **2015**, *9*, 62.

27. Silveira, S. M. D.; Cunha Júnior, A.; Scheuermann, G. N.; Secchi, F. L.; Vieira, C. R. W. Chemical composition and antimicrobial activity of essential oils from selected herbs cultivated in the South of Brazil against food spoilage and foodborne pathogens. *Ciência Rural*, **2012**, *42*, 1300-1306.

28. Moghaddam, A. M. D.; Shayegh, J.; Mikaili, P.; Sharaf, J. D. Antimicrobial activity of essential oil extract of *Ocimum basilicum* L. leaves on a variety of pathogenic bacteria. *J. Med. Plants Res.*, **2011**, *5*, 3453-3456.

***In vitro* Antimicrobial and Antioxidant Activity Evaluation of *Melampyrum arvense* L. var. *elatius* Boiss. and *Sedum spurium* M. Bieb. Extracts**

Ayşe Esra Karadağ^{1*}, Fatma Tosun¹

¹ Istanbul Medipol University, School of Pharmacy, Department of Pharmacognosy, Istanbul, Turkey

ABSTRACT

Sedum spurium M. Bieb. (Crassulaceae) is a common ornamental plant, whereas, *Melampyrum arvense* L. var. *elatius* Boiss. (Orobanchaceae) is a semi-parasitic plant and grows naturally in the fields. In this study, the dichloromethane and ethyl acetate extracts of *M. arvense* and *S. spurium* were evaluated for their *in vitro* antioxidant and antimicrobial activities. The antioxidant activity was evaluated by DPPH[•]-ABTS[•] methods. The antimicrobial activity of *S. spurium* and *M. arvense* extracts was determined using the *in vitro* broth microdilution assay against following human pathogenic strains; *Staphylococcus aureus* ATCC 6538, *Enterococcus faecalis* ATCC 29212, *Escherichia coli* NRLL B-3008, *Helicobacter pylori* ATCC 43504, *Mycobacterium smegmatis* ATCC 25291, *Mycobacterium avium* ssp. *avium* and *Pseudomonas aeruginosa* ATCC 10145.

The extracts showed weak antimicrobial activity against Gram-negative/positive bacteria, having the MIC values of 500-1000 µg/mL. Antibacterial activity was not observed against *Mycobacteria* at 2000 µg/mL. In addition, antioxidant activity of *M. arvense* ethyl acetate extract was higher than those of the other extracts.

Keywords: *Melampyrum arvense*, *Sedum spurium*, Antibacterial, Antioxidant, *Mycobacteria*

INTRODUCTION

Melampyrum L. genus is an annual and semi-parasitic plant group. It is represented by two species, *M. arvense* and *M. pratense* in the Flora of Turkey¹. Iridoid glycosides were the major bioactive secondary metabolites of

*Corresponding Author: Ayşe Esra Karadağ, e-mail: aeguler@medipol.edu.tr

Ayşe Esra Karadağ ORCID Number: 0000-0002-3412-0807

Fatma Tosun ORCID Number: 0000-0003-2533-5141

(Received 28 January 2019, accepted 26 February 2019)

Melampyrum species². The previous *in vitro* studies showed that *Melampyrum* extracts have antioxidant, protein kinase C inhibitory, antimalarial, cytotoxic and antiprotozoal activities³⁻⁵ and it is used as animal fodder traditionally⁶. *Sedum* L. is represented by 43 species in Turkey⁷⁻⁸. It is reported that several *Sedum* species have wound healing properties and were used as diuretic and laxative and as well as for the treatment of various diseases such as hemorrhoids in folk medicine⁹⁻¹¹. The major components of *Sedum* species have been described as alkaloids and flavonoids in previous studies¹²⁻¹⁶.

The aim of the present study was evaluation of the antimicrobial and antioxidant activities of *M. arvense* and *S. spurium* extracts. The phenolic compound composition of the extracts was analyzed by High Performance-Liquid Chromatography (HPLC).

METHODOLOGY

Plant Material and Extraction

M. arvense and *S. spurium* were collected in the vicinity of Trabzon-Tonya and Trabzon-Hamsiköy, respectively. Plants were identified by Prof. M. Vural and voucher specimens have been deposited at Herbarium of the Department of Pharmacognosy, School of Pharmacy, Istanbul Medipol University, Istanbul, Turkey. (Voucher specimens no. IMEF: 1055 and IMEF: 1142 resp.) The air-dried and coarsely ground aerial parts of plant material were macerated with 70% ethanol. The extract was filtered and evaporated to dryness *in vacuo* (Heidolph, Germany), and then dissolved in a water-ethanol (90:10) mixture and extracted with dichloromethane and ethyl acetate, respectively.

Antioxidant Activity

DPPH[•] and ABTS[•] Scavenging Assay

The antioxidant capacity was determined in terms of hydrogen donating or radical scavenging ability using DPPH[•] by its capability to bleach the stable radical¹⁷. The reaction mix contained 100 µM DPPH[•] in methanol and dichloromethane or ethyl acetate extracts. After 30 min, absorbance was read at 517 nm by using a UV-Vis spectrophotometer (UV-1800, Shimadzu, Japan) at 25 ± 2°C and the radical scavenging activity (RSA) was determined as the percentage of radical reduction as follows:

$$\text{DPPH}^{\bullet} \text{ RSA } \% = \left[\frac{\text{Absorbance}_{\text{control}} - \text{Absorbance}_{\text{test sample}}}{\text{Absorbance}_{\text{control}}} \right] \times 100$$

The total antioxidant activity of the samples was measured using the ABTS radical cation decolorization assay¹⁸. ABTS[•] was produced by reacting 7 mM

aqueous ABTS[•] with 2.45 mM potassium persulfate. The reaction mixture was left at room temperature overnight (12–16 h) in the dark. The resulting intensely colored ABTS radical cation was diluted with ethanol. Absorbance was measured at 734 nm at room temperature. The assay was performed in triplicate. Negative controls in which 990 µL ethanol was substituted for ABTS[•] were used. The assay was carried out on Trolox as a positive control¹⁹. The results were expressed as IC₅₀ as follows:

$$\text{ABTS}^{\bullet}\text{ RSA } \% = \left[\frac{\text{Absorbance}_{\text{control}} - \text{Absorbance}_{\text{test sample}}}{\text{Absorbance}_{\text{control}}} \right] \times 100$$

Each experiment was performed in triplicate. The IC₅₀ value of the extracts was calculated from a calibration graph. Test results are presented as mean ± standard deviation (SD). Statistical analysis of antioxidant test results was completed using one-way ANOVA with the SPSS 23.0 software. A difference in the mean values of $P < 0.05$ was considered to be statistically significant.

Antimicrobial Activity

The antimicrobial activity of the extracts was determined using the broth microdilution assay²⁰ to determine the minimum inhibitory concentrations (MIC). *Staphylococcus aureus* ATCC 6538, *Enterococcus faecalis* ATCC 29212, *Escherichia coli* NRLL B-3008, and *Pseudomonas aeruginosa* ATCC 10145 strains were grown in Mueller Hinton Broth (MHB) at 37°C in aerobic conditions for 24 h. All microorganisms were standardized to McFarland No: 0.5.

Helicobacter pylori ATCC 43504 strain was grown for 24 hours in Brucella broth containing 5% (v/v) horse blood and 10% (h/h) fetal bovine serum at 37°C in an anaerobic incubator (5% CO₂). After incubation at 37°C, 100 µL *H. pylori* (2x10⁷ CFU/mL) strain was transferred to the microplate evaluation²¹⁻²². Diluted bacterial suspensions were added to each well and then allowed to incubate at 37 °C for further 24 h.

Mycobacteria strains were inoculated in Middlebrook 7H11 agar and incubated in aerobic conditions at 37 °C for 4-5 days. The microorganism was transferred to media and incubated for a further five days. Diluted bacterial suspensions (10⁶ CFU/mL) were added to each well and then allowed to incubate at 37 °C for 5 days²³⁻²⁵.

Test samples stock solution was prepared in dimethyl sulfoxide and serial dilutions were prepared for each sample. The minimum non-reproductive concentration was reported as minimum inhibitory concentration (MIC). The MIC was calculated as the mean of three repetitions.

HPLC Analysis

The HPLC analyses studied on an Agilent (1200 LC) and UV-Vis detector (G1314A). HPLC was run on an Agilent C18 column (4.6 x 250 mm x 5 μ m) and its temperature was maintained at 40°C. The mobile phases were Solvent A: Acetonitrile: Water (10:90, v/v) and Solvent B: Acetonitrile: Water (90:10, v/v). The composition of solvent B was increased from 15% to 100% in 35 min, and at a flow rate of 0.6 mL/min. The injection volume is 10 μ L²⁶. Phenolic compounds were identified by matching their retention times against those of the standards analyzed under the same conditions (Figure 1).

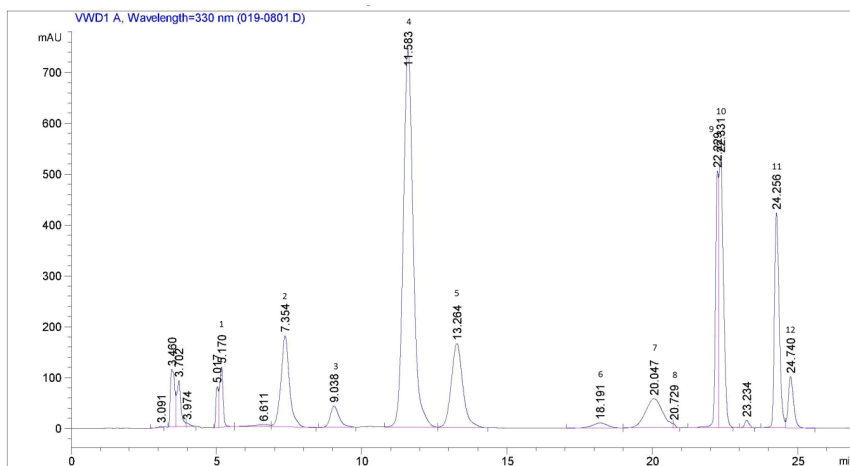


Figure 1. HPLC Chromatogram of References

1, Chlorogenic acid (RT: 5.1); 2, Caffeic acid (RT: 7.3); 3, Luteolin-O-Glycoside (RT: 9.03); 4, Coumaric acid (RT: 11.5); 5, Ferulic acid (RT: 13.2); 6, Rosmarinic acid (RT: 18.1); 7, Myrcetin (RT: 20.04); 8, Eriodictyol (RT: 20.7); 9, Luteolin (RT: 22.2); 10, Quercetin (RT: 22.3); 11, Apigenin (RT: 24.2); 12, Gallic acid (RT: 24.7)

RESULTS AND DISCUSSION

Antioxidant Activity

Antioxidant activities of the ethyl acetate and dichloromethane extracts of *M. arvensis* and *S. spurium* were measured by the ability to scavenge DPPH free radicals and ABTS radical scavenging method, by comparing with Ascorbic acid and Trolox, respectively. Antioxidant capacities were expressed by IC₅₀ values, indicating the extracts concentrations scavenge 50% of ABTS radical. It was observed that ethyl acetate extract of *M. arvensis* has higher antioxidant capacity than those of the other extracts. The results were shown in Table

1. Although there is no detailed study of antioxidant activity on *M. arvensis*, the results of previous studies on antioxidant activities other *Melampyrum* species were similar to those of the current study results^{3, 27}. As shown in a previous study²⁸, phenolic compounds found in the *M. barbatum* extract may be responsible for the antioxidant activity. To the best of our knowledge, this is the first report on the antioxidant capacity of *M. arvensis* extract.

Table 1. ABTS and DPPH radical scavenging activities of extracts

ABTS and DPPH radical scavenging activities + [IC ₅₀ ± SD (mg/mL)]					
	1	2	3	4	References
ABTS*	0,19 ± 0,04	1,43 ± 0,03	1.54 ± 0,04	2.01 ± 0,03	0,015 ± 0,001 (Trolox)
DPPH*	0,16 ± 0,03	1,13 ± 0,04	1.41 ± 0,03	1,97 ± 0,04	0,002 ± 0,001 (Ascorbic acid)

1: *M. arvensis* ethyl acetate extract; 2: *M. arvensis* dichloromethane extract; 3: *S. spurium* ethyl acetate extract; 4: *S. spurium* dichloromethane extract

Antimicrobial Activity

Antimicrobial activities of *M. arvensis* and *S. spurium* extract were evaluated according to their MIC values against various strains. Table 2 shows antimicrobial activities of *M. arvensis* and *S. spurium* extracts against bacterial strains. The results revealed that the extracts have weak antimicrobial activity against Gram-negative/positive bacteria with the MIC values in the range to 500-1000 µg/mL. Antibacterial activity was not observed against *Mycobacterias* at 2000 µg/mL. In a previous study, antimicrobial activity of *S. spurium* essential oil was evaluated²⁹ but this is the first report on antimicrobial activity evaluation of *S. spurium* extracts. Also, the results obtained by Tosun and co-workers in a previous study of different *Mycobacteria* strains on the *S. spurium* extract were similar to the results of the current study³⁰.

Table 2. Antimicrobial activity of extracts (MICs in µg/mL).

Bacteria Sample	E. a.	S. a.	P. a.	E. f.	H. p.	M. a.	M. s.
1	>2000	1000	500	500	>2000	>2000	>2000
2	>2000	1000	500	500	>2000	>2000	>2000
3	>2000	>2000	>2000	1000	>2000	>2000	>2000
4	>1000	>2000	>2000	1000	1000	>2000	>2000
Chloramphenicol	8	8	>32	16	16	-	-
Tetracycline	16	0.25	>16	0.025	0.025	-	-
Amikacin	-	-	-	-	-	250	250

1: *M. arvense* ethyl acetate extract; 2: *M. arvense* dichloromethane extract; 3: *S. spurium* ethyl acetate extract; 4: *S. spurium* dichloromethane extract

E.a.: *Escherichia coli*; *S.a.*: *Staphylococcus aureus*; *Pa.*: *Pseudomonas aeruginosa*; *E.f.*: *Enterococcus faecalis*; *H.p.*: *Helicobacter pylori*; *M.a.*: *Mycobacterium avium*; *M.s.*: *Mycobacterium smegmatis*

HPLC Analysis

The phytochemical constituents of the extracts were analyzed using HPLC technique. The phenolic compounds of *M. arvense* ethyl acetate extract was characterized as chlorogenic acid, caffeic acid, luteolin-7-O-glycoside, coumaric acid, ferulic acid, and quercetin (Figure 2). The high antioxidant capacity of *M. arvense* ethyl acetate extract may be due to the aforementioned phenolic compounds. It was reported that the phenolic compounds were responsible for the antioxidant activity in the previous studies on *Melampyrum* species³. In addition, eriodictyol, luteolin and quercetin were detected in *S. spurium* ethyl acetate extract by HPLC (Figure 3).

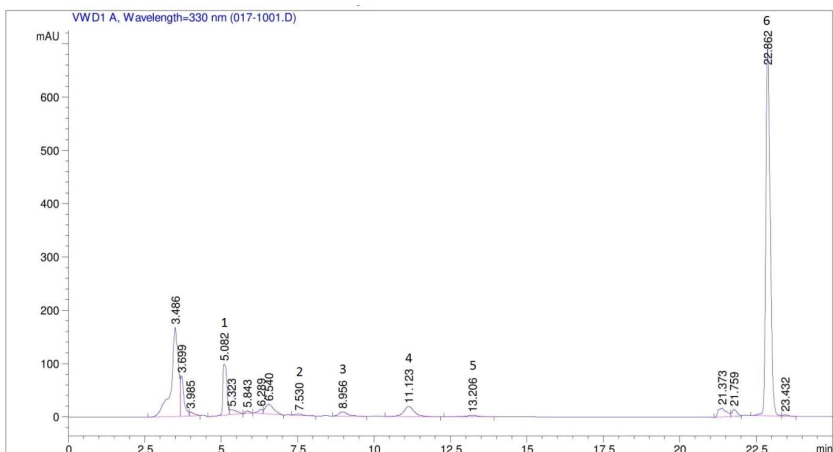


Figure 2. HPLC Chromatogram of *M. arvense* methanol extract

1, Chlorogenic acid (RT: 5.082); 2, Caffeic acid (RT: 7.5); 3, Luteolin-O-Glycoside (RT: 9.03); 4, Coumaric acid (RT: 11.5); 5, Ferulic acid (RT: 13.206); 6, Quercetin (RT: 22.3)

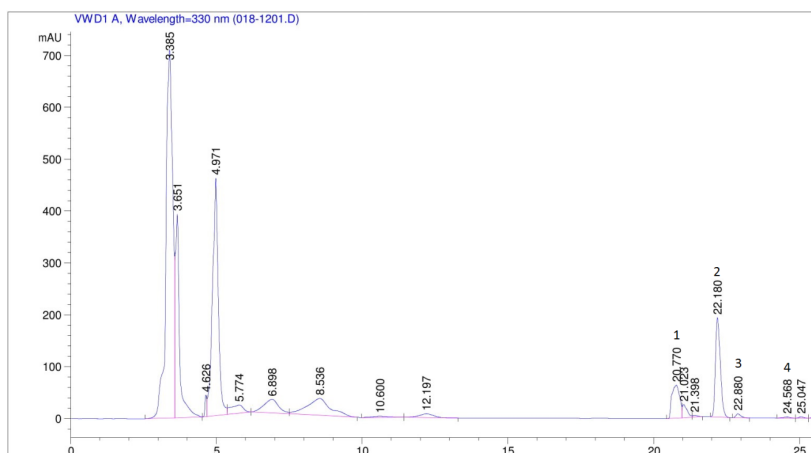


Figure 3: HPLC Chromatogram of *S. spurium* methanol extract

1, Eriodictyol (RT: 20.7); 2, Luteolin (RT: 22.2); 3, Quercetin (RT: 22.3)

REFERENCES

1. Davis, P.H. In *Flora of Turkey and the East Aegean Islands*, Vol 6, Edinburgh University Press, Edinburgh, **1978**.
2. Damtoft, S.; Hansen, S. B.; Jacobsen, B.; Jensen, S. R.; Nielsen, B. J. Iridoid glucosides from *Melampyrum*. *Phytochemistry*. **1984**, *23*, 2387-2389.
3. Štajner, D.; Popović, B. M.; Boža, P.; Kapor, A. Antioxidant capacity of *Melampyrum barbatum*—Weed and medicinal plant. *Phytother. Res.* **2009**, *23*, 1006-1010.
4. Kirmizibekmez, H.; Atay, I.; Kaiser, M.; Brun, R.; Cartagena, M. M.; Carballeira, N. M.; Yeşilada E.; Tasdemir, D. Antiprotozoal activity of *Melampyrum arvense* and its metabolites. *Phytother. Res.* **2011**, *25*, 142-146.
5. Galkin, A.; Jokela, J.; Wahlsten, M.; Tammela, P.; Sivonen, K.; Vuorela, P. Discovering protein kinase C active plants growing in Finland utilizing automated bioassay combined to LC/ MS. *Nat. Prod. Commun.* **2009**, *4*, 139-142.
6. Korkmaz, M.; Karakuş, S.; Selvi, S.; Çakılcıoğlu, U. Traditional knowledge on wild plants in Üzümlü (Erzincan-Turkey). *Indian J. Trad. Know.* **2016**, *15*, 538-545.
7. Hart, H.; Alpınar, K. *Sedum L.* In: Güner, A.; Özhatay, N.; Ekim, T.; Başer, K. H. C., *Flora of Turkey and the East Aegean Islands*, Vol. 11. Edinburgh, Edinburgh University Press, **2000**, pp 127.
8. Chamberlain, D. F. *Sedum L.* (Crassulaceae). In: Davis PH, ed., *Flora of Turkey and the East Aegean Islands*, Vol. 4, Edinburgh, Edinburgh University Press, **1972**, pp 224.
9. Baytop, T. In *Therapy with Medicinal Plants in Turkey-Past and Present*, 2nd ed.; Nobel Publishers: Istanbul, **1999**, pp 480.
10. Zeybek, N.; Zeybek, U. In *Farmasotik Botanik*, Ege University Press, Izmir, **1994**, pp 390.
11. Karahan, F.; Oz, I.; Demircan, N.; Stephenson, R. Succulent plant diversity in Turkey: Stonecrops (Crassulaceae). *Haseltonia*, **2006**, *12*, 41-54.
12. Bandyukova, V. A.; Shinkarenko, A. L. Paper-chromatographic determination of flavonoids in high-altitude plants of the Teberda reservation. *Farm Zh*, **1965**, *26*, 37-41.
13. Franck, B. Sedum alkaloids. II. Alkaloids in *Sedum acre* and related species. *Ber.* **1958**, *91*, 2803-2818.
14. Stevens, J. F.; Hart, H. T.; Elema, E. T. Flavonoid variation in Eurasian *Sedum* and *Sempervivum*. *Phytochemistry*, **1996**, *41*, 503-512.
15. Gill, S.; Raszeja, W.; Szykiewicz, G. Occurrence of nicotine in some species of the genus *Sedum*. *Farmacja Polska*, **1979**, *35*, 151-153.
16. Franck, B.; Hartmann, W. The *Sedum* alkaloids. *Abhandl Deut Akad Wiss Berlin KI. Chem. Geol. Biol.* **1963**, *4*, 111-119.
17. Blois, M. S. Antioxidant determinations by the use of a stable free radical. *Nature*. **1958**, *181*, 1199.
18. Re, R.; Pellegrini, N.; Proteggente, A.; Pannala, A.; Yang, M.; Rice-Evans, C. Antioxidant activity applying an improved ABTS radical cation decolorization assay. *Free Rad. Biol. Med.* **1999**, *26*, 1231-1237.

19. Okur, M. E.; Ayla, Ş.; Çiçek Polat, D.; Günal, M. Y.; Yoltaş, A.; Biçeroğlu, Ö. Novel insight into wound healing properties of methanol extract of *Capparis ovata* Desf. var. *palaestina* Zohary fruits. *J. Pharm. Pharmacol.* **2018**, *70*, 1401-1413.
20. Clinical and Laboratory Standards Institute M7-A7. In *Methods for Dilution Antimicrobial Susceptibility Tests for Bacteria That Grow Aerobically*, Approved Standard-Seventh Edition; CLSI document A. Wayne, Pa. USA. **2006**, 26.
21. EUCAST clinical breakpoints for *Helicobacter pylori*. European Committee on Antimicrobial Susceptibility Testing, **2011**.
22. Whitmire, J. M.; Merrell, D. S. Successful culture techniques for *Helicobacter* species: general culture techniques for *Helicobacter pylori*. *Methods Mol. Biol.* **2012**, *921*, 17-27.
23. Clinical and Laboratory Standards Institute, In *Susceptibility testing of Mycobacteria, Nocardiae, and Other Aerobic Actinomycetes*, Approved Standard; CLSI document M24-A. Wayne, Pa., **2003**, USA.
24. Lee, S. M.; Kim, J.; Jeong, J.; Park, Y. K.; Bai, G.; Lee, E. Y.; Lee, M. K.; Chang, C. L. Evaluation of the Broth Microdilution Method Using 2,3-Diphenyl-5-thienyl-(2)-tetrazolium Chloride for Rapidly Growing *Mycobacteria* Susceptibility Testing, *J. Korean Med. Sci.* **2007**, *22*, 784-90.
25. Chung, G. A.; Aktar, Z.; Jackson, S.; Duncan, K. High-Throughput Screen for Detecting Antimycobacterial Agents. *Antimicrob. Agents Chemother.* **1995**, *39*, 2235-2238.
26. Toplan, G. G.; Kurkcuoglu, M.; Goger, F.; İşcan, G.; Ağalar, H. G.; Mat, A.; Baser, K. H. C.; Koyuncu, M.; Saryar, G. Composition and biological activities of *Salvia veneris* Hedge growing in Cyprus. *Ind. Crop. Prod.* **2017**, *97*, 41-48.
27. Háznagy-Radnai, E.; Wéber, E.; Czige, S.; Berkecz, R.; Csédő, K.; Hohmann, J. Identification of iridoids, flavonoids and triterpenes from the methanolic extract of *Melampyrum bihariense* A. Kern. and the antioxidant activity of the extract. *Chromatographia*, **2014**, *77*, 1153-1159.
28. Galishevskaya, E. E.; Petrichenko, V. M. Phenolic compounds from two *Melampyrum* species. *Pharm. Chem. J.* **2010**, *44*, 497-500.
29. Yaylı, N.; Yaşar, A.; Yılmaz İskender, N.; Yaylı, N.; Cansu, T. B.; Coşkunçelebi, K.; Karaoğlu, Ş. Chemical constituents and antimicrobial activities of the essential oils from *Sedum pallidum* var. *bithynicum* and *S. spurium* grown in Turkey. *Pharm. Biol.* **2010**, *48*, 191-194.
30. Tosun, F.; Akyüz Kızılay, Ç.; Şener, B.; Vural, M. The evaluation of plants from Turkey for *in vitro* antimycobacterial activity. *Pharm. Biol.* **2005**, *43*, 58-63.

Preparation and *In vitro* Characterization of a Fluconazole Loaded Chitosan Particulate System

Gülsel Yurtdaş Kırmılioğlu^{1*}, Evrim Yenilmez¹, Ebru Başaran¹, Yasemin Yazan¹

¹Anadolu University, Faculty of Pharmacy, Department of Pharmaceutical Technology, 26470 Eskişehir, Türkiye

ABSTRACT

In the present study fluconazole (FZ) was successfully incorporated into cationic chitosan nanoparticles prepared by spray-drying method aiming dermal delivery. Particle size and zeta potential measurements, drug content, morphological, thermal and XRD analyses and FZ quantification by HPLC analyses were performed for characterizing the formulations prepared. Release behavior of FZ from the nanoparticles was determined using a Franz-diffusion cell. Thermal and XRD analyses results indicated that FZ was molecularly dispersed in chitosan nanoparticles. Cationic chitosan nanoparticles released FZ for 180 minutes indicative of the extended release of the drug. *In vitro* characterization results demonstrated that chitosan nanoparticles seem to be promising for enhancement of dermal delivery of FZ and could decrease potential side effects and reduce the potential of drug resistance.

Keywords: Fluconazole, Chitosan, Nanoparticles, Spray-drying, Franz-diffusion cell.

INTRODUCTION

Incorporation techniques of lipophilic drug active ingredients with poor aqueous solubility are used particularly in pharmaceutical technology for drug delivery design. Advantages of encapsulation include enhanced stability of labile drugs, controlled drug release and improved drug bioavailability.¹

Dermal delivery by topical preparations such as creams, gels and lotions are limited due to the barrier characteristics of *Stratum corneum*. This limitation hinders the drug deposition and leads to relatively poor stability of active

*Corresponding Author: Gülsel Yurtdaş Kırmılioğlu, e-mail: gyurtdas@anadolu.edu.tr

Gülsel Yurtdaş Kırmılioğlu ORCID Number: 0000-0001-8897-0885

EvrımYenilmez ORCID Number: 0000-0002-7979-0089

Ebru Başaran ORCID Number: 0000-0003-2104-2069

Yasemin Yazan ORCID Number: 0000-0002-7492-1668

(Received 08 March 2019, accepted 22 March 2019)

agents by direct exposure to UV light. ²

Fluconazole (FZ) is a triazole antifungal agent (**Figure 1**) with poor aqueous solubility administered either orally or intravenously.³ It is used in the treatment of oropharyngeal and esophageal candidiasis, urinary tract infections, pneumonia, peritonitis and serious systemic candidal infections.^{4,5} Adverse effects of FZ were reported to be related to the gastro-intestinal tract including abdominal pain, diarrhea, flatulence, nausea and vomiting. Other side effects associated with FZ are headache, dizziness, leucopenia, thrombocytopenia, hyperlipidemias, and raise in liver enzyme values. Serious hepatotoxicity was also reported while anaphylaxis, angioedema and skin reaction were rarely reported.⁵

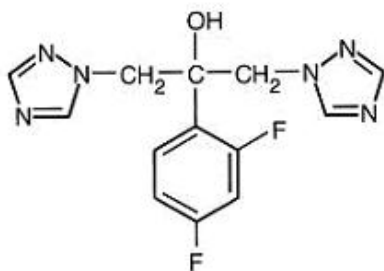


Figure 1. Chemical structure of fluconazole

Several classes of antifungal agents can be used in the treatment of candidiasis. However, among the factors influencing the efficacy of therapy is the immunity of the patient. Clinical failure following therapy may exist in patients with advanced immunodeficiency. In such cases, high doses of drugs or the use of multiple agents may be required thereby increasing the risk of serious side effects. To avoid this complication, entrapment of antifungal agents like FZ in a particulate delivery system can be used with several advantages such as the possibility of targetting the drug to the desired site in a controlled/sustained pattern. In this manner, therapeutic efficacy may be increased while reducing the side effects.^{6,7} Some antifungal agents have been entrapped in particulate delivery system and promising results were observed in animal models and clinical therapy. These studies include mainly the polyene drugs, represented by amphotericin B and nystatin.^{7,8} There are many studies regarding azole antifungal particulate drug delivery systems. ^{9,10}

Chitosan gained an increasing interest as a pharmaceutical excipient.¹¹ Chitosan is a hydrophilic, biocompatible and biodegradable polymer with low toxicity. It was investigated extensively for pharmaceutical and medical purposes including incorporation of therapeutic agents, proteins, enzymes, DNA and cells, formulation for oral vaccines and stabilization of liposomes.^{12,13} Among the pharmaceutical applications of chitosan are the use as a vehicle for directly compressed tablets, as a disintegrant, a binder, a granulating agent in ground mixtures, as a drug carrier for sustained release preparations as well as a co-grinding diluent for the enhancement of dissolution rate and bioavailability of water insoluble drugs.¹⁴ Furthermore, chitosan has mucoadhesive properties due to the molecular attraction formed by electrostatic interactions between positively charged chitosan and negatively charged mucosal surfaces.^{15,16}

Spray drying represents a single-step, cheap, continuous and scalable process dedicated for converting liquids into dry, free-flowing powders which enables the production of particles with controlled size and morphological aspects.¹⁷ Spray drying also eliminates the addition of crosslinking agent minimizes the swelling of chitosan based nanoparticles.¹² Therefore, spray drying technology was utilized in this study for the formulation of cationic nanoparticles using advantages of the method.

The objective of this study was to formulate chitosan-based cationic particulate systems containing FZ with high encapsulation efficiency and prolonged effect for reducing side effects and improving its stability. Chitosan nanoparticles were prepared by the spray-drying technique for topical skin fungal infections. Particle size, particle size distribution and thermal behaviour of the polymeric lattice were analyzed. Drug loading and release of the incorporated FZ were analyzed using a validated HPLC method.

METHODOLOGY

Materials

FZ was a kind gift from Bilim İlaç (Türkiye). Chitosan was purchased from Fluka Chemicals (Germany), acetic acid from Sigma-Aldrich (Germany) and ethanol from Carlo Erba (Italy). Sodium chloride, methanol and acetonitrile were the products of Merck (Germany).

Preparation of chitosan nanoparticles

Formulations were prepared using Mini Spray Dryer (B-190, BUCHI, Switzerland). The spray dryer was connected to the Inert Loop B-295 (Buchi Labortechnik AG, Switzerland) due to the organic solvent. Carbon dioxide gas was used at a flow rate of 120 L.min⁻¹. The residual oxygen level in the system was controlled below 4%.

When preparing particulate systems by spray-drying method, it has to be kept in the mind that production parameters such as size of nozzle, feeding pump rate, inlet temperature and compressed air flow rate, affect the particle size.^{12,18} It was reported that smaller particles are formed with lower feeding pump rate and smaller nozzle size. In addition, smaller particles are formed with greater volume of air input where particle size is not dependent inlet temperature in the range of 120-180°C.¹²

Briefly, FZ and chitosan were dissolved in 96% (v/v) ethanol and 2% (v/v) acetic acid solutions, respectively. The solutions were mixed and homogenized at 1500 rpm for 3 hours. The final clear solution was then spray-dried with an inlet temperature of 145°C ± 1°C and an outlet temperature of 50°C ± 3°C. White dry powders were obtained and kept in tightly closed vials at room temperature until being analyzed. The placebo formulation was prepared as described above without the addition of FZ. These were bare, empty nanoparticles.

Composition of the formulations was kept as simple as possible (**Table 1**).

Table 1. Compositions of the formulations prepared

CODE	FZ	Chitosan	Acetic acid	Ethanol
Placebo	-	2 g	240 mL (%2 v/v)	240 mL
C-FZ-1	0.2 g	2 g	240 mL (%2 v/v)	240 mL
C-FZ-2	0.5 g	2 g	240 mL (%2 v/v)	240 mL

Characterization of chitosan nanoparticles

Particle size and zeta potential analyses

Particle size, particle size distribution (PDI) and zeta potential measurements of the formulations prepared were performed on freshly prepared samples using Malvern Nano ZS (Zetasizer Nano Series, Worcestershire, UK). Samples of all formulations were dispersed in double distilled water (adjusted to a constant conductivity of 50 µS.cm⁻¹ using 0.9% NaCl) just prior to analyses. All analyses were repeated in triplicate at 25°C ± 2°C.

Morphology

The particle shape and surface characteristics of the freshly prepared nanoparticle formulations and FZ were investigated by scanning electron microscope (SEM) (HITACHI TM3030Plus Tabletop Microscope, Japan) at 25°C ± 2°C. Samples were coated with a thin layer gold under argon to avoid charging under the electron beam.

Thermal analysis

Thermal behaviors and the interactions between FZ and chitosan were analyzed using differential scanning calorimetry (DSC) (DSC-60, Shimadzu Scientific Instruments, Columbia, MI, USA). In DSC analyses, the heating rate of $10^{\circ}\text{C}\cdot\text{min}^{-1}$ was employed in the temperature range of 50°C - 200°C . Analyses were carried out under nitrogen with a scan rate of $5\text{ K}\cdot\text{min}^{-1}$.

X-ray diffractometry analysis

Dry powder X-ray diffractometry (XRD) analyses were performed using RIKAGU D/Max-3C (Japan). The XRD analysis range was 2°C - 40°C over 2θ with $2^{\circ}\text{C}\cdot\text{min}^{-1}$ scanning rate, with 40 kV voltage and current intensity level of 30 mA.

Pure FZ and placebo formulation were also analyzed and those XRD spectra were used as references in evaluating the chitosan nanoparticles containing FZ.

Determination of FZ content of chitosan nanoparticles

For the quantification of FZ incorporated into FZ formulations, accurately weighed (5 mg) formulations were dissolved in acetic acid (2%, v/v) solution and ethanol (5 mL, 4:1) mixture and agitated at 4000 rpm for 3 min. 1 mL of supernatant was collected. Drug content of nanoparticles was determined using the reversed-phase HPLC method equipped with a pump (LC 10-AD), a UV detector (SPD-20A), a data station (Shimadzu, Japan) and C_{18} column (250 mm x 4.6 mm i.d. and $5\ \mu\text{m}$ particle size). The mobile phase consisting of distilled water (tetrabutylammonium hydrogen sulfate): acetonitrile (75:25, v/v) was degassed prior to the analysis. The flow rate was $1\text{ mL}\cdot\text{min}^{-1}$ with an injection volume of $25\ \mu\text{L}$. The oven temperature was adjusted to $30^{\circ}\text{C} \pm 1^{\circ}\text{C}$ and FZ was monitored at 223 nm.

In vitro release studies of FZ from chitosan nanoparticles

In vitro release studies were performed using Franz diffusion cells.² The diffusion cells were thermoregulated with a water jacket at 32°C . Polypropylene membrane was placed on a Franz diffusion cell after keeping it 20 minutes in the donor compartment. The receptor chamber was filled with distilled water. 1000 μg of formulation was applied to the donor compartment. 0.5 mL aliquots were withdrawn from the receptor compartment at specific time intervals. The amounts withdrawn were replaced by the fresh distilled water. The amount of FZ in aliquots was analyzed by a validated HPLC method and release profiles were obtained.

RESULTS AND DISCUSSION

Preparation of chitosan nanoparticles

In this study, spray-drying method was successfully used to prepare chitosan nanoparticles since it does not involve toilsome procedures and avoids the use of harsh cross-linking agents and organic solvents which might possibly trigger chemical reactions with the active agent.¹⁹

Characterization of chitosan nanoparticles

Particle size and zeta potential measurements

Particle size is one of the important physical properties of colloidal systems. Particle size distribution of the formulation is especially significant in the physical stability and activity of colloidal systems.²⁰ It was also found that the size of nanoparticles play an important role in their adhesion to and interaction with the biological cells.²¹ Particle sizes of formulations were found to be 552.50 ± 10.30 nm and 648.25 ± 8.81 nm for C-FZ-1 and C-FZ-2, respectively (**Table 2**). It was found that decrease in the amount of FZ in formulations was in parallel with the relative decrease in average particle size.

Table 2. Mean particle size, PDI and zeta potential values of formulations prepared (SE: Standard error) (n=3)

Code	Particle size (nm) \pm SE	PDI \pm SE	Zeta Potential (mV) \pm SE
Placebo	410.00 ± 11.41	0.480 ± 0.018	7.0 ± 4.1
C-FZ-1	552.50 ± 10.30	0.450 ± 0.083	38.4 ± 0.2
C-FZ-2	648.25 ± 8.81	0.313 ± 0.051	40.4 ± 2.3

The acceptable value for PDI is 0.05-0.7; values greater than 0.7 indicate very broad size distribution and probably no suitability for dynamic light scattering technique.²² As shown in **Table 2**, acceptable PDI values were obtained for all batches. Also, PDI data showed that the homogeneity increased with the addition of FZ into the formulations.²³

Zeta potential of nanoparticles is commonly used to characterize the surface property of nanoparticles. Results showed that zeta potentials measured were 38.4 ± 0.2 mV and 40.4 ± 2.3 mV for C-FZ-1 and C-FZ-2, respectively, which may be attributed to the positive charges on polymeric matrices indicating adequate physical stability. Cationic chitosan nanoparticles with mucoadhesive properties may interact with the negatively charged of skin and open up the tight junctions of epithelial cells to allow the paracellular transport pathway resulting in an increase in bioavailability of the active agents.^{16,21}

Morphology

SEM images of pure FZ and formulations were demonstrated in **Figure 2**. SEM images showed that all formulations prepared were nearly in spherical shape while some of the spheres reminded the collapsed balloons with smooth surfaces. Crystalline structure of FZ was not observed in the formulations indicating successful incorporation of FZ into the polymeric matrices.²⁴

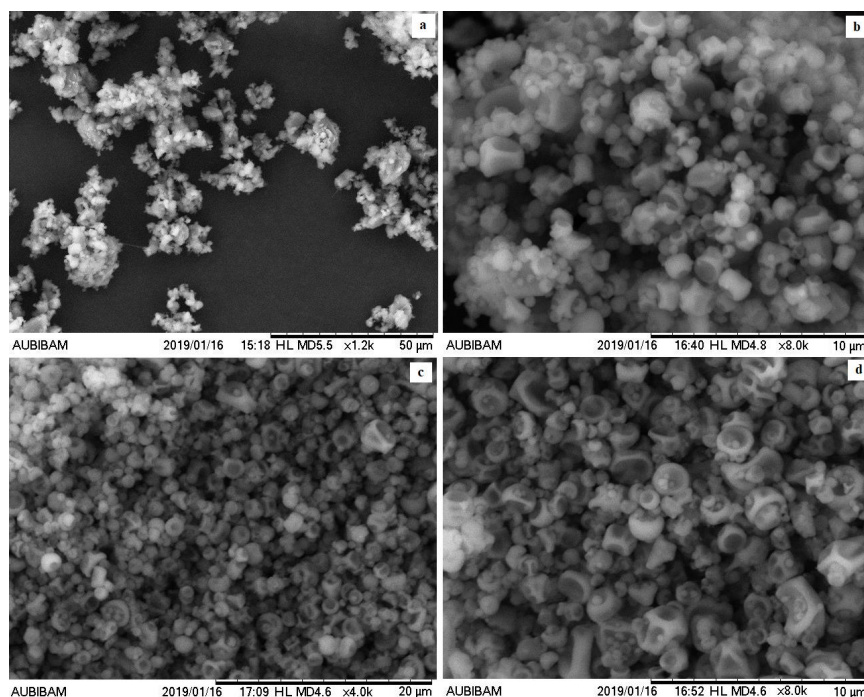


Figure 2. SEM images of pure fluconazole and chitosan nanoparticles prepared (a: FZ, b: placebo formulation, c: C-FZ-1, d: C-FZ-2).

Thermal analysis

DSC was in order to determine the incorporation of FZ into the polymeric network and also the status of polymer and active agent after spray-drying process.¹¹

The thermogram of FZ shows the simple thermal behaviour of the drug (**Figure 3a**). The sharp endothermic peak the observed at 142.66°C is the first order solid-liquid phase transition corresponding to the melting of the drug.³ Placebo formulation (**Figure 3b**) was characterized by its amorphous state since no endothermic peak was observed. In the DSC thermogram of formula-

tions, sharp peak belonging to FZ was not observed (**Figure 3c**). There may be two explanations of this peak disappearance. First explanation is the molecular incorporation of FZ into chitosan nanoparticles. When FZ was molecularly dispersed within the polymeric matrix resulting in a solid solution, the endothermic peak of FZ has disappeared.^{11,12,25} Second explanation is the dilution effect of the polymer network. When the ratio of drug:polymer is so small, the massive amount of polymer shades the endothermic peak of the drug.²⁶

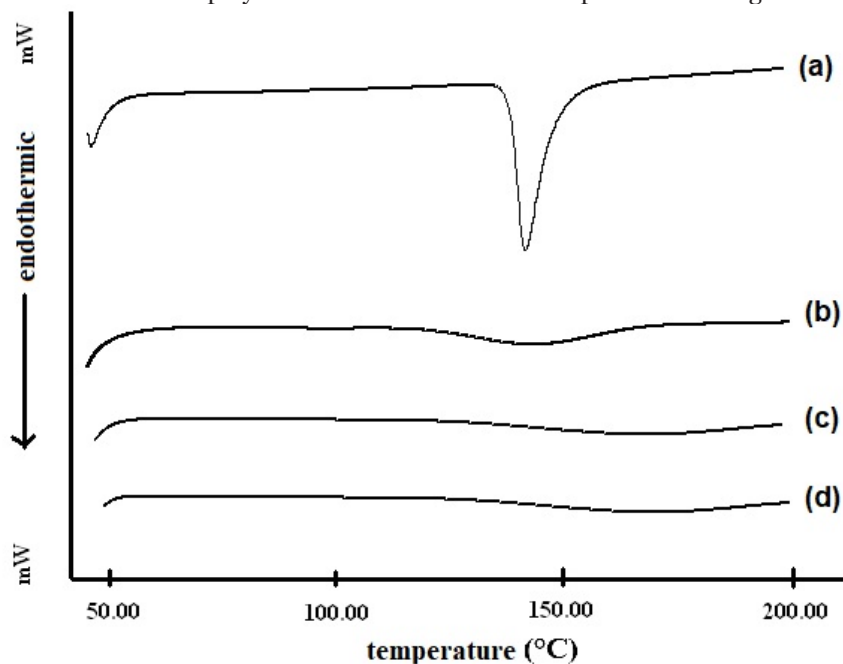


Figure 3. DSC thermograms of pure fluconazole and chitosan nanoparticles prepared (a: FZ, b: placebo formulation, c: C-FZ-1, d: C-FZ-2).

X-ray diffractometry analysis

DSC and XRD play a prominent role in the characterization of polymeric matrices because they are able to provide structural information on the dispersed particles.²⁷ Therefore, in this study for better evaluation of the crystalline polymeric structure of polymeric particles DSC and XRD analyses were performed simultaneously.

Dry powder XRD analyses of nanoparticles confirmed the DSC results showing the amorphous state of the polymeric network. XRD patterns of pure FZ, placebo and formulations were demonstrated in **Figure 4**. The FZ spectrum

shows several sharp diffraction peaks typical of its crystalline state (**Figure 4a**) while placebo and FZ-containing formulations were of amorphous state with no sharp XRD peaks in the spectra (**Figure 4b and Figure 4c**). In the patterns of the FZ loaded formulations, peaks corresponding to FZ disappeared, indicating that dispersion in an amorphous form.^{13,26}

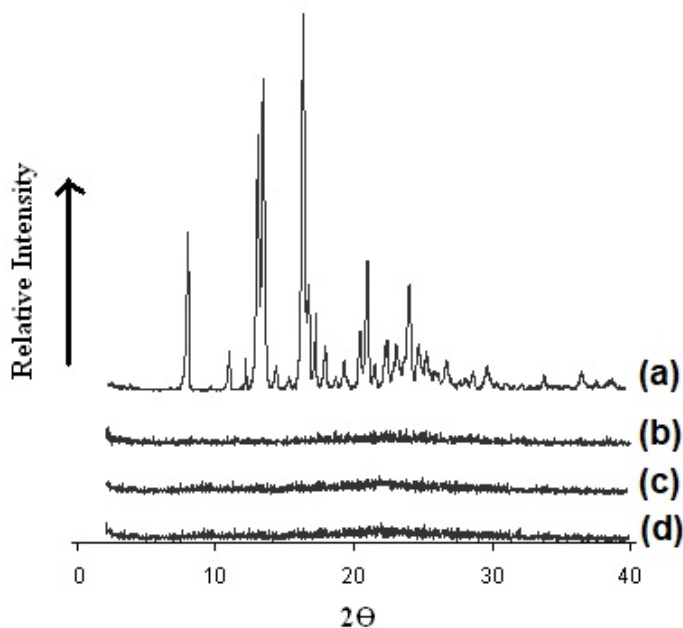


Figure 4. X-ray diffraction of patterns of pure fluconazole and chitosan nanoparticles prepared (a: FZ, b: placebo formulation, c: C-FZ-1, d: C-FZ-2).

Determination of FZ content of formulations

A validated HPLC method used for the determination of FZ demonstrated that the incorporation efficiency of FZ in formulations were found to be 8.99 ± 0.54 % and 12.04 ± 2.05 % (mean \pm SE), for C-FZ-1 and C-FZ-2, respectively. It is evident from the data that incorporation efficiency was affected by the drug: polymer ratio. The results revealed that the incorporation efficiency of formulations was increased with increasing concentration of the active agent in the formulations.²¹ Relatively low incorporation efficiency of nanoparticles prepared may be attributed to the spray-drying parameters such as nozzle diameter, spraying rate or viscosity of the spraying solution.

In vitro drug release

In vitro dissolution test plays an important role in drug formulation development and quality control. It can be used not only primary tool to observe the consistency and stability of drug products but also as a relatively rapid and inexpensive process to estimate *in vivo* absorption of a drug formulation.¹¹

The *in vitro* release profile of FZ from formulations were shown in **Figure 5**. Franz diffusion cell analyses results showed that the release of FZ from formulations were 26.12 % and 29.52 % at the end of 180 minutes for C-FZ-1 and C-FZ-2, respectively. Flux (J) and permeation coefficient (k_p) values were determined using the slope of the steady-state portion of the amount of the drug permeated and divided by time. The steady-state flux (J_s) of FZ from the formulations were calculated to be $9.7 \times 10^{-2} \pm 0.001 \mu\text{g} \cdot \text{cm}^{-2} \cdot \text{h}^{-1}$ and $1.2 \times 10^{-1} \pm 0.0001 \mu\text{g} \cdot \text{cm}^{-2} \cdot \text{h}^{-1}$ while permeability coefficient (k_p) was determined to be $3.10 \times 10^{-3} \pm 0.001 \text{ cm} \cdot \text{h}^{-1}$ and 4.0565×10^{-4} for the C-FZ-1 and C-FZ-2, respectively. The results indicated that the release of FZ from the formulations varied depending on time.²

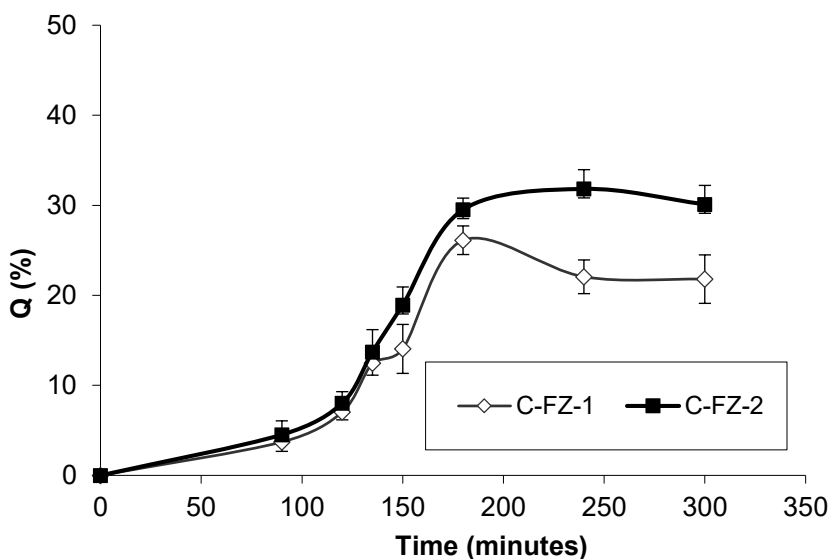


Figure 5. *In vitro* release profile of FZ from FZ loaded chitosan nanoparticles.

FZ was successfully incorporated into chitosan nanoparticles using a spray-drying method. *In vitro* characteristics of nanoparticles prepared were analyzed to confirm incorporation of FZ into the polymeric structure. When submicron sized with homogenous size distribution and nearly spherical nanoparticles

were prepared. DSC and XRD assays confirmed decrease in FZ crystallinity in cationic nanoparticles. Chitosan nanoparticles released FZ for 180 minutes indicative of the extended release of the drug, which will reduce the side effects in treating the infections induced by *Candida albicans*. With the cationic and mucoadhesive properties of chitosan-based system, nanoparticles will ensure longer residence at the infection site, providing a favorable release profile for the FZ for the dermal delivery.

Conclusively, chitosan nanoparticles may be good alternative for delivery of FZ, which need to be, investigated further using *in vivo* tests before final decision.

CONFLICT OF INTEREST

The authors declare no conflict of interest, financial or otherwise.

REFERENCES

1. Pandey, R.; Ahmad, Z.; Sharma, S.; Khuller, G. K. Nano-Encapsulation of Azole Antifungals: Potential Applications to Improve Oral Drug Delivery. *Int. J. Pharm.* **2005**, *301*, 268-276.
2. Yenilmez, E.; Başaran, E.; Yazan, Y. Release Characteristics of Vitamin E Incorporated Chitosan Nanoparticles and *In Vitro-In Vivo* Evaluation for Topical Application. *Carbohydr. Polym.*, **2011**, *84*, 807-811.
3. Yurtdaş, G.; Demirel, M.; Genç, L. Inclusion Complexes of Fluconazole with β -Cyclodextrin: Physicochemical Characterization and *In Vitro* Evaluation of Its Formulation. *J. Inc. Phenom. Macrocycl. Chem.* **2011**, *70*, 429-435.
4. Al-Marzouqi, A. H.; Elwy, H. M.; Shehadi, I.; Adem, A. Physicochemical Properties of Antifungal Drug-Cyclodextrin Complexes Prepared by Supercritical Carbon Dioxide and by Conventional Techniques. *J. Pharm. Biomed. Anal.*, **2009**, *49*, 227-233.
5. Sweetman, S.C., Fluconazole. In *Martindale: The Complete Drug Reference*, 36th ed. The Pharmaceutical Press: London, England, 2009; pp. 532.
6. Otsubo, T.; Maesaki, S.; Hossain, M.A.; Yamamoto, Y.; Tomono, K.; Tashiro, T.; Seki, J.; Tomii, Y.; Sonoke, S.; Kohno, S. *In Vitro* and *In Vivo* Activities of NS-718, A New Lipid Nanosphere Incorporating Amphotericin B, Against *Aspergillus Fumigatus*. *Antimicrob. Agents Chemother.* **1999**, *43*, 471-475.
7. Assis, D. N.; Mosqueira, V. C. F.; Vilela, J. M. C.; Andrade, M. S.; Cardoso, V. N. Release Profiles and Morphological Characterization by Atomic Force Microscopy and Photon Correlation Spectroscopy of 99m Technetium-Fluconazole Nanocapsules. *Int. J. Pharm.*, **2008**, *349*, 152-160.
8. Mehta, R. T.; Hopfer, R. L.; McQueen, T.; Juliano, R. L., Lopez-Berestein, G. Toxicity and Therapeutic Effects in Mice of Liposome-Encapsulated Nystatin for Systemic Fungal Infections. *Antimicrob. Agents Chemother.*, **1987**, *31*, 1901-1903.
9. Duret, C.; Wauthoz, N.; Sebti, T.; Vanderbist, F.; Amighi, K. New Inhalation-Optimized Itraconazole Nanoparticle-Based Dry Powders for The Treatment of Invasive Pulmonary Aspergillosis. *Int. J. Nanomedicine*, **2012**, *7*, 5475-5489.

10. Modi, J.; Joshi, G.; Sawant, K. Chitosan Based Mucoadhesive Nanoparticles of Ketconazole for Bioavailability Enhancement: Formulation, Optimization, *In Vitro* and *Ex Vivo* Evaluation. *Drug Dev. Ind. Pharm.*, **2013**, *39*, 540-547.
11. Yurtdaş-Kırımlioğlu, G.; Özer, S.; Büyükköroğlu, G.; Yazan, Y. Formulation and *In Vitro* Evaluation of Moxifloxacin Hydrochloride-Loaded Polymeric Nanoparticles. *Lat. Am. J. Pharm.*, **2018**, *37*, 1850-1862.
12. He, P.; Davis, S. S.; Illum, L. Chitosan Microspheres Prepared by Spray Drying. *Int. J. Pharm.*, **1999**, *187*, 53-65.
13. Grcic', J. F.; Voinovichb, D.; Moneghinib, M.; Lac'ana, B. C.; Magarotto, L.; Jalsenjak, I. Chitosan Microspheres with Hydrocortisone and Hydrocortisone-Hydroxypropyl- β -Cyclodextrin Inclusion Complex. *Eur. J. Pharm. Sci.*, **2000**, *9*, 373-379.
14. Sinha, V. R.; Singla A. K.; Wadhawan, S.; Kaushik, R.; Kumria, R.; Bansal, K.; Dhawan, S. Chitosan Microspheres as A Potential Carrier for Drugs. *Int. J. Pharm.*, **2004**, *274*, 1-33.
15. Shimoda, J.; Onishi, H.; Machida, Y. Bioadhesive Characteristics of Chitosan Microspheres To The Mucosa of Rat Small Intestine. *Drug Dev. Ind. Pharm.*, **2001**, *27*, 567-576.
16. Kockisch, S.; Rees, G. D.; Young, S.A.; Tsibouklis, J.; Smart, J.D. Polymeric Microspheres for Drug Delivery To The Oral Cavity: An *In Vitro* Evaluation of Mucoadhesive Potential. *J. Pharm. Sci.* **2003**, *92*, 1614-1623.
17. Re, M. Formulating Drug Delivery Systems by Spray Drying. *Dry Technol.* **2006**, *24*, 433-446.
18. Corrigan, D. O.; Healy, A. M.; Corrigan, O. I. Preparation and Release of Salbutamol from Chitosan and Chitosan Co-Spray Dried Compacts and Multiparticulates. *Eur J Pharm Biopharm.* **2006**, *62*, 295-305.
19. Agnihotri, S.A.; Mallikarjuna, N. N., Aminabhavi, T.A. Recent Advances on Chitosan-Based Micro- and Nanoparticles in Drug Delivery. *J Control Release.* **2004**, *100*, 5-28.
20. Takka, S.; Acartürk, F.; Ağabeyoğlu, İ.; Çelebi N.; Değim, T.; Değim, Z. Önformülasyon. In: Modern Farmasötik Teknoloji; Acartürk, F., Ağabeyoğlu, İ., Çelebi, N., Çelebi, T., Değim, T., Değim, Z., Doğanay, T., Takka, S., Tirnaksız, F., Eds.; Ankara, 2007; pp. 119-140.
21. Yurtdaş-Kırımlioğlu, G.; Yazan, Y. Formulation and *In Vitro* Characterization of Polymeric Nanoparticles Designed for Oral Delivery of Levofloxacin Hemihydrate, *Euro Int. J. Sci. Technol.* **2016**, *5*, 148-157.
22. Hasan, A. A.; Sabry, S. A.; Abdallah, M. H.; El-Damasy, D. A. Formulation and *In Vitro* Characterization of Poly(DL-Lactide-co-Glycolide)/Eudragit® RLPO or RS30D Nanoparticles as an Oral Carrier of Levofloxacin Hemihydrate. *Pharm. Dev. Technol.* **2016**, *21*, 655-663.
23. Lopedota, A.; Trapani, A.; Cutrignelli, A.; Chiarantini, L.; Pantucci, E.; Curci, R.; Manuali, E.; Trapani, G. The Use of Eudragit® RS 100/Cyclodextrin Nanoparticles for The Transmucosal Administration of Glutathione. *Eur. J. Pharm. Biopharm.*, **2009**, *72*, 509-520.
24. Yurtdaş-Kırımlioğlu, G.; Öztürk, A.A. Levocetirizine Dihydrochloride Loaded Chitosan Nanoparticles: Formulation and *In Vitro* Evaluation, *Turk. J. Pharm. Sci.* [Online early Access]. DOI: 10.4274/tjps.34392. Published online: September 20, 2018.

25. Cavalli, R.; Peira, E.; Caputo, O.; Gasco, M. R. Solid Lipid Nanocarriers as Carriers of Hydrocortisone and Progesterone Complexes with β -Cyclodextrins. *Int. J. Pharm.*, **1999**, *182*, 59-69.
26. Agnihotri, S. M.; Vavia, P. R. Diclofenac-Loaded Biopolymeric Nanosuspensions for Ophthalmic Application. *Nanomedicine: NBM*. **2009**, *5*, 90-95.
27. Bunjes, H.; Unruh, T. Characterization of Lipid Nanoparticles by Differential Scanning Calorimetry X-ray and Neutron Scattering. *Adv. Drug Deliv. Rev.* **2007**, *59*, 379-402.

REVIEW ARTICLES

Pharmaceutical Properties of Marine Polyphenols: An Overview

Vo Thanh Sang^{1*}, Ngo Dai Hung², Kim Se-Kwon³

¹ NTT Institute of Hi-Technology, Nguyen Tat Thanh University, Ho Chi Minh City, Vietnam.

² Faculty of Natural Sciences, Thu Dau Mot University, Thu Dau Mot City, Binh Duong Province, Vietnam.

³ Department of Marine Life Science, College of Ocean Science and Technology, Korea Maritime and Ocean University, Busan 606-791, Korea.

ABSTRACT

Natural products are non-drug materials that have applied for prevention or treatment of health problem. The use of natural products as pharmaceutical ingredients has got much attention by consumers nowadays. Among them, marine organisms are currently considered as a huge source for the discovery of pharmaceutical agents. During the last decades, numerous novel agents have been achieved from marine organisms and many of them have potential application in pharmaceutical industry. Notably, marine algae are known to be one of the most important producers of variety of chemically active metabolites. Especially, phlorotannins, a polyphenol from brown algae, have been revealed to possess numerous biological activities such as UV-protective, anti-oxidant, anti-viral, anti-allergic, anti-cancer, anti-inflammatory, anti-diabetes, and anti-obesity activities. Therefore, phlorotannins are promising agents for development of pharmaceutical products. This contribution focuses on phlorotannins from brown algae and presents potential application in pharmaceutical field due to its biological activities and health benefit effects.

Keywords: Natural product, Pharmaceutical, Phlorotannins, Algae, Bioactivity.

INTRODUCTION

The marine environment represents approximately half of the global biodiversity. It is a rich source of structurally diverse and biologically active metabolites, which are important for the discovery of potential therapeutic agents^{1, 2}. During the last decades, marine organisms have received much attention in screening marine natural products for their biomedical and pharmaceutical potentials³⁻⁵. Various marine organisms such as algae, tunicates, sponges, soft

*Corresponding Author: Vo Thanh Sang, email: vtsang@ntt.edu.vn; Tel.: +84 28 6271 7296

Vo Thanh Sang ORCID Number: 0000-0002-6726-3257

Ngo Dai Hung ORCID Number: 0000-0002-4025-1694

Kim Se-Kwon ORCID Number: 0000-0001-6507-9539

(Received 03 December 2018, accepted 15 January 2019)

corals, bryozoans, sea slugs, mollusks, echinoderms, fishes, microorganisms, etc. have been subjected for isolation of numerous novel compounds. Consequently, numerous active agents such as lipid, protein, peptide, amino acid, neurotoxins, polysaccharides, chlorophyll, carotenoids, vitamins, minerals, and unique pigments have been discovered. Many of these substances have been demonstrated to possess interesting biological activities⁶⁻¹⁴. Notably, marine algae are known to be one of the most important producers of biomass in the marine environment. Algae are very simple chlorophyll-containing organisms composed of one cell or grouped together in colonies or as organisms with many cells¹⁵. Therefore, they vary greatly in size from unicellular of 3–10 µm to giant kelps up to 70-meter-long. Algae are identified as the microalgae which are found in both benthic and littoral habitats and also throughout the ocean waters as phytoplankton and the macroalgae (seaweeds) which occupy the littoral zone. Phytoplankton comprises diatoms, dinoflagellates, green and yellow–brown flagellates, and blue–green algae while seaweeds are classified into green algae, brown algae, and red algae. Marine algae are known to be a good source of healthy food due to their low content in lipids, high concentration in polysaccharides, natural richness in minerals, polyunsaturated fatty acids and vitamins. Especially, seaweeds are able to produce a great variety of secondary metabolites characterized by a broad spectrum of biological activities such as anti-coagulation, anti-virus, anti-oxidant, anti-allergy, anti-cancer, anti-inflammation, anti-obesity, anti-diabetes, anti-hypertension, neuroprotection, and immunomodulation¹⁶⁻¹⁹. Therefore, marine algae are believed to be a promising source to provide not only novel biologically active substances for the development of pharmaceuticals but also essential compounds for human nutrition²⁰.

The Phaeophyceae (brown algae) is a large group of marine multicellular algae, including various seaweeds. They play an important role in marine environments, both as food and for the habitats they form. Although the division Phaeophyta consists of 13 orders according to the classification of Bold and Wynne¹⁵, only three orders namely *Laminariales*, *Fucales*, and *Dictyotales* have been extensively researched for their phytochemicals. The most studied species of these orders are *Laminaria*, *Ecklonia*, *Undaria*, *Himantalia*, *Sargassum*, and *Dictyota*. Brown seaweeds are rich in polysaccharide, polyphloroglucinol phenolic compounds, and other secondary metabolites such as terpenes, carotenoids, and oxylipins²⁰. Notably, marine brown algae accumulate a variety of phloroglucinol-based polyphenols, as phlorotannins. These phlorotannins consist of phloroglucinol units linked to each other in various ways, and are of wide occurrence among marine brown algae^{21, 22}. Among marine brown algae,

Ecklonia cava, *Ecklonia stolonifera*, *Ecklonia kurome*, *Eisenia bicyclis*, *Ishige okamurae*, *Sargassum thunbergii*, *Hizikia fusiformis*, *Undaria pinnatifida*, and *Laminaria japonica* have been reported for phlorotannins with health beneficial biological activities²².

PHLOROTANNINS

Sources and distribution

Phlorotannins have only been found to exist within brown algae and may constitute up to 15% of the dry weight of brown algae²³. The concentration of phlorotannins is highly variable among different brown seaweeds as well as among different geographical areas. The fucoid species from the Atlantic and the temperate Pacific contain higher concentration of phlorotannins as compared to those obtained from the tropical Pacific²⁴. It was found that phlorotannins have mostly focused on Fucoaceae (*Ascophyllum nodosum* and *Fucus vesiculosus*), Sargassaceae (*Sargassum spinuligerum* and *Carpophyllum angustifolium*), and Cystoseiraceae (*Cystophora retroflexa* and *C. torulosa*) with concentrations ranging from 20 to 250 mg/g dry matter²⁵⁻²⁹. They tend to be concentrated within the outer cortical layers, physode, and the mitotic meristematic and meiotic sporogenous tissues³⁰. In addition, Laminariaceae brown algae, such as *Eisenia bicyclis*, *Ecklonia cava*, *Ecklonia kurome* were also found to contain a significant amount of phlorotannins^{31, 32}.

Structural diversity and classification

Phlorotannins are formed by the polymerization of phloroglucinol (1,3,5-trihydroxybenzene) monomer units. They are highly hydrophilic components with a wide range of molecular sizes ranging between 126 Da and 650 kDa. The monomeric units are linked through aryl-aryl bonds and diaryl ether bonds forming different subgroups of phlorotannins³³. Phlorotannins can be grouped according to the criteria of interphloroglucinol linkages into three primary types including fucols, phlorethols, and fucophlorethols³⁴. Fucols is formed by only phenyl linkages, while phlorethols is formed by only aryloether bonds and fucophlorethols is formed by both aryloether and phenyl linkages³⁵. The structural diversity of phlorotannins increases by adding the number of phloroglucinol units. Each of the primary groups can be grouped into linear or branched phlorotannins. In fucols, the interphloroglucinol links at meta-relative position construct of the linear phlorotannin such as tetrafucol-A and the branched phlorotannin such as tetrafucol-B, which were isolated from *Fucus vesiculosus*^{36, 37}. Moreover, longer oligomers of phlorotannin such as pentafucols and heptafucols were purified from *Scytothamnus australis*³³ and *Analipus japoni-*

*cas*³⁸. The linear phlorethols such as triphlorethol C and tetraphlorethols A and B were isolated from *Laminaria ochroleuca*³⁹. The branched phlorethols include tetraphlorethol C from *Ecklonia maxima*⁴⁰, pentaphlorethol B and hexaphlorethol A from *Cystophora retroflexa*²⁷. Furthermore, an additional hydroxyl group on the terminal monomer unit forms other structural motifs of phlorethols such as bifuhalol, trifuhalol A, and trifuhalol B^{41, 42}. The isofuhalols such as isotrifuhalol has an extension unit that bind between meta-oriented phloroglucinol units and it bears the additional hydroxyl group⁴³. Some fuhalols with more than one additional hydroxyl group have been called hydroxyfuhalols, such as hydroxytrifuhalol B⁴⁴. In addition, another subgroup of phlorethols, the eckols, includes a 1,4-dibenzodioxin system, such as the trimers eckol and dioxinodehydroeckol⁴⁰, the tetramers 2-phloroeckol and 7-phloroeckol⁴⁵⁻⁴⁷. In fucophlorethols, the combinations of C-C and C-O-C linkages allow the formation of various compounds in linear, branched and heterocyclic fashions. The linear fucophlorethols is fucodiphlorethol-B⁴⁸, meanwhile the branched fucophlorethols is bisfucotriphlorethol A²⁵, and heterocyclic fucophlorethols is phlorofucofuroeckol A⁴⁹.

Biosynthesis of phlorotannins

Phlorotannins are biosynthesized via the acetate-malonate pathway, also known as the polyketide pathway, in a process which may involve a polyketide synthase-type enzyme complex⁵⁰. However, the exact biosynthetic pathway for phlorotannins is unknown up to now. Therefore, methodologies that monitor phlorotannin synthesis at the genetic or enzymatic levels could be useful to reveal some of the uncertainties regarding phlorotannin biosynthesis⁵¹. Firstly, two molecules of acetyl co-enzyme A are converted into malonyl co-enzyme A through the addition of carbon dioxide. This addition changes the acetyl methyl group into a highly reactive methylene. Secondly, the process of polymerization is assisted to occur with the low required energy. During further synthesis steps, the carbon dioxide, which was added as an activator, is lost. Thirdly, a polyketide chain consisting of an acid moiety is formed, and the co-enzyme is lost. The polyketide chain is transformed by intermolecular ring closure and elimination of water to produce hexacyclic ring systems. Triketide, the cyclization product, is not stable and thus undergoes transformation into the thermodynamically more stable aromatic form, phloroglucinol, consisting of three phenolic hydroxyl groups⁵². The polymerization of phloroglucinol in different ways results in formation of various phlorotannins.

Physiological properties

Phlorotannins are found in physodes, which contribute to the development of the cell wall of brown algae⁵³. It has suggested that phlorotannins are likely to be integral structural components of brown-algal cell walls⁵⁴. They are bound to the cell wall during maturation of the plant⁵⁵. Phenolic compounds are bound with four major types of bonds including hydrophobic, hydrogen, ionic, and covalent bond to increase the strength⁵⁶. The cell wall (alginic acid) and phlorotannins are linked via covalent bonds including the ester bond and the hemiacetal bond, thus requiring strong conditions to degrade. Moreover, phlorotannins have a putative role in brown algal reproduction due to exposing on the surface of the recently fertilized zygotes where they may prevent multiple fertilizations by inhibiting spermatozoid movement⁵³.

A characteristic of phlorotannins is their plasticity to a variety of environmental factors including nutrient environment⁵⁷, light⁵⁸, depth⁵⁹, salinity⁶⁰, grazing⁶¹ or other mechanical wounding⁶². Such plasticity may represent inducible defense against herbivory²³. Suggestions for other adaptive roles for phlorotannins include protection against ultraviolet radiation⁶³ or function as anti-fouling substances⁶⁴. The suggested defensive role of phlorotannins is due to deterring feeding by herbivores⁶⁵ and decreasing their assimilation efficiency by binding with proteins in the gut^{66, 67}.

PHARMACEUTICAL PROPERTIES OF PHLOROTANNINS

Antioxidant and UV-protective activities

The oxidants such as superoxide anion radicals, hydroxyl radical species, and hydrogen peroxide are often generated by biological oxidation reactions of exogenous factors⁶⁸. It is well-known that oxidants are involved in signal transduction and gene activation and can contribute to host cell and organ damage⁶⁹. Therefore, scavenging of oxidant is considered to be important to control various diseases. Interestingly, phlorotannins from marine brown algae have been evidenced to be effective to scavenge oxidants in non-cellular and cellular systems. According to Ahn and colleagues, the antioxidant activities of three phlorotannins including phloroglucinol, eckol and dieckol purified from *Ecklonia cava* collected in Jeju Island have been investigated⁷⁰. It reported that all the phlorotannins have the potential DPPH, alkyl, hydroxyl and superoxide radical scavenging activities. Eckol exhibit the most strong antioxidant activity via scavenging 93% of DPPH. Moreover, these phlorotannins were effective to protect DNA against H₂O₂-induced damage. In the same trend, Kang and colleagues have also investigated the cytoprotective effect of eckol from

E. cava against oxidative stress induced cell damage in Chinese hamster lung fibroblast (V79-4) cells⁷¹. Eckol was effective to reduce H₂O₂-induced cell death in V79-4 cells, inhibit radiation-induced cell damage, and scavenge intracellular ROS production. Moreover, eckol was able to increase the activity of catalase and its protein expression via increasing phosphorylation of extracellular signal-regulated kinase and activity of nuclear factor κB. In another study of Kang and colleagues, triphlorethol-A from *E. cava* was found to reduce intracellular hydrogen peroxide generated by gamma-ray radiation, thus protecting against radiation-induced membrane lipid peroxidation, cellular DNA damage, and cell death⁷². Furthermore, triphlorethol-A augments cellular antioxidant defense capacity through induction of HO-1 expression via ERK-Nrf2-ARE signaling pathway, thereby protecting cells from oxidative stress⁷³. Notably, Li and colleagues have isolated several phlorotannins from *E. cava* such as phloroglucinol, eckol, fucodiphloroethol G, phlorofucofuroeckol A, dieckol, and 6,6'-bieckol. All phlorotannins were found to possess antioxidant properties via scavenging free radicals, protecting membrane protein from oxidant-induced damage, enhancing cellular glutathione level in RAW264.7 cell line⁷⁴. Likewise, several phlorotannins including phloroglucinol, eckol, dieckol, eckstolonol and triphloroethol A from *E. cava* were investigated for their activity against AAPH-induced oxidative stress toxicity in zebrafish embryos⁷⁵. All phlorotannins were able to scavenge intracellular ROS, prevent lipid peroxidation and reduce AAPH-induced cell death in zebrafish embryos. In an *in vivo* study, the role of eckol from *E. cava* as a radioprotective agent against the gamma ray-induced damage has been investigated by Park and colleagues⁷⁶. It has been determined that eckol significantly decreased the mortality of lethally irradiated mice via improving the hematopoietic recovery, repairing the damaged DNA in immune cells and enhancing their proliferation. Therefore, eckol is considered as a potential candidate for adjuvant therapy of radiation-exposed cancer patients. Recently, the antioxidant properties of phlorotannins from brown seaweed *Cystoseira trinodis* and *Carpophyllum flexuosum* was investigated⁷⁷⁻⁷⁸. It indicated that the antioxidant activities of these seaweed were due to phlorotannins content and structure.

UV radiation has a strong oxidative component, and photo-oxidative stress has been directly linked to skin photo-damage and associated with abnormal cutaneous reactions such as epidermal hyperplasia, accelerated breakdown of collagen, and inflammatory responses. Herein, dieckol from *E. cava* has been found to be able to inhibit melanogenesis and protect against photo-oxidative stress induced by UV-B radiation⁷⁹. The inhibitory activity on melanogenesis was evidenced via suppression of tyrosinase and melanin synthesis. Meanwhi-

le, protective activity was observed via scavenging intracellular ROS, preventing DNA damage, and increasing cell viability. Additionally, Fucofuroeckol-A from *E. stolonifera* was also found as protective agent against UVB-induced allergic reaction in RBL-2H3 mast cells⁸⁰. It was revealed that F-A significantly suppress mast cell degranulation via decreasing histamine release as well as intracellular Ca^{2+} elevation induce by UVB. Notably, the protective activity of F-A against mast cell degranulation was found due to scavenging ROS production. According to Klervi and colleagues, the ethyl acetate fraction of brown macroalga (*Halidrys siliquosa*) appeared to be a broad-spectrum UV-A absorber⁸¹. This activity was found due to the present of four phenolic compounds including trifluhalols, tetrafluhalols, diphlorethols, and triphlorethols. These results indicated that phlorotannins from brown algae have potential protective effects against UV radiation, which might be applied in cosmeceutical industries.

Antimicrobial activity

Infectious diseases caused by bacteria and fungi are still a major threat to public health, despite the tremendous progress in human medicine. Increasing resistance of clinically important bacteria to existing antibiotics is a major problem throughout the world⁸². The discovery of novel antimicrobial compounds for clinical application is necessary to check the global crisis of antibiotic resistance. In this regard, phlorotannins from brown algae have been found to possess antimicrobial effect against food-borne pathogenic bacteria, antibiotic resistance bacteria, and pathogenic fungi. According to Nagayama and colleagues, the oral administration of phlorotannins from *E. kurome* on mice results in effective inhibition against methicillin-resistant *Staphylococcus aureus* (MRSA). The minimum bactericidal concentrations (MBCs) of eckol, phlorofucofuroeckol A, dieckol, and 8,8'-bieckol against *Campylobacter jejuni* were 0.08, 0.08, 0.03, and 0.03 $\mu\text{mol/ml}$, respectively. At twice the MBCs, all *Vibrio parahaemolyticus* were killed within 0.5-2 h, while catechins showed little bactericidal activity within 4 h⁸³. Furthermore, Lee and collaborators have determined that dieckol from *E. stolonifera* exhibited antibacterial activity against methicillin-susceptible *S. aureus* (MSSA) and MRSA in a range of minimum inhibitory concentrations (MICs) of 32 to 64 $\mu\text{g/ml}$ ⁸⁴. The MICs of ampicillin against two standard strains of MRSA were dramatically reduced from 512 to 0.5 $\mu\text{g/ml}$ in combination with 1/4 MIC of dieckol (16 $\mu\text{g/ml}$). Likewise, Phlorofucofuroeckol-A from *E. bicyclis* were also showed anti-MRSA activity with MIC of 32 $\mu\text{g/ml}$ and synergistic action against MRSA in combination with β -lactam antibiotics ampicillin, penicillin, and oxacillin⁸⁵.

Thereby, phlorotannins- β -lactam antibiotics combinations exert a synergistic effect against MRSA, indicating the promising treatment of MRSA infections. In addition, it has shown that phlorofucofuroeckol-A from *E. cava* and *E. bicyclis* exhibited effective inhibition against *Propionibacterium acnes*, which may be useful as natural additives in anti-acne cosmetic products^{86, 87}. Although the relationship between the structure and anti-bacterial activity of the phlorotannins is limited, their inhibitory activity may be suggested to depend on the degree of polymerization of phlorotannin derivatives.

Besides, the purified phlorotannins extracts from three brown seaweeds including *Cystoseira nodicaulis*, *C. usneoides*, and *Fucus spiralis* displayed their antifungal activity against human pathogenic yeast and filamentous fungi⁸⁸. It was revealed that *C. albicans* ATCC 10231 was the most susceptible among yeast, while *Epidermophyton floccosum* and *Trichophyton rubrum* were the most susceptible among dermatophytes. It was found that *C. nodicaulis* and *C. usneoides* seem to act by affecting the ergosterol composition of the cell membrane of yeast and dermatophyte, respectively. Meanwhile, *F. spiralis* influenced the dermatophyte cell wall composition by reducing the levels of chitin. Moreover, phlorotannins from *F. spiralis* inhibited the dimorphic transition of *Candida albicans*, leading to the formation of pseudohyphae with diminished capacity to adhere to epithelial cells. On the other hand, the potential fungicidal activity of dieckol from *E. cava* was also found due to inhibition of *Trichophyton rubrum* associated with dermatophytic nail infections in human⁸⁹.

Anti-HIV activity

Human immunodeficiency virus type-1 (HIV-1) is the cause of acquired immune deficiency syndrome (AIDS) which has been a major human viral disease with about 33.2 million people infected worldwide up to now^{90, 91}. Antiviral agents that interfere with HIV at different stages of viral replication have been developed^{92, 93}. However, failure in anti-AIDS treatment⁹² is observed by the emergence of resistant virus, cross-resistance to drugs and cell toxicity^{94, 95}. Therefore, the search for potential candidates containing higher inhibitory activity against various HIV strains is increasing in pharmaceutical industry. Accordingly, phlorotannins from brown algae have been revealed to possess anti-HIV activity. For the first time, Ahn et al. (2004) reported that 8,8'-bieckol and 8,4'''-dieckol from *E. cava* exhibited an inhibitory effect on HIV-1 reverse transcriptase and protease⁹⁶. The inhibition against reverse transcriptase of 8,8'-bieckol with a biaryl linkage (IC_{50} , 0.5 μ M) is ten-fold higher than that of 8,4'''-dieckol with a diphenyl ether linkage (IC_{50} , 5.3 μ M), although these two phlorotannins are dimers of eckol. They have suggested that the steric hind-

rance of the hydroxyl and aryl groups near the biaryl linkage of 8,8'-bieckol caused to the potent inhibitory activity. Moreover, 8,8'-bieckol selectively inhibits reverse transcriptase over protease and inhibitory effect is comparable to the positive control nevirapine (IC_{50} , 0.28 μ M). Moreover, kinetic study showed that 8,8'-bieckol inhibited the RNA-dependent DNA synthesis activity of HIV-1 reverse transcriptase noncompetitively against dUTP/dTTP with a K_i value of 0.78 μ M. Meanwhile, this compound also exhibited an uncompetitive inhibition (K_i , 0.23 μ M) with respect to a homopolymeric template/primer, $(rA)_n(dT)_{15}$. A possible suggestion for this phenomenon is that 8,8'-bieckol binds to HIV-1 reverse transcriptase only after the template/primer initially binds to the enzyme. Furthermore, Ahn et al. (2006) has shown that diphlorethohydroxycarmalol from *I. okamurae* also has inhibitory effect on HIV-1⁹⁷. This compound exhibited inhibitory effects on HIV-1 reverse transcriptase and integrase with IC_{50} values of 9.1 μ M and 25.2 μ M, respectively. However, diphlorethohydroxycarmalol did not show an inhibitory activity against HIV-1 protease. In the same trend, 6,6'-bieckol from *E. cava* has been found as a potent wild inhibition against HIV-1 induced syncytia formation, lytic effects, and viral p24 antigen production⁹⁸. This phlorotannin has selectively inhibited the activity of HIV-1 reverse transcriptase enzyme with an IC_{50} of 1.07 μ M without any cytotoxicity. Recently, Kwon and colleagues have found that phlorotannins including eckol, 7-phloroeckol, phlorofucofuroeckol, and dieckol possessed antiviral activities with IC_{50} range of 10.8 – 22.5 μ M against porcine epidemic diarrhea virus⁹⁹. These phlorotannins were completely blocked binding of viral spike protein to sialic acids at less than 36.6 μ M by hemagglutination inhibition. Notably, phlorofucofuroeckol and dieckol inhibited viral replication with IC_{50} values of 12.2 and 14.6 μ M in the post-treatment assay, respectively. Interestingly, phlorofucofuroeckol and dieckol inhibited both viral entry by hemagglutination inhibition and viral replication by inhibition of viral RNA and viral protein synthesis, but not viral protease.

Anti-allergic activity

Allergic disease including allergic rhinitis, asthma, and atopic eczema are among the commonest causes of chronic ill-health. It is caused by an exaggerated reaction of the immune system to harmless environmental substances, such as animal dander, house dust mites, foods, pollen, insects, and chemical agents^{100, 101}. Allergic reaction is characterized by the excessive activation of mast cells and basophils by immunoglobulin E (IgE) from B cells, resulting in the release of preformed inflammatory mediators from secretory granules such as histamine and β -hexosaminidase, the generation and secretion of the newly

synthesized substances such as leukotrienes, prostaglandins, and cytokines¹⁰². These mediators cause allergic inflammatory responses due to airway constriction, mucous production, and recruitment of inflammatory cells. So far, a large number of anti-allergic agents from natural products have been identified based on the specific assay system or screening approaches. Recently, phlorotannins from brown algae have been determined as potential natural inhibitors of allergic reactions due to suppression of allergic degranulation, inhibition of hyaluronidase enzyme, and blockade of FcεRI activities. Several bioactive phloroglucinol derivatives including fucodiphloroethol G, eckol, dieckol, 6,6'-bieckol, phlorofucofuroeckol A, and 1-(3',5'-dihydroxyphenoxy)-7-(2'',4'',6-trihydroxyphenoxy)-2,4,9-trihydroxydibenzo-1,4-dioxin were isolated from *E. cava* and evidenced against A23187 or FcεRI-mediated histamine release from KU812 and RBL-2H3 cells^{103, 32}. Especially, dieckol, 6,6'-bieckol, and fucodiphloroethol G exhibited a significantly inhibitory activity with IC₅₀ range of 27.80 – 55.12 μM. The inhibitory mechanism of these compounds was determined to be due to blocking the binding activity between IgE and FcεRI. Similarly, Shim et al. (2009) have proved that phlorotannins of dioxinodehydroeckol and phlorofucofuroeckol A from *E. stolonifera* induced a suppression of the cell surface FcεRI expression, and total cellular protein and mRNA levels of the FcεRI α chain in KU812 cells¹⁰⁴. Further, both of these compounds exerted inhibitory effects against intracellular calcium elevation and histamine release from anti-FcεRI α chain antibody (CRA-1)-stimulated cells. In another study, phlorotannin PFF-B obtained from *E. arborea* exposed strong inhibitory activity against histamine and β-hexosaminidase release with IC₅₀ value of 7.8 μM^{105, 106}. Obviously, PFF-B had a 2.8–6.0 times greater inhibitory activity than those of epigallocatechin gallate (IC₅₀=22.0 μM) or Tranilast (IC₅₀=46.6 μM), a clinically used anti-allergic drug¹⁰⁷. Thus, these bioactive phloroglucinol derivatives were suggested as a promising candidate for the design of novel inhibitor of FcεRI-mediated allergic reaction. For the first time, the anti-allergenicity of phlorotannin from four edible seaweed species of *Fucus* genus was evaluated by Barbosa and colleagues¹⁰⁸. It was found that *Fucus* was able to inhibit mast cell degranulation via decreasing histamine and beta-hexosaminidase release from the activated RBL-2H3 cells, contributing to the valorisation of *Fucus* spp. both as food and for nutraceutical applications.

Hyaluronidase depolymerizes the polysaccharide hyaluronic acid in the extracellular matrix of connective tissue, which is found both in organs and in body fluids. It is mainly known to be involved in the permeability of the vascular system¹⁰⁹ and allergic reaction^{110, 111}. Interestingly, various phlorotannins such

as phlorofucofuroeckol A, dieckol, and 8,8'-bieckol from *E. bicyclis* are able to inhibit hyaluronidase enzyme with IC_{50} values of 140, 120, and 40 μM , respectively¹¹². The effect of these phlorotannins against hyaluronidase enzyme is stronger than well-known inhibitors such as catechins ($IC_{50}=620 \mu\text{M}$) and sodium cromoglycate ($IC_{50}=270 \mu\text{M}$). Notably, 8,8'-bieckol, the strongest hyaluronidase inhibitor among the tested phlorotannins, acted as a competitive inhibitor with an inhibition constant of 35 μM . Likewise, several phlorotannins of 6,6'-bieckol, 6,8'-bieckol, 8,8'-bieckol, PFF-A, and PFF-B from *E. arborea* were also confirmed as strong inhibitors of hyaluronidase^{113, 114}.

Anti-inflammatory activity

Inflammation is a critically important aspect of host responses to various stimuli including physical damage, ultra violet irradiation, microbial invasion, and immune reactions^{115, 116}. It is associated with a large range of mediators that initiate the inflammatory response, recruit and activate other cells to the site of inflammation¹¹⁷. However, excessive or prolonged inflammation can prove harmful, contributing to the pathogenesis of a variety of diseases, including chronic asthma, rheumatoid arthritis, multiple sclerosis, inflammatory bowel disease, psoriasis, and cancer¹¹⁶. Currently, several classes of drugs such as corticosteroids, nonsteroidal anti-inflammatory drugs, and aspirin are used to treat the inflammatory disorders. All these therapeutics help to alleviate the symptoms but, especially after long-term and high-dose medication, they can have quite substantial side-effects. Therefore, there is still a vital need for the development of new anti-inflammatory drugs with satisfactory tolerability for long-term use. Herein, phlorotannins have been evidenced as potential agents for down-regulation of inflammatory responses. Phlorotannin-rich extracts of *E. cava* showed significant suppression of PGE_2 generation in LPS-treated RAW 246.7 cells, and significant inhibition of human recombinant interleukin-1 α -induced proteoglycan degradation¹¹⁸. Moreover, the phlorotannin-rich the fermented *E. cava* processing by-product extract was reported to inhibit NO and PGE_2 production, suppress the inducible nitric oxide synthase (iNOS) and cyclooxygenase-2 (COX-2) expressions, and attenuate interleukin-1 β and interleukin-6 production in lipopolysaccharide stimulated RAW 264.7 cells¹¹⁹. Recently, phlorotannin 6,6'-bieckol from *E. cava* was found to inhibit NO and PGE_2 production by suppressing the expression of iNOS and COX-2 at the mRNA and protein levels in LPS-stimulated primary macrophages and RAW 264.7 macrophage cells¹²⁰. Moreover, 6,6'-bieckol down-regulated the production and mRNA expression of the inflammatory cytokines TNF- α and IL-6. The pretreatment of 6,6'-bieckol decreased LPS-induced transactivation

of nuclear factor-kappa B (NF- κ B) and nuclear translocation of p50 and p65 subunits of NF- κ B, thus inhibiting LPS-induced NF- κ B binding to the TNF- α and IL-6 promoters. On the other hand, Kim and collaborators have evidenced that phlorofucofuroeckol A from *E. stolonifera* attenuated the productions and expression of NO, PGE₂, and pro-inflammatory cytokines such as IL-1 β , IL-6, and TNF- α in LPS-stimulated microglia. Profoundly, phlorofucofuroeckol A treatment showed inactivation of c-Jun NH₂-terminal kinases (JNKs), p38 mitogen-activated protein kinase (MAPK), Akt, and NF- κ B¹²¹. Likewise, Kim et al. (2009) have shown the inhibitory activity of this phlorofucofuroeckol A on NO and PGE₂ production and iNOS and COX-2 expression in RAW 264.7 murine macrophage cells¹²². Besides, phlorotannins from *E. arborea* also exhibited inhibitory effect on NO production in LPS-stimulated RAW 264.7 cells¹²³ and mouse ear edema induced by arachidonic acid, 12-O-tetradecanoyl phorbol-13-acetate, and oxazolone¹²⁴. Notably, 8,8'-bieckol from *E. bicyclis* showed the pronouncedly inhibitory effects on soybean lipoxygenases and 5-lipoxygenases with IC₅₀ values of 38 and 24 μ M, respectively. Meanwhile, dieckol presented a significant inhibition of COX-1 with inhibition rate of 74.7%¹²⁵. Similarly, 6,6'-bieckol, 6,8'-bieckol, 8,8'-bieckol, PFF-A, and PFF-B from *E. arborea* were also confirmed as strong inhibitors of phospholipase A₂, cyclooxygenase, and lipoxygenases, which correlated to suppression in synthesis and release of leukotriene and prostaglandin from RBL cells¹¹⁴. Recently, phlorotannin-rich extract of the edible brown alga *E. cava* against hyper-inflammatory response in LPS-induced septic shock mouse model was also investigated¹²⁶. Dieckol, a major compound in the extract, reduced mortality, tissue toxicity, and serum levels of the inflammatory factors in septic mice and suppressed the septic shock through negative regulation of pro-inflammatory factors via the NIK/TAK1/IKK/I κ B/NF κ B and Nrf2/HO-1 pathways. In addition, Barbosa and colleagues have demonstrated the marked potential of *Fucus* sp. and their phlorotannin-purified extracts to act upon different mediators important in the pathophysiology of inflammatory-related conditions¹²⁷. The anti-inflammatory potential of the purified phlorotannin extracts in both cell and cell-free systems was observed. Therefore, the phlorotannin extracts from *Fucales* arise as potentially beneficial in inflammation-related conditions, effectively acting upon enzymatic and non-enzymatic inflammatory target.

Anti-cancer activity

Cancer can be defined as a disease in which a group of abnormal cells grow uncontrollably by disregarding the normal rules of the cell division¹²⁸. Cancers may be caused in one of three ways, namely incorrect diet, genetic predisposition, and via the environment. At least 35% of all cancers worldwide are caused

by an incorrect diet. Meanwhile, genetic predisposition caused about 20% of cancer cases, thus leaving the majority of cancers being associated with a host of environmental carcinogens¹²⁹. It is necessary to avoid exposure to cancer-causing biological, chemical, and physical agents, and consume chemo-preventive agents to reduce cancer risk. A promising approach is associated with natural products that are available as anti-cancer agents against commonly occurring cancers occurring worldwide^{130, 131}. Recently, phlorotannins have been reported as novel promising anti-cancer agent for breast cancer. Kong et al. (2009) has indicated that dioxinodehydroeckol from *E. Cava* exerted anti-proliferative activity against human breast cancer cells via induction of apoptosis¹³². Dioxinodehydroeckol treatment caused the increase in caspase (-3 and -9) activity, DNA repair enzyme poly-(ADP-ribose) polymerase (PARP) cleaved, and pro-apoptotic gene (Bax, p53, and p21) and the decrease in anti-apoptotic gene Bcl-2 and NF-κB activation. Moreover, phlorotannins-rich extracts from *Palmaria*, *Ascophyllum* and *Alaria* also inhibited the proliferation of colon cancer cells¹³³. On the other hand, the anti-cancer activity of *S. muticum* polyphenol-rich seaweed was shown via inhibiting breast cancer cell proliferation with IC₅₀ of 22 µg/ml and inducing apoptosis from 13% to 67% by accumulation of cells at sub-G1 phase¹³⁴. Parys et al. (2010) reported that trifucodiphloretol A, trifucotriphloretol A and fucotriphloretol A from *Fucus vesiculosus* were the potential chemo-preventive agents due to their capacity to inhibit the activity of aromatase related to carcinogenesis from breast cancers¹³⁵. For the first time, Kim and colleagues have determined the inhibitory effects of phlorotannins isolated from *E. cava* on MMP activities in cultured human cell lines without any cytotoxic effect¹³⁶. Recently, the anti-proliferative effect of various brown algae including *Cystoseira crinita*, *Cystoseira stricta*, and *Sargassum vulgare* on the human epithelial cell line Caco-2 was evidenced via arresting in G phases along with an increment in sub-diploid cell population¹³⁷. The anti-proliferative effect of these algae was correlated with their polyphenol and flavonoid contents. Moreover, the phlorotannins recovered from hydrothermal treatment of *Sargassum muticum* were showed the anti-proliferative properties against lung adenocarcinoma A549 cells and colon carcinoma HCT-116 cells¹³⁸. These results imply that seaweeds which are rich in phlorotannins may be used in anti-cancer drug research programs.

Anti-diabetic activity

Diabetes mellitus is a chronic metabolic disorder involved in hyperglycaemia, resulting from the deficiency in the production of insulin by the pancreas. Up to now, numerous therapeutics have been proposed to control hyperglycaemia in diabetic patients. Especially, α-amylase and α-glucosidase are enzymes related

to hyperglycaemia due to the starch hydrolysis and release of the glucose monomers for subsequent absorption by the small intestine. Therefore, the inhibition of these enzymes reduces the availability of free glucose monomers and consequently decreases blood glucose levels¹³⁹. Rengasamy et al. (2013) has isolated three phlorotannins including dibenzo (1,4) dioxine-2,4,7,9-tetraol and eckol from *E. maxima* and evaluated their alpha-glucosidase inhibitory activities¹⁴⁰. The inhibitory activities of dibenzo (1,4) dioxine-2,4,7,9-tetraol and eckol on enzyme alpha-glucosidase were 33.7 and 11.2 μM , respectively. A phenolic-rich extract from *Ascophyllum* was effective to inhibit α -amylase and α -glucosidase with IC_{50} of 0.1 $\mu\text{g}/\text{ml}$ GAE and 20 $\mu\text{g}/\text{ml}$ GAE¹³³. The presence of fucophloroethol structures with degrees of polymerization from 3 to 18 monomer units in *Fucus distichus* is responsible for its inhibition on α -glucosidase and α -amylase, with IC_{50} values of 0.89 and 13.9 $\mu\text{g}/\text{ml}$ ¹⁴¹. Moreover, dieckol and eckol from *Eisenia bicyclis* exhibited the inhibitory activity on α -amylase up to 97.5 and 87.5% at 1 mM ¹⁴². Meanwhile, α -glucosidase was inhibited by phlorofucofuroeckol-A, dieckol, and 7-phloroecol from *E. stolonifera* and eckol and dioxinodehydroeckol from *E. bicyclis* with IC_{50} of 1.37, 1.61, 6.13, 22.78, and 34.6 μM , respectively¹⁴³. The ingestion of methanolic extract of *E. stolonifera* suppressed the increase in plasma glucose and lipid peroxidation levels in unfasted KK-A(y) mice¹⁴⁴. Furthermore, various phlorotannins from *E. stolonifera* exhibited the inhibitory activities on aldose reductase, which are highly implicated in hyperglycemia and oxidative stress. The IC_{50} values of phloroglucinol derivatives are 21.95 - 125.45 μM ¹⁴⁵. Besides, dieckol from *E. cava* has evidenced prominent inhibitory effect against alpha-glucosidase and alpha-amylase with IC_{50} values of 0.24 and 0.66 mM , respectively. The increase of postprandial blood glucose levels were significantly suppressed in the dieckol administered group in the streptozotocin-induced diabetic mice¹⁴⁶. Recently, three phlorotannins, eckol, dieckol and phlorofucofuroeckol-A from *E. bicyclis* were revealed for their anti-diabetic activity of alloxan-induced type1 and insulin-induced type 2 in the zebrafish model¹⁴⁷. Notably, the inhibition of the catalytic reaction of α -glucosidase by minor phlorotannin derivatives from *E. cava* were demonstrated with IC_{50} values ranging from 2.3 ± 0.1 to 59.8 ± 0.8 μM . Compounds 2–5 inhibited the catalytic reaction of α -glucosidase in non-competitive and competitive manners¹⁴⁸.

Anti-obesity

Obesity is a major obstacle in human health and life quality, resulting in many chronic diseases. It is due to a chronic imbalance between energy intake and energy expenditure, leading to the increased fat storage¹⁴⁹. Interestingly, a series of anti-obesity components derived from marine origin have been found,

especially phlorotannins. Herein, three phlorotannins from *E. stolonifera* including phloroglucinol, eckol, and phlorofuocufuroeckol A significantly inhibited lipid accumulation in 3T3-L1 cells via reducing the expression of adipocyte marker genes such as proliferator activated receptor γ and CCAAT/enhancer-binding protein α ¹⁵⁰. Meanwhile, phlorotannin dieckol from *E. cava* exhibited great potential adipogenesis inhibition and down-regulated the expression of peroxisome proliferator-activated receptor- γ , CCAAT/enhancer-binding proteins, sterol regulatory element-binding protein 1 (SREBP1) and fatty acid binding protein 4¹⁵¹. Moreover, diphloretohydroxycarmalol (DPHC) from *Ishige okamurae* was showed to inhibit population growth and induce apoptosis in 3T3-L1 preadipocytes¹⁵². The peptidyl prolyl cis/trans isomerase Pin1 enhances the uptake of triglycerides and the differentiation of fibroblasts into adipose cells in response to insulin stimulation. However, phlorotannin called 974-B from *E. kurome* was showed to inhibit the differentiation of mouse embryonic fibroblasts and 3T3-L1 cells into adipose cells without inducing cytotoxicity, suggesting a lead drug candidate for obesity-related disorders¹⁵³.

Other biological activities

According to Ahn et al. (2010), phloroglucinol from *E. cava* possesses the activation activity on immune response. The phloroglucinol elicited the proliferation of lymphocytes without cytotoxicity and enhanced IL-2 production by activating the nuclear factor-kappaB (NF- κ B) signaling pathway¹⁵⁴.

Inhibition of angiotensin I-converting enzyme (ACE) activity is the most common mechanism underlying the lowering of blood pressure. Dieckol from *E. cava* was found as potent ACE inhibitor with IC_{50} value of 1.47 mM. It is a non-competitive inhibitor against ACE according to Lineweaver-Burk plots¹⁵⁵. Meanwhile, eckol, phlorofuocufuroeckol A, and dieckol from *E. stolonifera* were also determined to manifest the marked inhibitory activity against ACE, with IC_{50} values of 70.82, 12.74, and 34.25 μ M, respectively¹⁵⁶.

Neurodegenerative diseases are characterized by progressive dysfunction and death of neurons. Recently, neuroprotective effects of phlorotannins from brown seaweed have been evidenced by various experimental models. Um and colleagues have reported that phlorotannin-rich fraction from *Ishige foliacea* brown seaweed prevents the scopolamine-induced memory impairment in mice¹⁵⁷. It reduced acetylcholinesterase activity in the brain and significantly decreased lipid peroxidation levels, but increased glutathione levels and superoxide dismutase activity. Moreover, the expression levels of brain-derived neurotrophic factor, tropomyosin receptor kinase B, the phosphorylated extracellular signal-regulated kinase, and cyclic AMP-response element-binding

protein were increased by *I. foliacea* phlorotannin. In addition, the neuroprotective effect of dieckol from *E. cava* on rotenone-induced oxidative stress in a human dopaminergic neuronal cell line SH-SY5Y was also determined by Cha and colleagues¹⁵⁸. Dieckol reduced the intracellular reactive oxygen species and cytochrome C release, cell death, and α -synuclein aggregation in SH-SY5Y cells. Likewise, it was found that eckmaxol, a phlorotannin from *E. maxima*, could produce neuroprotective effects in SH-SY5Y cells via directly acting on glycogen synthase kinase 3β ¹⁵⁹. Accordingly, phlorotannin from the brown algae could be a potential therapeutic agent for the prevention of neurodegenerative diseases.

RESULTS AND DISCUSSION

Finding the safe and efficient agents from natural products for prevention and treatment of chronic diseases are always necessary. Herein, phlorotannins from brown algae have been identified with various biological activities and health benefit effects. The extensive discoveries of phlorotannins underlying structure-activity relationship will provide clear evidence on their actions against diseases. Moreover, the further studies due to the bioavailability involving in liberation, absorption, distribution, metabolism, and elimination phases will ensure the bio-efficacy of phlorotannins. Collectively, phlorotannins from brown algae are believed to play an important role in the development of promising pharmaceutical products that can prevent and/or treat various chronic diseases.

ACKNOWLEDGEMENT

This review is supported by Nguyen Tat Thanh University, Ho Chi Minh city, Vietnam.

CONFLICT OF INTEREST

There are no conflicts to declare.

REFERENCES

1. Faulkner, D. J. Marine natural products. *Nat Prod Rep.* **2002**, *19*, 1–48.
2. Blunt, J. W.; Copp, B. R.; Munro, M. H.; Northcote, P. T.; Prinsep, M. R. Marine natural products. *Nat Prod Rep.* **2010**, *27*, 165–237.
3. Molinski, T. F.; Dalisay, D. S.; Lievens, S. L.; Saludes, J. P. Drug development from marine natural products. *Nat Rev Drug Discov.* **2009**, *8*, 69–85.
4. Mayer, A. M.; Glaser, K. B; Cuevas, C.; Jacobs, R. S.; Kem, W.; Little, R. D.; McIntosh, J. M.; Newman, D. J.; Potts, B. C.; Shuster, D. E. The odyssey of marine pharmaceuticals: a current pipeline perspective. *Trends Pharmacol Sci.* **2010**, *31*, 255–265.

5. Mayer, A. M. S.; Glaser, K. B. Marine Pharmacology and the Marine Pharmaceuticals Pipeline. *The FASEB J.* **2013**, *27*, 1167-7
6. Ngo, D. H.; Wijesekara, I.; Vo, T. S.; Ta, Q. V.; Kim, S. K. Marine food-derived functional Ingredients as potential antioxidants in the food industry: An overview. *Food Res Int.* **2011**, *44*, 523-529.
7. Ngo, D. H.; Ryu, B.; Vo, T. S.; Himaya, S. W.; Wijesekara, I.; Kim, S. K. Free radical scavenging and angiotensin-I converting enzyme inhibitory peptides from Pacific cod (*Gadus macrocephalus*) skin gelatin. *Int J Biol Macromol.* **2011**, *49*, 1110-1116.
8. Ngo, D. H.; Vo, T. S.; Ngo, D. N.; Wijesekara, I.; Kim, S. K. Biological activities and potential health benefits of bioactive peptides derived from marine organisms. *Int J Biol Macromol.* **2012**, *51*, 378-383.
9. Ngo, D. H.; Ryu, B.; Kim, S. K. Active peptides from skate (*Okamejei kenojei*) skin gelatin diminish angiotensin-I converting enzyme activity and intracellular free radical-mediated oxidation. *Food Chem.* **2014**, *143*, 246-255.
10. Vo, T. S.; Kim, S. K. Potential Anti-HIV Agents from Marine Resources: An Overview, *Mar Drugs.* **2010**, *8*, 2871-2892.
11. Vo, T. S.; Ngo, D. H.; Ta, Q.V.; Kim, S. K. Marine organisms as a therapeutic source against herpes simplex virus infection. *Eur J Pharm Sci.* **2011**, *44*, 11-20.
12. Vo, T. S.; Kong, C. S.; Kim, S. K. Inhibitory effects of chitooligosaccharides on degranulation and cytokine generation in rat basophilic leukemia RBL-2H3 cells. *Carbohydr Polym.* **2011**, *84*, 649-655.
13. Vo, T. S.; Kim, S. K. Fucoidan as a natural bioactive ingredient for functional foods. *J Funct Foods.* **2013**, *5*, 16-27.
14. Vo, T. S.; Kim, S. K. Down-regulation of histamine-induced endothelial cell activation as potential anti-atherosclerotic activity of peptides from *Spirulina maxima*. *Eur J Pharm Sci.* **2013**, *50*, 198-207.
15. Bold, H. C.; Wynne, M. J. In *Introduction to the algae structure and reproduction*, 2nd ed.; Prentice-Hall Inc: New York, 1985.
16. Gamal, A. A. Biological importance of marine algae. *Saudi Pharm J.* **2010**, *18*, 1-25.
17. Vo, T. S.; Ngo, D. H.; Kim, S. K. Potential Targets for Anti-Inflammatory and Anti-Allergic Activities of Marine Algae: An Overview. *Inflamm Allergy Drug Targets.* **2012**, *11*, 90-101.
18. Vo, T. S.; Ngo, D. H.; Kim, S. K. Marine algae as a potential pharmaceutical source for anti-allergic therapeutics. *Process biochem.* **2012**, *47*, 386-394.
19. Lincoln, R. A.; Strupinski, S.; Walker, J. M. Bioactive compounds from algae. *Life Chem Rep.* **1991**, *8*, 97-183.
20. Gupta, S.; Abu-Ghannam, N. Bioactive potential and possible health effects of edible brown seaweeds. *Trends Food Sci Technol.* **2011**, *22*, 315-326.
21. Singh, I. P.; Bharate, S. B. Phloroglucinol compounds of natural origin. *Nat Prod Rep.* **2006**, *23*, 558-591.
22. Li, Y. X.; Wijesekara, I.; Li, Y.; Kim, S. K. Phlorotannins as bioactive agents from brown

- algae. *Process Biochem.* **2011**, *46*, 2219–2224.
23. Targett, N. M.; Arnold, T. M. Predicting the effects of brown algal phlorotannins on marine herbivores in tropical and temperate oceans. *J Phycol.* **1998**, *34*, 195–205.
24. Arnold, T. M.; Targett, N. M. To grow and defend: lack of trade-offs for brown algal phlorotannins. *Oikos.* **2003**, *100*, 406–408.
25. Glombitza, K. W.; Hauperich, S. Phlorotannins from the brown alga *Cystophora torulosa*. *Phytochemistry.* **1997**, *46*, 735–740.
26. Glombitza, K. W.; Schmidt, A. Trihydroxyphlorethols from the brown alga *Carpophyllum angustifolium*. *Phytochemistry.* **1999**, *51*, 1095–1100.
27. Sailler, B.; Glombitza, K. W. Phlorethol and fucophlorethol from the brown alga *Cystophora retroflexa*. *Phytochemistry.* **1999**, *50*, 869–881.
28. Toth, G. B.; Pavia, H. Water-borne cues induce chemical defense in a marine alga (*Ascophyllum nodosum*). *Prot Natl Acad Sci USA.* **2000**, *97*, 14418–14420.
29. Arnold, T. M.; Targett, N. M.; Tanner, C. E.; Hatch, W. I. Evidence for methyl jasmonate-induced phlorotannin production in *Fucus vesiculosus* (*Phaeophyceae*). *J Phycol.* **2001**, *37*, 1026–1029.
30. Shoenwaelder, M. E. A. The occurrence and cellular significance of physodes in brown algae. *Phycologia.* **2002**, *41*, 125–139.
31. Nakamura, T.; Nagayama, K.; Uchida, K.; Tanaka, R. Antioxidant activity of phlorotannins isolated from the brown alga *Eisenia bicyclis*. *Fisheries Sci.* **1996**, *62*, 923–926.
32. Le, Q. T.; Li, Y.; Qian, Z. J.; Kim, M. M.; Kim, S. K. Inhibitory effects of polyphenols isolated from marine alga *Ecklonia cava* on histamine release. *Process Biochem.* **2009**, *44*, 168–176.
33. Glombitza, K. W.; Pauli, K. Fucols and phlorethols from the brown alga *Scytothamnus australis* Hook. et Harv. (*Chnoosporaceae*). *Bot Mar.* **2003**, *46*, 315–320.
34. Isaza Martı́nez, J. H.; Torres Castañeda, H. G. Preparation and Chromatographic Analysis of Phlorotannins. *J Chromatogr Sci.* **2013**, *51*, 825–838.
35. Keusgen, M.; Glombitza, K. W. Phlorethols, fuhalols and their derivatives from the brown alga *Sargassum spinuligerum*. *Phytochemistry.* **1995**, *38*, 975–985.
36. Glombitza, K. W.; Rauwald, H. W.; Eckhardt, G. Fucole, Polyhydrox yologiphenyle aus *Fucus vesiculosus*. *Phytochemistry.* **1975**, *14*, 1403–1405.
37. Truus, K.; Vaher, M.; Koel, M.; Mähar, A.; Taure, I. Analysis of bioactive ingredients in the brown alga *Fucus vesiculosus* by capillary electrophoresis and neutron activation analysis. *Anal Bioanal Chem.* **2004**, *379*, 849–852.
38. Glombitza, K. W.; Zieprath, G. Phlorotannins from the brown alga *Analipus japonicas*. *Planta Medica.* **1989**, *55*, 171–175.
39. Koch, M.; Glombitza, K. W.; Eckhard, G. Phlorotannins of *Phaeophyceae Laminaria ochroleuca*. *Phytochemistry.* **1980**, *19*, 1821–1823.
40. Glombitza, K. W.; Vogels, H. P. Antibiotics from algae. XXXV. Phlorotannins from *Ecklonia maxima*. *Planta Medica.* **1985**, *51*, 308–312.

41. Glombitza, K. W.; Rosener, H. U.; Müller, D. Bifuhalol und Diphlorethol aus *Cystoseira tamariscifolia*. *Phytochemistry*. **1975**, *14*, 1115–1116.
42. Glombitza, K. W.; Forster, M.; Eckhardt, G. Polyhydroxyphenyläther aus der *Phaeophyceae Sargassum muticum*. *Phytochemistry*. **1978**, *17*, 579–580.
43. Grosse-Damhues, J.; Glombitza, K. W. Isofuhalols, a type of phlorotannin from the brown alga *Chorda filum*. *Phytochemistry*. **1984**, *23*, 2639–2642.
44. Glombitza, K. W.; Li, S. M. Hydroxyphlorethols from the brown alga *Carpophyllum maschalocarpum*. *Phytochemistry*. **1991**, *30*, 2741–2745.
45. Yoon, N. Y.; Chung, H. Y.; Kim, H. R.; Choi, J. S. Acetyl- and butyrylcholinesterase inhibitory activities of sterols and phlorotannins from *Ecklonia Stolonifera*. *Fisheries Sci.* **2008**, *74*, 200–207.
46. Yoon, N.Y.; Eom, T. K.; Kim, M. M.; Kim, S. K. Inhibitory effect of phlorotannins isolated from *Ecklonia cava* on mushroom tyrosinase activity and melanin formation in mouse B16F10 melanoma cells. *J Agric Food Chem.* **2009**, *57*, 4124–4129.
47. Lee, S. H.; Yong, L.; Karadeniz, F.; Kim, M. M.; Kim, S. K. α -Glucosidase and α -amylase inhibitory activities of phloroglucinal derivatives from edible marine brown alga, *Ecklonia cava*. *J Sci Food Agr.* **2009**, *89*, 1552–1558.
48. Glombitza, K. W.; Keusgen, M.; Hauperich, S. Fucophlorethols from the brown algae *Sargassum spinuligerum* and *Cystophora torulosa*. *Phytochemistry*. **1997**, *46*, 1417–1422.
49. Eom, S. H.; Lee, S. H.; Yoon, N. Y.; Jung, W. K.; Jeon, Y. J.; Kim, S. K.; Lee, M. S.; Kim, Y. M. α -Glucosidase- and α -amylase-inhibitory activities of phlorotannins from *Eisenia bicyclis*. *J Sci Food Agric.* **2012**, *92*, 2084–2090.
50. Arnold, T. M.; Targett, N. M. Marine tannins: The importance of a mechanistic framework for predicting ecological roles. *J Chem Ecol.* **2002**, *28*, 1919–1934.
51. Amsler, C. D.; Fairhead, V. A. Defensive and sensory chemical ecology of brown algae. *Adv Bot Res.* **2006**, *43*, 1–91.
52. Waterman, P. G.; Mole, S. In *Analysis of phenolic plant metabolites*, Blackwell Scientific Publications: Oxford, 1994.
53. Schoenwaelder, M. E. A.; Wiencke, C. Phenolic compounds in the embryo development of several northern hemisphere fucoids. *Plant Biology.* **2000**, *2*, 24–33.
54. Schoenwaelder, M. E. A.; Clayton, M. N. Secretion of phenolic substances into the zygote wall and cell plate in embryos of *Hormosira* and *Acrocarpia* (Fucales, Phaeophyceae). *J Phycol.* **1998**, *34*, 969–980.
55. Peng, S.; Scalbert, A.; Monties, B. Insoluble ellagitannins in *Castanea sativa* and *Quercus petraea* woods. *Phytochemistry.* **1991**, *30*, 775–778.
56. Appel, H. M. Phenolics in ecological interactions - the importance of oxidation. *J Chem Ecol.* **1993**, *19*, 1521–1552.
57. Van Alstyne, K. L.; Pelletreau, K. N. Effects of nutrient enrichment on growth and phlorotannin production in *Fucus gardneri* embryos. *Mar Ecol Prog Ser.* **2000**, *206*, 33–43.
58. Cronin, G.; Hay, M. E. Effects of light and nutrient availability on the growth, secondary chemistry, and resistance to herbivory of two brown seaweeds. *Oikos.* **1996**, *77*, 93–106.

59. Peckol, P.; Krane, J. M.; Yates, J. L. Interactive effects of inducible defence and resource availability on phlorotannins in the north Atlantic brown alga *Fucus esiculosus*. *Mar Ecol Prog Ser.* **1996**, *138*, 209–217.
60. Jormalainen, V.; Honkanen, T. Multiple cues for phenotypic plasticity in phlorotannin production of the bladder wrack *Fucus esiculosus*. *Phycologia.* **2001**, *40*, 59–60.
61. Pavia, H.; Brock, E. Extrinsic factors influencing phlorotannin production in the brown alga *Ascophyllum nodosum*. *Mar Ecol Prog Ser.* **2000**, *193*, 285–294.
62. Hammerstroöm, K.; Dethier, M. N.; Duggins, D. O. Rapid phlorotannin induction and relaxation in five Washington kelps. *Mar Ecol Prog Ser.* **1998**, *165*, 293–305.
63. Pavia, H.; Cervin, G.; Lindgren, A.; Åberg, P. Effects of UV-B radiation and simulated herbivory on phlorotannins in the brown alga *Ascophyllum nodosum*. *Mar Ecol Prog Ser.* **1997**, *157*, 139–146.
64. Lau-Stanley, C. K.; Qian, P. Y. Phlorotannins and related compounds as larval settlement inhibitors of the tube-building polychaete *Hydroides elegans*. *Mar Ecol Prog Ser.* **1997**, *159*, 219–227.
65. Steinberg, P. D.; Estes, J. A.; Winter, F. C. Evolutionary consequences of food chain length in kelp forest communities. *Proc Natl Acad Sci USA.* **1995**, *92*, 8145–8148.
66. Stern, J. L.; Hagerman, A. E.; Steinberg, P. D.; Mason, P. K. Phlorotannin-protein interactions. *J Chem Ecol.* **1996**, *22*, 1877–1899.
67. Irelan, C. D.; Horn, M. H. Effects of macrophyte secondary chemicals on food choice and digestive efficiency of *Cebidichthys iolaceus* (Girard), an herbivorous fish of temperate marine waters. *J Exp Mar Biol Ecol.* **1991**, *153*, 179–194.
68. Cheeseman, K. H.; Slater, T. F. An introduction to free radical biochemistry. *British Med Bull.* **1993**, *49*, 481–489.
69. Li, Y. J.; Takizawa, H.; Kawada, T. Role of oxidative stresses induced by diesel exhaust particles in airway inflammation, allergy and asthma: their potential as a target of chemoprevention. *Inflamm Allergy Drug Targets.* **2010**, *9*, 300–305.
70. Ahn, G. N.; Kim, K. N.; Cha, S. H.; Son, C. B.; Lee, J.; Heo, M. S.; Yeo, I. K.; Lee, N. H.; Jee, Y. H.; Kim, J. S.; Heu, M. S.; Jeon, Y. J. Antioxidant activities of phlorotannins purified from *Ecklonia cava* on free radical scavenging using ESR and H₂O₂-mediated DNA damage. *Eur Food Res Technol.* **2007**, *22*, 71–79.
71. Kang, K. A.; Lee, K.H.; Chae, S.; Zhang, R.; Jung, M. S.; Lee, Y.; Kim, S. Y.; Kim, H. S.; Joo, H. G.; Park, J. W.; Ham, Y. M.; Lee, N. H.; Hyun, J. W. Eckol isolated from *Ecklonia cava* attenuates oxidative stress induced cell damage in lung fibroblast cells. *FEBS Lett.* **2005**, *579*, 6295–6304.
72. Kang, K. A.; Zhang, R.; Lee, K. H.; Chae, S.; Kim, B. J.; Kwak, Y. S.; Park, J. W.; Lee, N. H.; Hyun, J. W. Protective effect of triphlorethol-A from *Ecklonia cava* against ionizing radiation in vitro. *J Radiat Res.* **2006**, *47*, 61–68.
73. Kang, K. A.; Lee, K. H.; Park, J. W.; Lee, N. H.; Na, H. K.; Surh, Y. J.; You, H. J.; Chung, M. H.; Hyun, J. W. Triphlorethol-A induces heme oxygenase-1 via activation of ERK and NF- κ B related factor 2 transcription factor. *FEBS Lett.* **2007**, *581*, 2000–2008.
74. Li, Y.; Qian, Z. J.; Ryu, B.; Lee, S. H.; Kim, M. M.; Kim, S. K. Chemical components and

its antioxidant properties in vitro: an edible marine brown alga, *Ecklonia cava*. *Bioorgan Med Chem.* **2009**, *17*, 1963–1973.

75. Kang, M. C.; Cha, S. H.; Wijesinghe, W. A.; Kang, S. M.; Lee, S. H.; Kim, E. A.; Song, C. B.; Jeon, Y. J. Protective effect of marine algae phlorotannins against AAPH-induced oxidative stress in zebrafish embryo. *Food Chem.* **2013**, *138*, 950–955.

76. Park, E.; Ahn, G. N.; Lee, N. H.; Kim, J. M.; Yun, J. S.; Hyun, J. W.; Jeon, Y. J.; Wie, M. B.; Lee, Y. J.; Park, J. W.; Jee, Y. Radioprotective properties of eckol against ionizing radiation in mice. *FEBS Lett.* **2008**, *582*, 925–930.

77. Sathya, R.; Kanaga, N.; Sankar, P.; Jeeva, S. Antioxidant properties of phlorotannins from brown seaweed *Cystoseira trinodis* (Forsskål) C. Agardh. *Arab J Chem.* **2017**, *10*, S2608–S2614.

78. Zhang, R.; Yuen, A. K. L.; Magnusson, M.; Wright, J. T.; Nys, R. de.; Masters, A. F.; Maschmeyer, T. A comparative assessment of the activity and structure of phlorotannins from the brown seaweed *Carpophyllum flexuosum*. *Algal Res.* **2018**, *29*, 130–141.

79. Heo, S. J.; Ko, S. C.; Cha, S. H.; Kang, D. H.; Park, H. S.; Choi, Y. U.; Kim, D.; Jung, W. K.; Jeon, Y. J. Effect of phlorotannins isolated from *Ecklonia cava* on melanogenesis and their protective effect against photo-oxidative stress induced by UV-B radiation. *Toxicol In Vitro.* **2009**, *23*, 1123–1130.

80. Vo, T. S.; Kim, S. K.; Ryu, B.; Ngo, D. H.; Yoon, N. Y.; Bach, L. G.; Hang, N. T. N.; Ngo, D. N. The Suppressive Activity of Fucofuroeckol-A Derived from Brown Algal *Ecklonia stolonifera* Okamura on UVB-Induced Mast Cell Degranulation. *Mar Drugs.* **2018**, *16*, 1–9.

81. Klervi, L. L.; Gwladys, S.; Celine, C.; Laurence, C.; Stephane, C.; Fanny, G.; Maud, L.; Mayalen, Z.; Fabienne, G.; Nathalie, P.; Valerie, S. P. Sunscreen, antioxidant, and bactericide capacities of phlorotannins from the brown macroalga *Halidrys siliquosa*. *J Appl Phycol.* **2016**, *28*, 3547–3559.

82. Kaplan, S. L.; Mason, Jr. E. O. Management of infections due to antibiotic-resistant *Streptococcus pneumoniae*. *Clin Microbiol Rev.* **1998**, *11*, 628–644.

83. Nagayama, K.; Iwamura, Y.; Shibata, T.; Hirayama, I.; Nakamura, T. Bactericidal activity of phlorotannins from the brown alga *Ecklonia kurome*. *J Antimicrob Chemother.* **2002**, *50*, 889–893.

84. Lee, D. S.; Kang, M. S.; Hwang, H. J.; Eom, S. H.; Yang, J. Y.; Lee, M. S.; Lee, W. J.; Jeon, Y. J.; Choi, J. S.; Kim, Y. M. Synergistic effect between dieckol from *Ecklonia stolonifera* and β -lactams against methicillin-resistant *Staphylococcus aureus*. *Biotechnol Bioprocess Eng.* **2008**, *13*, 758–764.

85. Eom, S. H.; Kim, D. H.; Lee, S. H.; Yoon, N. Y.; Kim, J. H.; Kim, T. H.; Chung, Y. H.; Kim, S. B.; Kim, Y. M.; Kim, H. W.; Lee, M. S.; Kim, Y. M. In vitro antibacterial activity and synergistic antibiotic effects of phlorotannins isolated from *Eisenia bicyclis* against methicillin-resistant *Staphylococcus aureus*. *Phytother Res.* **2013**, *27*, 1260–1264.

86. Choi, J. S.; Lee, K.; Hong, Y. K.; Lee, B. B.; Cho, K. K.; Kim, Y. C.; Choi, I. S.; Kim, Y. D. Antibacterial activity of the phlorotannins dieckol and phlorofucofuroeckol-a from *Ecklonia cava* against *Propionibacterium acnes*. *Bot. Sci.* **2014**, *92*, 425–431.

87. Lee, J. H.; Eom, S. H.; Lee, E. H.; Jung, Y. J.; Kim, H. J.; Jo, M. R.; Son, K. T.; Lee, H. J.; Kim, J. H.; Lee, M. S.; Kim, Y. M. In vitro antibacterial and synergistic effect of phlorotannins

isolated from edible brown seaweed *Eisenia bicyclis* against acne-related bacteria. *Algae*. **2014**, *29*, 47-55.

88. Lopes, G.; Pinto, E.; Andrade, P. B.; Valentão, P. Antifungal Activity of Phlorotannins against Dermatophytes and Yeasts: Approaches to the Mechanism of Action and Influence on *Candida albicans* Virulence Factor. *PLoS ONE*. **2013**, *8*, e72203.

89. Lee, M. H.; Lee, K. B.; Oh, S. M.; Lee, B. H.; Chee, H. Y. Antifungal activities of dieckol isolated from the marine brown alga *Ecklonia cava* against *Trichophyton rubrum*. *Food Sci Biotechnol*. **2010**, *53*, 504-507.

90. Ojewole, E.; Mackraj, I.; Naidoo, P.; Govender, T. Exploring the use of novel drug delivery systems for antiretroviral drugs. *Eur J Pharm Biopharm*. **2008**, *70*, 697-710.

91. Govender, T.; Ojewole, E.; Naidoo, P. Polymeric nanoparticles for enhancing antiretroviral drug therapy. *Drug Deliv*. **2008**, *15*, 493-501.

92. Clavel, F.; Hance, A. J. HIV drug resistance. *N Engl J Med*. **2004**, *350*, 1023-1035.

93. Lee, S. A.; Hong, S. K.; Suh, C. I.; Oh, M. H.; Park, J. H.; Choi, B. W.; Park, S. W.; Paik, S. Y. Anti-HIV-1 efficacy of extracts from medicinal plants. *J Microbiol*. **2010**, *48*, 249-252.

94. Tantillo, C.; Ding, J.; Jacobo-Molina, A.; Nanni, R. G.; Boyer, P. L.; Hughes, S. H.; Pauwels, R.; Andries, K.; Janssen, P. A.; Arnold, E. Locations of anti-AIDS drug binding sites and resistance mutations in the three-dimensional structure of HIV-1 reverse transcriptase. Implications for mechanisms of drug inhibition and resistance. *J Mol Biol*. **1994**, *243*, 369-387.

95. Lipsky, J. J. Antiretroviral drugs for AIDS. *Lancet*. **1996**, *348*, 800-803.

96. Ahn, M. J.; Yoon, K. D.; Min, S. Y.; Lee, J. S.; Kim, J. H.; Kim, T. G.; Kim, S. H.; Kim, N. G.; Hu, H.; Kim, J. Inhibition of HIV-1 reverse transcriptase and protease by phlorotannins from the brown alga *Ecklonia cava*. *Biol Pharm Bull*. **2004**, *27*, 544-547.

97. Ahn, M. J.; Yoon, K. D.; Kim, C. Y.; Kim, J. H.; Shin, C. G.; Kim, J. Inhibitory activity on HIV-1 reverse transcriptase and integrase of a carmalol derivative from a brown alga, *Ishige okamurae*. *Phytother Res*. **2006**, *20*, 711-713.

98. Artan, M.; Li, Y.; Karadeniz, F.; Lee, S. H.; Kim, M. M.; Kim, S. K. Anti-HIV-1 activity of phloroglucinol derivative, 6,6-bieckol, from *Ecklonia cava*. *Bioorg Med Chem*. **2008**, *16*, 7921-7926.

99. Kwon, H. J.; Ryu, Y. B.; Kim, Y. M.; Song, N.; Kim, C. Y.; Rho, M. C.; Jeong, J. H.; Cho, K. O.; Lee, W. S.; Park, S. J. In vitro antiviral activity of phlorotannins isolated from *Ecklonia cava* against porcine epidemic diarrhea coronavirus infection and hemagglutination. *Bioorg Med Chem*. **2013**, *21*, 4706-4713.

100. Arshad, S. H. Does exposure to indoor allergens contribute to the development of asthma and allergy? *Curr Allergy Asthma Rep*. **2010**, *10*, 49-55.

101. Milián, E.; Díaz, A. M. Allergy to house dust mites and asthma. *P R Health Sci J*. **2004**, *23*, 47-57.

102. Galli, S. J.; Tsai, M.; Piliponsky, A. M. The development of allergic inflammation. *Nature*. **2008**, *454*, 445-454.

103. Li, Y.; Lee, S. H.; Le, Q. T.; Kim, M. M.; Kim, S. K. Anti-allergic effects of phlorotannins on histamine release via binding inhibition between IgE and FcεRI. *J Agric Food Chem*.

2008, 56, 12073–12080.

104. Shim, S. Y.; Choi, J. S.; Byun, D. S. Inhibitory effects of phloroglucinol derivatives isolated from *Ecklonia stolonifera* on FcεRI expression. *Bioorg Med Chem*. **2009**, 17, 4734–4739.
105. Sugiura, Y.; Matsuda, K.; Yamada, Y.; Nishikawa, M.; Shioya, K.; Katsuzaki, H.; Imai, K.; Amano, H. Isolation of a new anti-allergic phlorotannin, Phlorofucofuroeckol-B, from an edible brown alga, *Eisenia arborea*. *Biosci Biotechnol Biochem*. **2006**, 70, 2807–2811.
106. Sugiura, Y.; Matsuda, K.; Yamada, Y.; Nishikawa, M.; Shioya, K.; Katsuzaki, H.; Imai, K.; Amano, H. Anti-allergic phlorotannins from the edible brown alga, *Eisenia arborea*. *Food Sci Technol Res*. **2007**, 13, 54–60.
107. Matsubara, M.; Masaki, S.; Ohmori, K.; Karasawa, A.; Hasegawa, K. Differential regulation of IL-4 expression and degranulation by anti-allergic olopatadine in rat basophilic leukemia (RBL-2H3) cells. *Biochem Pharmacol*. **2004**, 67, 1315–1326.
108. Barbosa, M.; Lopes, G.; Valentão, P.; Ferreres, F.; Gil-Izquierdo, Á.; Pereira, D. M.; Andrade, P. B. Edible seaweeds' phlorotannins in allergy: A natural multi-target approach. *Food Chem*. **2018**, 265, 233–241.
109. Meyer, K. The biological significance of hyaluronic acid and hyaluronidase. *Physiol Rev*. **1947**, 27, 335–359.
110. Kakegawa, H.; Matsumoto, H.; Satoh, T. Inhibitory effects of some natural products on the activation of hyaluronidase and their antiallergic actions. *Chem Pharm Bull*. **1992**, 40, 1439–1442.
111. Kim, T. W.; Lee, J.H.; Yoon, K. B.; Yoon, D. M. Allergic reactions to hyaluronidase in pain management: A report of three cases. *Korean J Anesthesiol*. **2011**, 60, 57–59.
112. Shibata, T.; Fujimoto, K.; Nagayama, K.; Yamaguchi, K.; Nakamura, T. Inhibitory activity of brown algal phlorotannins against hyaluronidase. *Int J Food Sci Tech*. **2002**, 37, 703–709.
113. Sugiura, Y.; Matsuda, K.; Yamada, Y.; Imai, K.; Kakinuma, M.; Amano, H. Radical scavenging and hyaluronidase inhibitory activities of phlorotannins from the edible brown alga *Eisenia arborea*. *Food Sci Technol Res*. **2008**, 14, 595–598.
114. Sugiura, Y.; Matsuda, K.; Okamoto, T.; Yamada, Y.; Imai, K.; Ito, T.; Kakinuma, M.; Amano, H. The inhibitory effects of components from a brown alga, *Eisenia arborea*, on degranulation of mast cells and eicosanoid synthesis. *J Funct Foods*. **2009**, 1, 387–393.
115. Gordon, S. The role of the macrophage in immune regulation. *Res Immunol*. **1998**, 149, 685–688.
116. Gautam, R.; Jachak, S. M. Recent developments in anti-inflammatory natural products. *Med Res Rev*. **2009**, 29, 767–820.
117. Gallin, J. I.; and Snyderman, R. In *Overview in Inflammation: Basic Principles and Clinical Correlates*, 3rd ed.; Lippincott Williams & Wilkins: Philadelphia, 1999.
118. Kang, K.; Hwang, H. J.; Hong, D. H.; Park, Y.; Kim, S. H.; Lee, B. H.; Shin, H. C. Antioxidant and antiinflammatory activities of ventol, a phlorotannin-rich natural agent derived from *Ecklonia cava*, and its effect on proteoglycan degradation in cartilage explant culture. *Res Commun Mol Pathol Pharmacol*. **2004**, 115–116, 77–95.
119. Wijesinghe, W. A. J. P.; Ahn, G.; Lee, W. W.; Kang, M. C.; Kim, E. A.; Jeon, Y. J. Anti-inflammatory activity of phlorotannin-rich fermented *Ecklonia cava* processing by-product

extract in lipopolysaccharide-stimulated RAW 264.7 macrophages. *J Appl Phycol.* **2013**, *25*, 1207–1213.

120. Yang, Y. I.; Shin, H. C.; Kim, S. H.; Park, W. Y.; Lee, K. T.; Choi, J. H. 6,6'-Bieckol, isolated from marine alga *Ecklonia cava*, suppressed LPS-induced nitric oxide and PGE₂ production and inflammatory cytokine expression in macrophages: the inhibition of NFκB. *Int Immunopharmacol.* **2012**, *12*, 510-517.

121. Kim, A. R.; Lee, M. S.; Choi, J. W.; Utsuki, T.; Kim, J. I.; Jang, B. C.; Kim, H. R. Phlorofucofuroeckol A suppresses expression of inducible nitric oxide synthase, cyclooxygenase-2, and pro-inflammatory cytokines via inhibition of nuclear factor-κB, c-Jun NH₂-terminal kinases, and Akt in microglial cells. *Inflammation.* **2013**, *36*, 259-271.

122. Kim, A. R.; Shin, T. S.; Lee, M. S.; Park, J. Y.; Park, K. E.; Yoon, N. Y.; Kim, J. S.; Choi, J. S.; Jang, B. C.; Byun, D. S.; Park, N. K.; Kim, H. R. Isolation and identification of phlorotannins from *Ecklonia stolonifera* with antioxidant and anti-inflammatory properties. *J Agric Food Chem.* **2009**, *57*, 3483-3489.

123. Jung, H. A.; Jin, S. E.; Ahn, B. R.; Lee, C. M.; Choi, J. S. Anti-inflammatory activity of edible brown alga *Eisenia bicyclis* and its constituents fucosterol and phlorotannins in LPS-stimulated RAW264.7 macrophages. *Food Chem Toxicol.* **2013**, *59*, 199-206.

124. Sugiura, Y.; Tanaka, R.; Katsuzaki, H.; Imai, K.; Matsushita, T. The anti-inflammatory effects of phlorotannins from *Eisenia arborea* on mouse ear edema by inflammatory inducers. *J Funct Foods.* **2013**, *5*, 2019 – 2023.

125. Shibata, T.; Nagayama, K.; Tanaka, R.; Yamaguchi, K.; Nakamura, T. Inhibitory effects of brown algal phlorotannins on phospholipase A₂s, lipoxygenases and cyclooxygenases. *J Appl Phycol.* **2003**, *15*, 61–66.

126. Yang, Y. I.; Woo, J. H.; Seo, Y. J.; Lee, K. T.; Lim, Y.; Choi, J. H. Protective Effect of Brown Alga Phlorotannins against Hyper-inflammatory Responses in Lipopolysaccharide-Induced Sepsis Models. *J Agric Food Chem.* **2016**, *64*, 570-578.

127. Barbosa, M.; Lopes, G.; Ferreres, F.; Andrade, P. B.; Pereira, D. M.; Gil-Izquierdo, Á.; Valentão, P. Phlorotannin extracts from Fucales: Marine polyphenols as bioregulators engaged in inflammation-related mediators and enzymes. *Algal Res.* **2017**, *28*, 1–8.

128. Hail, Jr. N. Mitochondria: a novel target for the chemoprevention of cancer. *Apoptosis.* **2005**, *10*, 687–705.

129. Reddy, L.; Odhav, B.; Bhoola, K. D. Natural products for cancer prevention: a global perspective. *Pharmacol. Ther.* **2003**, *99*, 1– 13.

130. Nirmala, M. J.; Samundeeswari, A.; Sankar, P. D. Natural plant resources in anti-cancer therapy-A review. *Res Plant Biol.* **2011**, *1*, 01-14.

131. Bhanot, A.; Sharma, R.; Noolvi, M. N. Natural sources as potential anti-cancer agents: A review. *Int J Phytomedicine.* **2011**, *3*, 09-26.

132. Kong, C. S.; Kim, J. A.; Yoon, N. Y.; Kim, S. K. Induction of apoptosis by phloroglucinol derivative from *Ecklonia cava* in MCF-7 human breast cancer cells. *Food Chem Toxicol.* **2009**, *47*, 1653-1658.

133. Nwosu, F.; Morris, J.; Lund, V. A.; Stewart, D.; Ross, H. A.; McDougall, G. J. Anti-proliferative and potential anti-diabetic effects of phenolic-rich extracts from edible marine algae. *Food Chem.* **2011**, *126*, 1006–1012.

134. Namvar, F.; Mohamad, R.; Baharara, J.; Zafar-Balanejad, S.; Fargahi, F.; Rahman, H. S. Antioxidant, antiproliferative, and antiangiogenesis effects of polyphenol-rich seaweed (*Sargassum muticum*). *Biomed Res Int.* **2013**, *604787*.
135. Parys, S.; Kehraus, S.; Krick, A.; Glombitza, K. W.; Carmeli, S.; Klimo, K.; Gerhäuser, C.; König, G. M. In vitro chemopreventive potential of fucophlorethols from the brown alga *Fucus vesiculosus* L. by anti-oxidant activity and inhibition of selected cytochrome P450 enzymes. *Phytochemistry.* **2010**, *71*, 221–229.
136. Kim, M. M.; Ta, Q. V.; Mendis, E.; Rajapakse, N.; Jung, W. K.; Byun, H. G.; Jeon, Y. J.; Kim, S. K. Phlorotannins in *Ecklonia cava* extract inhibit matrix metalloproteinase activity. *Life Sci.* **2006**, *79*, 1436–1443.
137. Alghazeer, R.; Howell, N.; El-Naili, M.; Awayn, N. Anticancer and Antioxidant Activities of Some Algae from Western Libyan Coast. *Nat Sci.* **2018**, *10*, 232–246.
138. Casas, M. P.; Rodríguez-Hermida, V.; Pérez-Larrán, P.; Conde, E.; Liveri, M. T.; Ribeiro, D.; Fernandes, E.; Domínguez, H. In vitro bioactive properties of phlorotannins recovered from hydrothermal treatment of *Sargassum muticum*. *Sep Purif Technol.* **2016**, *167*, 117–126.
139. Thilagam, E.; Parimaladevi, B.; Kumarappan, C.; and Mandal, S. C. α -Glucosidase α -amylase inhibitory activity of *Senna surattensis*. *J Acupunct Meridian Stud.* **2013**, *6*, 24–30.
140. Rengasamy, K. R.; Aderogba, M. A.; Amoo, S. O.; Stirk, W. A.; Van Staden, J. Potential antiradical and α -glucosidase inhibitors from *Ecklonia maxima* (Osbeck) Papenfuss. *Food Chem.* **2013**, *141*, 1412–1415.
141. Kellogg, J.; Grace, M. H.; Lila, M. A. Phlorotannins from Alaskan seaweed inhibit carbolytic enzyme activity. *Mar Drugs.* **2014**, *12*, 5277–5294.
142. Okada, Y.; Ishimaru, A.; Suzuki, R.; Okuyama, T. A new phloroglucinol derivative from the brown alga *Eisenia bicyclis*: Potential for the effective treatment of diabetic complications. *J Nat Prod.* **2004**, *67*, 103–105.
143. Moon, H. E.; Islam, N.; Ahn, B. R.; Chowdhury, S. S.; Sohn, H. S.; Jung, H. A.; Choi, J. S. Protein tyrosine phosphatase 1B and α -glucosidase inhibitory phlorotannins from edible brown algae *Ecklonia stolonifera* and *Eisenia bicyclis*. *Biosci Biotechnol Biochem.* **2011**, *75*, 1472–1480.
144. Iwai, K. Antidiabetic and antioxidant effects of polyphenols in brown alga *Ecklonia stolonifera* in genetically diabetic KK-Ay mice. *Plant Foods Hum Nutr.* **2008**, *63*, 163–169.
145. Jung, H. A.; Yoon, N. Y.; Woo, M. H.; Choi, J. S. Inhibitory activities of extracts from several kinds of seaweeds and phlorotannins from the brown alga *Ecklonia stolonifera* on glucose-mediated protein damage and rat lens aldose reductase. *Fish Sci.* **2008**, *74*, 1363–1365.
146. Lee, S. H.; Park, M. H.; Heo, S. J.; Kang, S. M.; Ko, S. C.; Han, J. S.; Jeon, Y. J. Dieckol isolated from *Ecklonia cava* inhibits α -glucosidase and α -amylase in vitro and alleviates post-prandial hyperglycemia in streptozotocin-induced diabetic mice. *Food Chem Toxicol.* **2010**, *48*, 2633–2637.
147. Kim, E. B.; Nam, Y. H.; Kwak, J. H.; Kang, T. H. Anti-diabetic activity of phlorotannin from *Eisenia bicyclis* in Zebrafish, a model of type 1 and 2 diabetes. *Planta Med.* **2015**, *81*, PW_112.

148. Park, S. R.; Kim, J. H.; Jang, H. D.; Yang, S. Y.; Kim, Y. H. Inhibitory activity of minor phlorotannins from *Ecklonia cava* on α -glucosidase. *Food Chem.* **2018**, *257*, 128-134.
149. Kaila, B.; and Raman, M. Obesity: a review of pathogenesis and management strategies. *Can J Gastroentero.* **2008**, *22*, 61-68.
150. Jung, H. A.; Jung, H. J.; Jeong, H. Y.; Kwon, H. J.; Ali, M. Y.; Choi, J. S. Phlorotannins isolated from the edible brown alga *Ecklonia stolonifera* exert anti-adipogenic activity on 3T3-L1 adipocytes by downregulating C/EBP α and PPAR γ . *Fitoterapia.* **2014**, *92*, 260-269.
151. Ko, S. C.; Lee, M.; Lee, J. H.; Lee, S. H.; Lim, Y.; and Jeon, Y. J. Dieckol, a phlorotannin isolated from a brown seaweed, *Ecklonia cava*, inhibits adipogenesis through AMP-activated protein kinase (AMPK) activation in 3T3-L1 preadipocytes. *Environ Toxicol Pharmacol.* **2013**, *36*, 1253-1260.
152. Park, M. H.; Jeon, Y. J.; Kim, H. J.; Han, J. S. Effect of diphlorethohydroxycarmalol isolated from *Ishige okamurae* on apoptosis in 3t3-L1 preadipocytes. *Phytother Res.* **2013**, *27*, 931-936.
153. Mori, T.; Hidaka, M.; Ikuji, H.; Yoshizawa, I.; Toyohara, H.; Okuda, T.; Uchida, C.; Asano, T.; Yotsu-Yamashita, M.; Uchida, T. A high-throughput screen for inhibitors of the prolyl isomerase, Pin1, identifies a seaweed polyphenol that reduces adipose cell differentiation. *Biosci Biotechnol Biochem.* **2014**, *78*, 832-838.
154. Ahn, G.; Park, E.; Park, H. J.; Jeon, Y. J.; Lee, J.; Park, J. W.; Jee, Y. The classical NF-kB pathway is required for phloroglucinol-induced activation of murine lymphocytes. *Biochim Biophys Act.* **2010**, *1800*, 639-645.
155. Wijesinghe, W. A Ko, S. C.; Jeon, Y. J. Effect of phlorotannins isolated from *Ecklonia cava* on angiotensin I-converting enzyme (ACE) inhibitory activity. *Nutr Res Pract.* **2011**, *5*, 93-100.
156. Jung, H. A.; Hyun, S. K.; Kim, H. R.; Choi, J. S. Angiotensin-converting enzyme I inhibitory activity of phlorotannins from *Ecklonia stolonifera*. *Fish. Sci.* **2006**, *72*, 1292-1299.
157. Um, M. Y.; Lim, D. W.; Son, H. J.; Cho, S.; Lee, C. Phlorotannin-rich fraction from *Ishige foliacea* brown seaweed prevents the scopolamine-induced memory impairment via regulation of ERK-CREB-BDNF pathway. *J Funct Foods*, **2018**, *40*, 110-116.
158. Cha, S. H.; Heo, S. J.; Jeon, Y. J.; Park, S. M. Dieckol, an edible seaweed polyphenol, retards rotenone-induced neurotoxicity and α -synuclein aggregation in human dopaminergic neuronal cells. *RSC Adv.* **2016**, *6*, 110040-110046.
159. Wang, J.; Zheng, J.; Huang, C.; Zhao, J.; Lin, J.; Zhou, X.; Naman, C. B.; Wang, N.; Gerwick, W. H.; Wang, Q.; Yan, X.; Cui, W.; He, S. Eckmaxol, a Phlorotannin Extracted from *Ecklonia maxima*, Produces Anti- β -amyloid Oligomer Neuroprotective Effects Possibly via Directly Acting on Glycogen Synthase Kinase 3 β . *ACS Chem Neurosci.* **2018**, *9*, 1349-1356.

